1521-0103/383/2/129–136$35.00
THE JOURNAL OF PHARMACOLOGY AND EXPERIMENTAL THERAPEUTICS

dx.doi.org/10.1124/jpet.122.001322
J Pharmacol Exp Ther 383:129–136, November 2022

The Journal of PHARMACOLOGY And Experimental Therapeutics

A Novel Truncated Liver Enriched Antimicrobial Peptide-2 Palmitoylated at its N-Terminal Antagonizes Effects of Ghrelin

Lucie Hola, Blanka Zelezna, Alena Karnosova, Jaroslav Kunes, Jean-Alain Fehrentz, Severine Denoyelle, Sonia Cantel, Miroslava Blechova, David Sykora, Aneta Myskova, and Lenka Maletınska

Institute of Organic Chemistry and Biochemistry, Czech Academy of Sciences, Prague, Czech Republic (L.H., B.Z., A.K., J.K., M.B., A.M., L.M.); Institute of Physiology, Czech Academy of Sciences, Prague, Czech Republic (J.K.); First Faculty of Medicine, Charles University, Prague, Czech Republic (L.H., A.K.); University of Chemistry and Technology, Prague, Czech Republic (D.S., A.M.); and IBMM, Univ Montpellier, CNRS, ENSCM, Montpellier, France (J.A.F., S.C., S.D.)

Received May 20, 2022; accepted August 3, 2022

ABSTRACT

Ghrelin is secreted in the stomach during fasting and targets the growth hormone secretagogue receptor (GHSR1a) in the hypothalamus and brainstem to exert its orexigenic effect. Recently, liver enriched antimicrobial peptide-2 (LEAP2) was identified as an endogenous high-affinity GHSR1a antagonist. LEAP2 is a 40-amino acid peptide with two disulfide bridges and GHRS1a affinity in the N-terminal hydrophobic part. In this study, we tested modified truncated N-terminal peptide LEAP2 (1-14), along with its myristoylated, palmitoylated, and stearoylated analogs, to determine their affinity GHSR1a with affinity similar to that of natural LEAP2, and lipidization significantly enhanced the affinity of LEAP2(1–14) to GHSR1a. According to the beta-lactamase reporter gene response, the natural GHSR1a agonist ghrelin activated the receptor with nanomolar EC_{50}. LEAP2(1-14) analogs behaved as inverse agonists of GHSR1a and suppressed internal activity of the receptor with EC_{50} values in the 10^{8} M range. LEAP2(1-14) analogs significantly lowered acute food intake in overnight fasted mice, and palmitoylated LEAP2(1-14) was the most potent. In free-fed mice, all LEAP2(1-14) analogs significantly decreased the orexigenic effect of the stable ghrelin analog [Dpr^3]Ghrelin. Moreover, palmitoylated LEAP2(1-14) inhibited the growth hormone (GH) release induced by [Dpr^3]Ghrelin and exhibited an increased stability in rat plasma compared with LEAP2(1-14). In conclusion, palmitoylated LEAP2(1-14) had the most pronounced affinity for GHSR1a, had an anorexigenic effect, exhibited stability in rat plasma, and attenuated [Dpr^3]Ghrelin-induced GH release. Such properties render palmitoylated LEAP2(1-14) a promising substance for antiobesity treatment.

CANCE STATEMENT

The agonist and antagonist of one receptor are rarely found in one organism. For ghrelin receptor (growth hormone secretagogue receptor, GHSR), endogenous agonist ghrelin and endogenous antagonist/inverse agonist liver enriched antimicrobial peptide-2 (LEAP2) co-exist and differently control GHSR signaling. As ghrelin has a unique role in food intake regulation, energy homeostasis, and cytoprotection, lipidized truncated LEAP2 analogs presented in this study could serve not only to reveal the relationship between ghrelin and LEAP2 but also for development of potential anti-obesity agents.

Introduction

Liver-expressed antimicrobial peptide 2 (LEAP2) is a peptide of 40 amino acids originally isolated from human blood in 2003 (Krause et al., 2003). LEAP2 is expressed mainly in the liver and jejunum (Ge et al., 2018). LEAP2 has two disulfide bonds and folds into a cationic globular structure (Henriques et al., 2010). In early studies (Krause et al., 2003), LEAP2 was reported to show in vitro antimicrobial activities at a micromolar concentration. However, LEAP2 physiologic concentration in plasma is in the nanomolar range (Mani et al., 2019). Moreover, the LEAP2 peptide sequence is highly conserved from fish to mammals (Li et al., 2021), implying that LEAP2 performs other important functions in addition to being an antimicrobial peptide. Ge et al. tested the activation of 168 known human G-protein coupled receptors by LEAP2 in agonist and antagonist modes (Ge et al., 2018). LEAP2 fully inhibited growth hormone secretagogue receptor 1a (GHSR1a), receptor of the orexigenic hormone ghrelin.

The ghrelin-GHSR1a system is involved in multiple biologic functions, such as growth hormone (GH) secretion, food intake, reward-seeking behaviors, cardiovascular functions and glucose homeostasis (Zigman et al., 2006). These diversified functions

This work was supported by the Czech Science Foundation [22-11155S] and Czech Academy of Sciences [RVO:61388963, RVO:67985823].
No author has an actual or perceived conflict of interest with the contents of this article.
dx.doi.org/10.1124/jpet.122.001322.

ABBREVIATIONS: Dpr, diaminopropionic acid; ESI, electrospray ionization; GH, growth hormone; GHSR1a, growth hormone secretagogue receptor 1a; K_i, inhibition constant; LC, liquid chromatography; LEAP2, liver enriched antimicrobial peptide-2; MS, mass spectrometry; NPY, neuropeptide Y.

suggest the complexity of GHSR1a intracellular signaling. Ghrelin is secreted during fasting in the stomach and stimulates secretion of the orexigenic neuropeptides agouti-related protein and neuropeptide Y in agouti-related protein /neuropeptide Y neurons in the arcuate nucleus of hypothalamus (Cowley et al., 2003). Ghrelin consists of 28 amino acids and is unusual among peptide hormones because its Ser^3 is octanoylated (Kojima et al., 1999). Ghrelin without the acyl group can neither bind GHSR1a nor induce GH release (Sato et al., 2014).

The N-terminal fragment of LEAP2 is enriched with hydrophobic amino acids, such as Met^1, Pro^3, Phe^4, and Trp^5, allowing it to bind the same ligand-binding pocket on GHSR1a as ghrelin (Wang et al., 2019). LEAP2 competes with ghrelin for binding to GHSR1a and decreases the constitutive activity of GHSR1a, acting as an inverse agonist by stabilizing an inactive conformation of the receptor (M′Kadmi et al., 2019). LEAP2 inhibits the major effects of ghrelin in vivo. LEAP2 s.c. pretreatment was reported to attenuate the orexigenic effect of s.c. administered ghrelin in mice. Moreover, LEAP2 inhibits ghrelin-induced GH release (Ge et al., 2018). However, subsequently, other researchers showed that specifically intracerebroventricular, but not peripheral, administration of LEAP2 to rats suppressed central ghrelin functions, including Fos expression in hypothalamic nuclei, the promotion of food intake, blood glucose elevation, and body temperature reduction (Islam et al., 2020). Lean but also obese mice deficient in LEAP2 are more sensitive to the acute effects of administered ghrelin on food intake and GH secretion. LEAP2 deficiency lowers energy expenditure, reduces locomotor activity, and increases food intake in females chronically fed a high-fat diet, resulting in increased body weight, body length, and hepatic fat accumulation (Shankar et al., 2021).

The plasma levels of ghrelin and its inverse agonist LEAP2 have an opposite trend in fasting and feeding/refeeding in mice and humans. Similarly, the LEAP2 levels are higher and ghrelin levels are lower in morbidly obese humans than in lean ones. The LEAP2 to ghrelin ratio is an obvious marker of obesity and decreases with body weight loss in obese people (Mani et al., 2019).

Research investigating the interrelation between ghrelin and LEAP2 faces the following two very basic problems: first, the instability of ghrelin caused by the labile ester bond between octanoic acid and the hydroxyl of Ser^3, which is essential for ghrelin biologic activity, and second, the extremely difficult synthesis of LEAP2 complicated with two S-S bonds. These problems could be overcome by first using the ghrelin analog [Dpr^3]Ghrelin with Ser^3 replaced with diaminopropionic acid (Dpr) and octanoyl anchored to the peptide chain by stable amide bond (Bednarek et al., 2000; Maletınska et al., 2012) and second by using shorter N-terminal peptides of LEAP2, whose syntheses are feasible and which have preserved biologic activity (M′Kadmi et al., 2019).

The aim of this study was to design a series of novel truncated LEAP2 analogs to select the most stable and bioavailable GHSR1a inverse agonists. Biologically active LEAP2(1-14) was synthesized based on published data (M′Kadmi et al., 2019) and lipidized with different fatty acid residues (myristoyl, palmitoyl, or stearoyl) at its C-terminus as the N-terminal part of LEAP2 is essential for receptor binding (M′Kadmi et al., 2019). LEAP2(1-14) and its lipidized analogs were characterized by evaluating their binding affinity to GHSR1a, their ability to affect GHSR1a internal activity, their opposing effect on ghrelin orexigenic action and GH release in mice, and their stability in rat plasma. Out of the LEAP2 truncated lipidized analogs designed and tested in this study, palmitoylated LEAP2(1-14) showed the most potent inhibitory properties toward ghrelin-induced GHSR1 activation.

Materials and Methods

Peptide Synthesis

Ghrelin and [Dpr^3]Ghrelin Synthesis. Ghrelin and [Dpr^3]Ghrelin were assembled in a solid-phase ABI 433A synthesizer (Applied Biosystems, Foster City, CA) as previously described (Holubova et al., 2018). Ghrelin was used in the in vitro experiments, and its stable analog [Dpr^3]Ghrelin was used in the in vivo experiments. Lipidization with the corresponding fatty acid was performed on a fully protected peptide on resin as the last step (Maletınska et al., 2012). Peptide purification and identification were carried out by analytical high-performance liquid chromatography and mass spectrometry (MS). The purity of the synthesized peptides was greater than 95%.

LEAP-2(38-77) (#075-40) was obtained from Pheonix Pharmaceuticals (Burlingame, CA USA).

Synthesis of LEAP2(1-14) and Its Lipidized Analogs. Fmoc-^{1}Nle-^{2}Thr(tBu)-^{3}Pro-^{4}Phe-^{5}Trp(Boc)-^{6}Arg(Pbf)-^{7}Gly-^{8}Val-^{9}Ser(tBu)-^{10}Leu-^{11}Arg(Pbf)-^{12}Pro-^{13}Ile-^{14}Gly-^{15}bAla-^{16}Lys(Alloc)-NH_2 was assembled by solid-phase peptide synthesis starting from Agilent Amphisphere 40 RAM resin (0.36 mmol/g), 1100 mg of resin, 0.4 mmol, using Fmoc chemistry, HATU/DIEA coupling conditions, and piperidine/DMF for deprotection. All coupling steps (5 eq.) were performed twice for 10 minutes. After the completion of the synthesis, the Alloc group of Lys^{16} was deprotected twice in DCM using $Pd(PPh_3)_4$ 0.25 eq. and $PhSiH_3$ 25 eq. for 30 minutes. Then, the peptidyl resin was washed with DCM, dried, and divided into 4 equal parts. Lipidization was performed on three parts by coupling each part with the three corresponding acids (10 eq.) using BOP as a coupling agent (10 eq.) and DIEA as the base for 30 minutes. The fourth part was directly deprotected to yield LEAP2(1-14). Final deprotection was performed with a TFA/TIS/H_2O (95/2.5/2.5) mixture for 3 hours. Purification was performed on a Gilson PLC 2250 Preparative RP-high-performance liquid chromatography system (Villiers le Bel, France) using a preparative column (Waters DeltaPak C18 Radial-Pak Cartridge, 100 Å, 100x40 mm, 15 mm particle size) in the gradient mode at a flow rate of 50.0 ml/min. Buffer A was 0.1% TFA in water, and buffer B was 0.1% TFA in acetonitrile.

Peptide Characterization. The liquid chromatography (LC)/MS system consisted of a high-performance liquid chromatography -ZQ (Waters) equipped with an electrospray ionization (ESI) source. The analyses were carried out using a Phenomenex Kinetex column (C18, 100 Å, 100x2.1 mm, 2.6 mm). A flow rate of 0.5 ml/min and a gradient of 0–100% B over 5 minutes were used as follows: eluent A, water/ 0.1% HCO_2H; eluent B, ACN/0.1% HCO_2H. Positive-ion electrospray (ESI1) mass spectra were acquired from 100 to 1500 m/z with a scan time of 0.2 seconds. Nitrogen was used for both the nebulizing and drying gas. All peptides were characterized with a purity of at least 95%.

The structures of all peptides are shown in Fig. 1B.

Peptide Iodination. Ghrelin was iodinated at His^9 with Na[^{125}I] purchased from Izotop (Budapest, Hungary) using Iodo-Gen (Pierce, Rockford, IL, USA) according to (Maletinska et al., 2012). The identity of the peptides was verified by a matrix-assisted laser desorption/ionization time-of-flight Reflex IV mass spectrometer (Bruker Daltonics, Billerica, MA, USA). The specific activity of ^{125}I-ghrelin was 2000 Ci/mmol. Aliquots of purified radiolabeled ghrelin were dried by evaporation, kept at -20C and used in the binding studies within 1 month.

Cell Culture. T-REx Tango GHSR-bla U2OS cells overexpressing GHSR1a and containing a b-lactamase reporter gene under the control of an upstream activation site response element were obtained from Thermo Fisher Scientific, Inc. (Waltham, MA, USA). The cells were maintained at 37C in a humified incubator with 5% CO_2 in

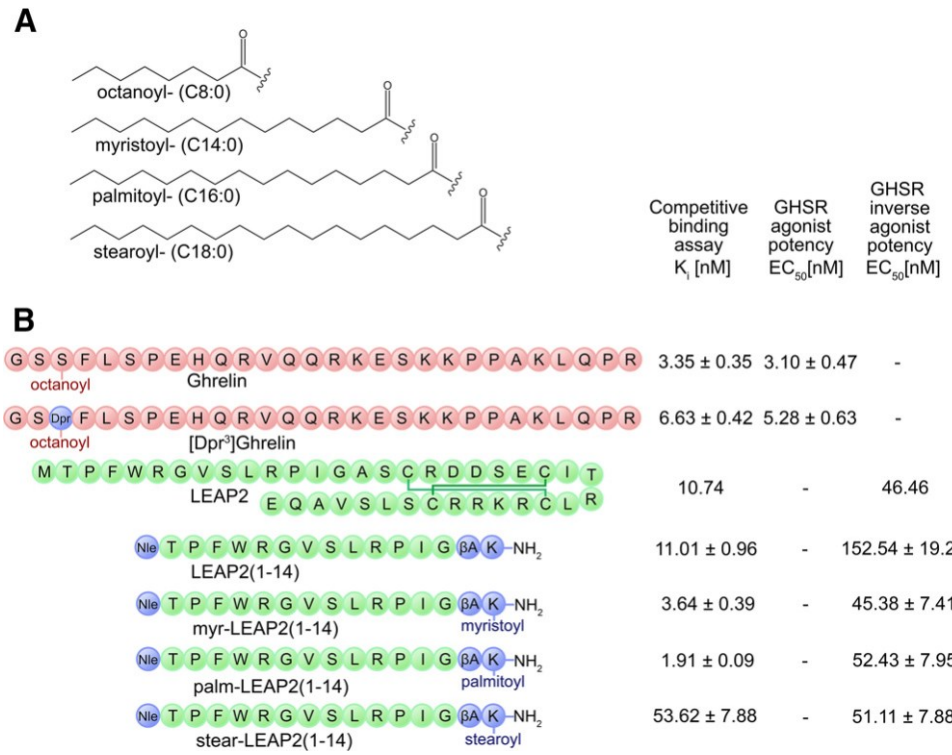

Fig. 1. Overview of lipid chains and sequences of ghrelin and LEAP2 analogs. (A) Fatty acid residues [C8, C14, C16, C18] applied in the current study. (B) Overview of sequences of ghrelin and LEAP2 analogs. Binding affinities of ghrelin and LEAP2 analogs to GHSR1a based on competi-tion with 125I-ghrelin as the means of Ki values ± S.E.M. Ki values were calculated using the Cheng-Prusoff equation. Agonist and inverse ago-nist effect of peptides on GHSR1a activation presented as the means EC_{50} values ± S.E.M. Data analyzed in GraphPad Software were performed in 3–5 independent experiments in duplicates.

McCoy's 5A medium supplemented with 10% dialyzed fetal bovine se-rum, 0.1 mM nonessential amino acids, 25 mM HEPES (pH 7.3), 1 mM sodium pyruvate, 1% streptomycin/penicillin, 200 lg/ml zeocin, 50 lg/ml hygromycin, and 100 lg/ml geneticin according to Thermo Fisher's protocol.

Competitive Binding Studies. The competitive binding studies were performed as previously described (Karnosova et al., 2021). In brief, T-REx Tango GHSR-bla U2OS cells were seeded on 24-well plates to reach a density of 20,000 cells/well, which was found to be optimal for the binding experiment. The cells were allowed to grow for 3 days. Sixteen hours before the experiment, doxycycline was added into a final concentration of 1.25 ng/ml. Ghrelin, LEAP2 and their analogs were used at final concentrations from 10^{12} to 10^{5} M to compete with 0.1 nM [^{125}I]-ghrelin. The incubations were performed in a total volume of 250 ll of binding buffer (50 mM Tris-Cl pH 7.4, 118 mM NaCl, 5 mM $MgCl_2$, 4.7 mM KCl, 0.1% BSA, and 2 g/l glucose) for 60 minutes at 23C. The cells were rinsed with wash buffer (20 mM Tris pH 7.4, 118 mM NaCl, 4.7 mM KCl, and 5 mM $MgCl_2$) and subsequently lysed in 0.1 M NaOH. Radioactivity was determined by gamma counting (Wizard 1470 Automatic Gamma Counter; PerkinElmer Life and Analytical Sciences, Waltham, MA). The experiments were carried out in duplicate at least three times.

Beta-Lactamase-Dependent Fluorescence Resonance Energy Transfer Assay. T-REx Tango GHSR-bla U2OS cells were used to study the agonist/inverse agonist/antagonist properties of ghrelin, LEAP2 and their analogs in a complementation assay for GHSR1a ac-tivity involving arrestin recruitment and expression of b-lactamase. The cells were plated at 10,000 cells/well in a 384-well plate in assay medium, and the assay was performed according to Thermo Fisher's protocol and according to our previous study (Holubova et al., 2018). Ghrelin, LEAP2 and their analogs were used at final concentrations ranging from 10^{12} to 10^{5} M. The fluorescent plate reader FlexSta-tion 3 was operated at a 409 nm excitation wavelength and a 460 or 530 nm emission wavelength via bottom read. The experiments were carried out in duplicate at least three times.

Experimental Animals. Male C57Bl/6J mice (Charles River, Sulzfeld, Germany) were housed at a temperature of 23C and a daily cycle of 12 hours of light and dark (light from 6:00 AM). The mice were given ad libitum water and standard chow diet of ssniff R/M-H (cat. no. V1534; Spezialdiäten GmbH, Soest, Germany), which con-tained 58%, 9%, and 33% of calories from carbohydrate, fat, and pro-tein, respectively. All experiments followed the ethical guidelines for animal experiments and the Act of the Czech Republic Nr. 246/1992 and were approved by the Committee for Experiments with Labora-tory Animals of the Academy of Sciences of the Czech Republic (deci-sion no. 38/2013 was issued on 8/4/2013).

Effect of LEAP2(1-14) and Its Lipidized Analogs on Acute Food Intake in Mice. Twelve-week-old mice were placed in sepa-rate cages for 1 week with free access to water and food pellets. Anorexigenic activity was tested in mice fasted for 17 hours. On the day of the food intake experiment, at 8:00 AM, the mice were s.c. injected with 150 ml of saline or LEAP2(1-14) analogs (dis-solved in saline) at a dose of 5 mg/kg of body weight (n 5 5). Thirty minutes after the injection, the mice were given preweighed food pellets. The anorexigenic effect of the LEAP2(1-14) analogs on the orexigenic activity of [Dpr^3] Ghrelin was tested in freely fed mice. On the day of the food intake experiment, at 8:00 AM, the mice were s.c. injected with 150 ml of saline or LEAP2(1-14) analogs (dissolved in saline) at a dose of 5 mg/kg of body weight (n 5 5). Fifteen minutes after the first injection, the mice were injected with saline or [Dpr^3]Ghrelin at a dose of 1 mg/kg of body weight. Fifteen minutes after the second injection, the mice were given preweighed food pellets. Food intake was monitored every 30 minutes

for at least 7 hours. The animals had free access to water during the experiment. The results are expressed in grams of food consumed.

GH Release After S.C. Administration of [Dpr^3]Ghrelin and Selected LEAP2(1-14) Analogs to Mice. The effects of LEAP2(1-14) and palm-LEAP2(1-14) on [Dpr^3]Ghrelin-induced GH release were determined in 8-week-old male C57BL/6J mice. At 8:00 AM, freely fed mice were s.c. injected with 200 ml of saline or peptide (dissolved in saline) at a dose of 10 mg/kg of body weight (n 5 5-8). Fifteen minutes after the first injection, the mice were injected with saline or [Dpr^3]Ghrelin at a dose of 1 mg/kg of body weight. Fifteen minutes after the second injection, the animals were sacrificed by decapitation, blood was collected, and the plasma was separated and stored at -80C until use. GH in the plasma samples was determined by a rat/mouse GH enzyme-linked immunosorbent assay kit (cat. no. EZRMGH-45K; Merck-Millipore, Burlington, Massachusetts, USA) according to the protocol recommended by the manufacturer.

Stability of Selected LEAP2(1-14) Analogs in Rat Plasma. The stability of LEAP2(1-14) and palm-LEAP2(1-14) in rat plasma was determined by LC combined with MS. For LC, an UltiMate 3000 (Thermo, USA) consisting of a DGP-3600SD pump, a WPS-3000SL autosampler, and a TCC-3000SD column compartment was used. The MS detection of the eluates from the LC system was performed with a Q-TRAP 3200 mass spectrometer (AB Sciex, Canada).

The LC–MS method used an XBridge Premier BEH C18, particle size 2.5 mm, VanGuard Fit, and 50x2.1 mm column (Waters, USA). Mobile phase A consisted of 0.1% HCOOH in water, and mobile phase B was 0.1% HCOOH in acetonitrile. The gradient time profile was as follows: 0–5 minutes, from 100% A to 100% B; 5–7 minutes 100% B; 7–7.2 minutes from 100% B to 100% A; and 7.2–12 minutes 100% A. The flow rate was 0.200 ml/min. The column was maintained at 25C, and the auto-sampler temperature was adjusted to 15C. The injection volume was 2 ll. For the analysis, the data acquisition and management software Analyst version 1.6 was employed (AB Sciex). Specific MS methods utilizing multiple reaction monitoring were devel-oped for the studied peptides. The general MS setup was as fol-lows: a turbo-V ion source equipped with an ESI probe in the positive mode, ion spray voltage 5500 V, curtain gas 15 psig, source temperature 450C, ion source gas (1) 50 psig, and ion source gas (2) 60 psig.

Stock solutions of LEAP2(1-14) and palm-LEAP2(1-14) were prepared by dissolving the compounds in 0.1% HCOOH/H_2O to a final concentration of 1 mg/ml. Blank rat plasma (90 ll) placed in 1.5 ml Protein LoBind Tubes (Eppendorf, USA), thermostated at 37C (Incubator NB-T205, N-Biotek, Korea), and spiked with 10 ll of the appropriate peptide solution. All stability experiments were carried out in triplicate. At specified time intervals, i.e., 0, 1, 2, 4, 8, and 24 hours, the plasma samples were taken up from the incubator, and the endogenous proteins were precipitated with 400 ml of 0.1% HCOOH in acetonitrile/H_2O, 8/2 (v/v) solution. Then, the samples were centrifuged for 5 minutes at 14,000 × g at 4C (Micro Star R17, VWR, Germany) be-fore the supernatant was transferred to 1.8-ml glass vials for the subsequent LC–MS analysis.

Statistical Analysis. The data are presented as the means ± S.E.M. The competitive binding experiments were analyzed by GraphPad Software (San Diego, CA, USA) according to Motulsky (Motulsky and Neubig, 2002). The competitive binding curves were plotted compared with the best fit of single-binding site models. The IC_{50} values were obtained from a nonlinear regression analysis, and the inhibition constants (K_i values) were calculated from the IC_{50} values using the Cheng-Prusoff equation (Cheng and Prusoff, 1973). The dissociation constant of the radioligand value obtained from the saturation binding experiments was 0.38 nM. The beta-lactamase assay results were analyzed by a nonlinear regression as log agonist versus response using GraphPad software. The EC_{50} values were determined as the concentration of the peptide that yielded 50% of the maximal response. The data are representative of at least three experiments, each performed in duplicate.

The data from the food intake and GH release experiments were calculated using GraphPad Prism software. A one-way and two-way ANOVA, followed by a Bonferroni post hoc test, was used when appropriate as described in the tables and figure legends; $P < 0.1$ was considered statistically significant.

Results

LEAP2, LEAP2(1-14) and Its Lipidized Analogs Compete with Ghrelin for Binding to GHSR1a. Based on previously published data, the affinity for GHSR1a of ghrelin, its stable analog [Dpr^3]Ghrelin (Holubova et al., 2018), LEAP2, LEAP2(1-14), and its lipidized analogs was studied. All peptides competed with ^{125}I-ghrelin for binding to GHSR1a overexpressed in U2OS cells; ghrelin and [Dpr^3]Ghrelin had a K_i in a nanomolar range as shown in Fig. 1. LEAP2 and its N-terminal fragment LEAP2(1-14) competed with ^{125}I-ghrelin for binding to GHSR1a with K_i in the 10^8 M range. Palmitoylation and myristoylation enhanced, but stearoylation lowered, the affinity of LEAP2(1-14) for GHSR1a.

LEAP2, LEAP2(1-14) and Its Lipidized Analogs Show Inverse Agonist and Antagonist Properties in a GHSR1a Activation Assay. GHSR1a activation was detected by a T-REx Tango GHSR-bla U2OS cell-based assay using a fluorometric microplate reader (FlexStation). Ghrelin and [Dpr^3]Ghrelin acted as strong GHSR1a agonists activating the receptor with a nanomolar EC_{50} (Figs. 1 and 2A). Natural LEAP2 and lipidized LEAP2(1-14) analogs acted as inverse agonists of GHSR1a and suppressed GHSR1a internal activity with EC_{50} values in the 10^8 M range. LEAP2(1-14) was a less effective inverse agonist, with an EC_{50} value that was three times higher.

Dose–response curves of ghrelin in the absence or presence of increasing concentrations of LEAP2 analogs served to determine the antagonist properties of all LEAP2 compounds. As shown in Fig. 2B, increasing the concentration of natural LEAP2 up to 1 lM increased the EC_{50} of ghrelin by more than ten times. In contrast, nonlipidized LEAP2(1-14) had lower antagonist activity (Fig. 2C). On the other hand, increasing the concentration of all lipidized LEAP2(1-14) analogs (Fig. 2, D–F) up to 1 lM increased the EC_{50} of ghrelin by more than one thousand times.

LEAP2(1-14) and Its Lipidized Analogs Decrease Acute Food Intake in Mice. The effects of s.c. administered LEAP2(1-14) and its lipidized analogs on acute food intake were tested in fasted mice (Fig. 3), and the cumulative food intake was recorded for 420 minutes after the administration of the peptides. LEAP2(1-14) and the myristoylated and stearoylated LEAP2(1-14) analogs showed a weak anorexigenic effect, but the palmitoylated analog strongly reduced the cumulative food intake in fasted mice.

The ability of LEAP2(1-14) and its lipidized analogs to modulate the orexigenic effects of [Dpr^3]Ghrelin in mice was tested in free-fed mice (Fig. 4, A–D). All peptides significantly reduced [Dpr^3]Ghrelin-induced food intake. LEAP2(1-14) and

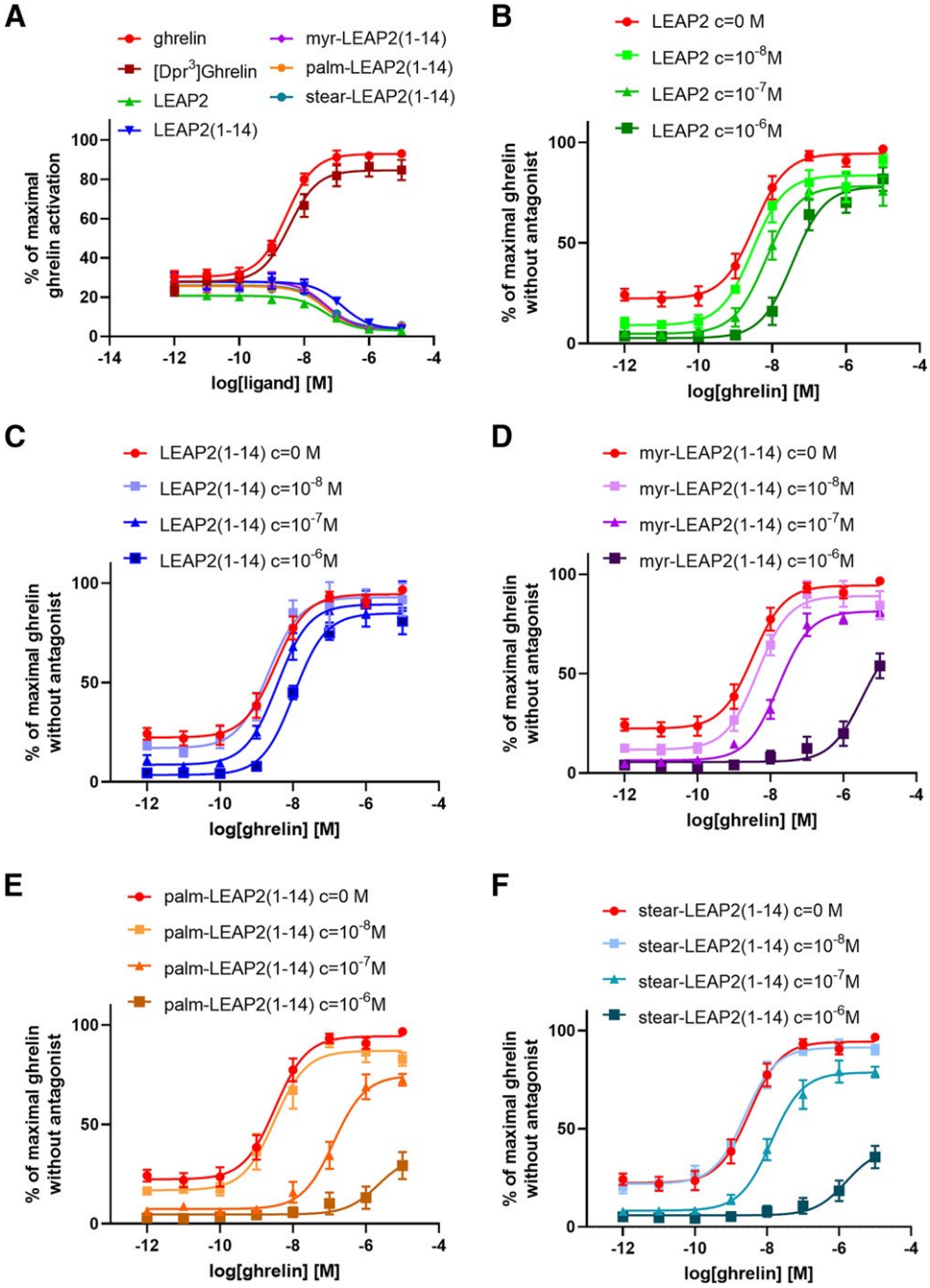

Fig. 2. Inverse agonist and antagonist GHSR1a activation potency. (A) Inverse agonist mode assay showing effect of LEAP2 compounds on inter-nal GHSR1a activation. (B–F) Antagonist mode assay showing effect of (B) LEAP2, (C) LEAP2(1-14), (D) myr-LEAP2(1-14), (E) palm-LEAP2(1-14), and (F) stear-LEAP2(1-14) on GHSR1a activation. The maximal ghrelin effect on U2OS cells expressing GHSR1a was standardized as 100%. Data are presented as the mean ± S.E.M. The experiments were performed in duplicates and repeated at least three times and analyzed using nonlinear regression.

myristoylated LEAP2(1-14) did not, but palmitoylated and stearoylated LEAP2(1-14) fully inhibited [Dpr^3]Ghrelin oregixenic action.

Palm-LEAP2(1-14) Analog Reduces [Dpr^3]Ghrelin-Induced GH Release. LEAP2(1-14) and its palmitoylated analog alone did not affect the plasma GH levels after an s.c. injection in 2-month-old mice. As the level of GH is naturally low in plasma, the ability of the peptides to inhibit [Dpr^3] Ghrelin-induced GH release was tested (Fig. 5). Palmitoylated LEAP2(1-14) significantly decreased the [Dpr^3] Ghrelin-induced release of GH. However, this effect on GH release was not observed after the administration of a nonlipidized LEAP2(1-14).

Stability of LEAP2(1-14) and Palm-LEAP2(1-14) in Rat Plasma. As clearly shown in Fig. 6, palm-LEAP2(1-14) is significantly more stable in blood plasma than its nonlipidized form. Thus, the lipidization of the original peptide improves its stability, which is highly desirable. Consequently, intact palm-LEAP2(1-14) lasts in living

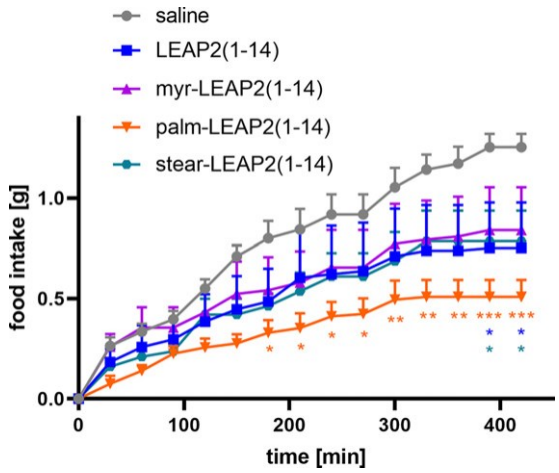

Fig. 3. Effect of LEAP2(1-14) analogs on cumulative food intake after s.c. administration to fasted mice. All LEAP2(1-14) analogs were administered s.c. at a dose of 5 mg/kg. The food intake was monitored every 30 minute for at least 7 hours (n 5 5). The data are presented as means ± S.E.M. and were analyzed by 2-way ANOVA followed by Bonferroni post hoc test. Significance is *P < 0.1; **P < 0.01; ***P < 0.001, versus saline-treated group (n 5 5).

organisms for a rather long time, and its action is protracted.

Discussion

N-terminal fragments of LEAP2 were previously shown to sustain inverse agonist properties toward GHSR1a and decrease ghrelin-induced food intake (M′Kadmi et al., 2019). As the lipidization of peptides is described as a potential tool to increase their stability and overcome their inability to cross the blood–brain barrier (Zhang and Bulaj, 2012), we lipidized the LEAP2(1-14) peptide. Palmitoic acid not only increased the stability of the peptide, but also its affinity and its inverse agonist action on the GHSR1a receptor. Palm-LEAP2(1-14) abrogated [Dpr^3]Ghrelin-induced effects on both food intake and GH release in mice.

LEAP2(1-14), which was used in this study, differs from the truncated N-terminal peptide in M′Kadmi's study (M′Kadmi et al., 2019) by a b-Ala-Lys-NH_2 linker employed for the subsequent lipidization (Fig. 1). In the in vitro studies, we confirmed that the lipidization of LEAP2(1-14) did not deteriorate its ability to bind to GHSR1a-transfected cells. LEAP2(1-14) and its lipidized analogs presented K_i values comparable to that of natural LEAP2 in the 10^9-10^8 M range. Palmitoylation and myristoylation even increased the affinity of LEAP2(1-14) for GHSR1a such that palm-LEAP2(1-14) had a higher affinity for the GHSR1a receptor than myr-LEAP2(1-14). Stearoylation slightly decreased the affinity of LEAP2(1-14) for GHSR1a but did not seem to reduce the in vivo effects of stear-LEAP2(1-14), suggesting that the better stability of the compound likely compensated for its decreased binding ability.

Based on the observation that LEAP2 did not affect GHSR1a-mediated b-arrestin recruitment, Ge et al. asserted that LEAP2 had no inverse agonist activity (Ge et al., 2018). However, this statement was disproved by M′Kadmi et al., who demonstrated the impact of LEAP2 on the basal level of inositol phosphate 1 (IP1) and the discovery that natural

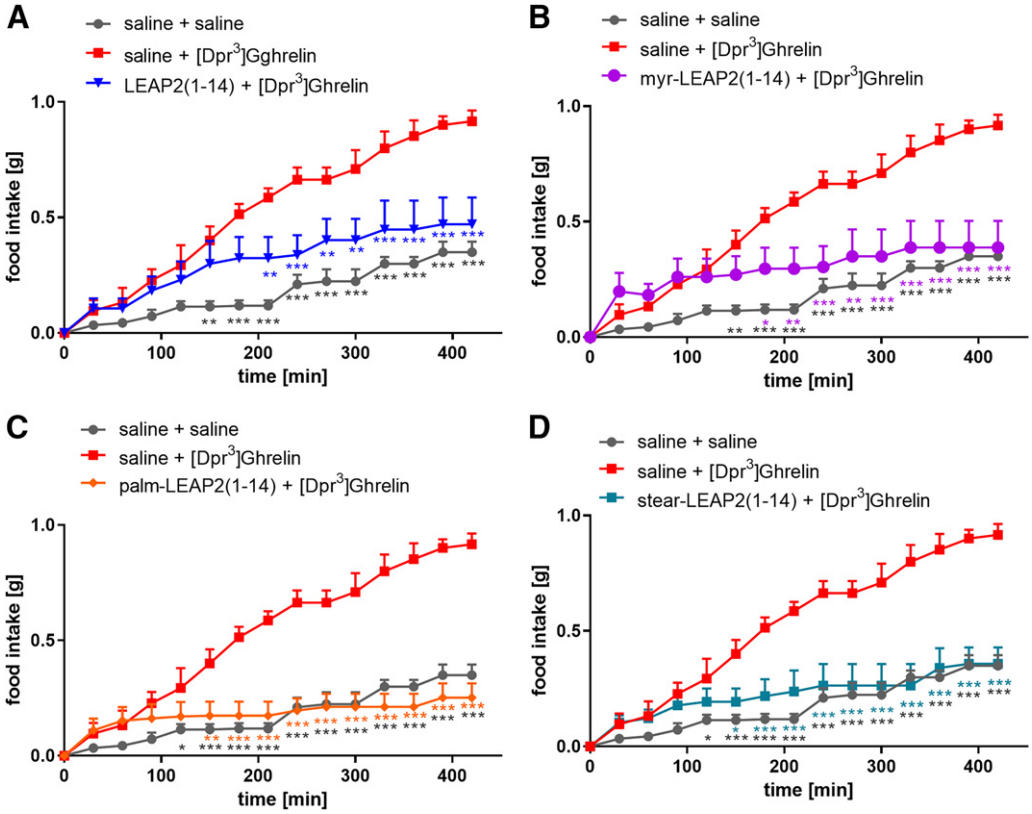

Fig. 4. Effect of LEAP2(1-14) analogs on [Dpr^3]Ghrelin-induced cumulative food intake after s.c. administration to free fed mice. All LEAP2(1-14) analogs were administered s.c. at a dose of 5 mg/kg, 15 minutes after injection, the mice were injected with saline or [Dpr^3]Ghrelin at dose of 1 mg/kg of body weight. The food intake was monitored every 30 minutes for at least 7 hours. Effect of (A) LEAP2(1-14), (B) myr-LEAP2(1-14), (C) palm-LEAP2(1-14), (D) teer-LEAP2(1-14). The data are presented as means ± S.E.M. and were analyzed by 1-way ANOVA followed by Bonfer-roni post hoc test. Significance is *P < 0.1; **P < 0.01; ***P < 0.001, versus saline 1 [Dpr^3]Ghrelin treated group (n 5 5).

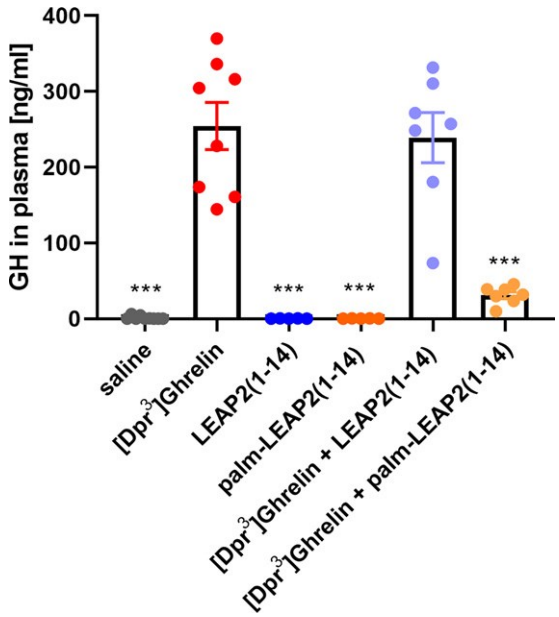

Fig. 5. Effect of LEAP2(1-14) and palm-LEAP2(1-14) on [Dpr^3]Ghrelin-induced GH release in 2-month-old mice. Mice were s.c. injected with 200 ml of saline or LEAP2(1-14) analogs at a dose of 10 mg/kg of body weight (n 5 5–8), and after 15 minutes with saline or [Dpr^3]Ghrelin at dose of 1 mg/kg of body weight. Blood was collected after 15 minutes, and GH was measured in blood plasma using a commercially available ELISA assay kit. Data are presented as means ± S.E.M. and were evaluated by 1-way ANOVA followed by Bonferroni post hoc test. Significance is *P < 0.1; **P < 0.01; ***P < 0.001, versus [Dpr^3]Ghrelin-treated group.

LEAP2 and its N-terminal fragments acted as inverse agonists (M′Kadmi et al., 2019). Moreover, M′Kadmi previously explained that b-arrestin recruitment at GHSR1a was low under basal conditions, which, thus, could lead to misleading results (M′Kadmi et al., 2015). All tested LEAP2-derived compounds decreased GHSR1a constitutive activity with an EC_{50} of 10 ^{8}10^{7} M (Figs. 1 and 2). Lipidized LEAP2(1-14) analogs had similar EC_{50} compared with that of natural LEAP2.

Furthermore, Ge et al. claimed that LEAP2 was a noncompetitive antagonist of GHSR1a (Ge et al., 2018). However, two other studies (M′Kadmi et al., 2019; Wang et al., 2019) showed that LEAP2 acted as a competitive antagonist of GHSR1a and that LEAP2 and ghrelin shared a common ligand-binding pocket on GHSR1a. In the present study, we verified that LEAP2 acts as a competitive antagonist (Fig. 2). Ghrelin's EC_{50} in the GHSR1a antagonist activity assay increased as the LEAP2 concentration increased, and LEAP2 did not change the maximal effect elicited by ghrelin (M′Kadmi et al., 2019). Similar to the inverse agonist assay, LEAP2(1-14) showed reduced antagonist activity compared with natural LEAP2. However, myr-LEAP2(1-14), palm-LEAP2(1-14) and stear-LEAP2(1-14) had even higher antagonist activity than natural LEAP2. Wang et al. explained that the differences across published studies (Ge et al., 2018; M′Kadmi et al., 2019), could be caused by the slow dissociation of LEAP2 from GHSR1a (Wang et al., 2019). LEAP2 preincubated with GHSR1a remains bound to the receptor, thus featuring non-competitive antagonism in certain assays (Wang et al., 2019). In our study, even though LEAP2 was preincubated with GHSR1a, it acted as a competitive antagonist. Non-competitive antagonism and also lack of constitutive activity reported by Ge et al. could be explained by the fact that in our study, incubation of LEAP2(1-14) analogs together with ghrelin was much longer than in Ge et al.'s study, and therefore there was enough time to establish equilibrium between ghrelin and LEAP2(1-14) analogs.

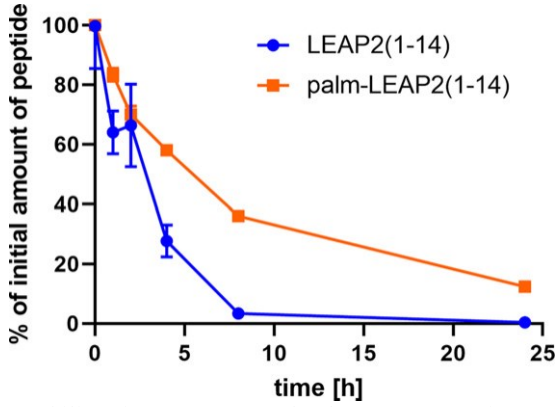

Fig. 6. Stability of LEAP2(1-14) and palm-LEAP2(1-14) in rat plasma monitored by LC-MS. Experiments in all time points were accomplished in triplicate. The data are presented as means ± S.E.M.

To investigate the antagonist properties of LEAP2 analogs in vivo, we focused on two well-established actions of ghrelin, namely, food intake (i) and GH release (ii).

(i) By activating GHSR1a in hypothalamic neurons, an orexigenic neural pathway is stimulated, resulting in increased food intake (Nakazato et al., 2001). Fasting is associated with increased levels of ghrelin; thus, we first tested the ability of LEAP2(1-14) and its lipidized analogs to affect fasting-induced food intake in mice (Fig. 3). We already know that N-terminal LEAP2 analogs decrease food intake in fasted mice similarly to natural LEAP2 (Fernandez et al., 2022; M′Kadmi et al., 2019). Particularly, palm-LEAP2(1-14) had the highest anorexigenic effect. We tested the ability of LEAP2 analogs to suppress the orexigenic effect of exogenously administered stable ghrelin analog [Dpr^3]Ghrelin used in our previous studies in free-fed mice (Maletinska et al., 2012). LEAP2(1-14) attenuated [Dpr^3]Ghrelin-induced food intake to the same extent as described by M′Kadmi (M′Kadmi et al., 2019). More interestingly, palm-LEAP2(1-14) and stear-LEAP2(1-14) fully inhibited [Dpr^3]Ghrelin-induced food intake (Fig. 4), while myr-LEAP2(1-14) was less potent in inhibition. Overall, these data indicate that palmitoylated LEAP2(1-14) suppresses orexigenic ghrelin function similarly to natural LEAP2 in previous studies (Ge et al., 2018) and is the best of all lipidized LEAP2(1-14) analogs. Following these results, we focused on palm-LEAP2(1-14) and nonlipidized LEAP2(1-14) to study GH release and conducted plasmatic stability experiments.

(ii) The activation of GHSR1a by ghrelin in pituitary cells led to robust GH release (Kojima et al., 1999) and natural LEAP2 suppressed ghrelin-induced GH secretion in mice (Ge et al., 2018; Islam et al., 2020). In this study (Fig. 5), we compared the ability of LEAP2(1-14) and its palmitoylated analog to inhibit [Dpr^3]Ghrelin-induced GH secretion. LEAP2(1-14) did not affect [Dpr^3]Ghrelin-induced GH release, while palm-LEAP2(1-14) inhibited such GH release. The

inability of LEAP2(1-14) to inhibit GH release might be caused by its lower stability or bioavailability in organisms compared with that of palm-LEAP2(1-14).

Finally, we tested the stability of LEAP2(1-14) and its palmitoylated analog in rat plasma (Fig. 6). The stability of palm-LEAP2(1-14) was significantly higher than that of LEAP2(1-14). The prolongation of the peptide half-life by lipidization is generally achieved by its increased binding to serum albumin, which carries free fatty acids and multiple other endogenous ligands and drugs in the blood (Kurtzhals et al., 1995). If the peptide is bound to albumin and does not circulate freely in the blood, its circulation time is prolonged (Made et al., 2014).

Taken together, the in vitro and in vivo properties of the N-terminal LEAP2 peptide LEAP2(1-14) and its analogs lipidized with myristic, palmitic, or stearic acid were tested and compared. All peptides exhibited a high binding affinity for GHSR1a-transfected cells and a high ability to inhibit GHSR1a constitutive activity, comparable to natural LEAP2. Palm-LEAP2(1-14) showed high in vivo stability and potent anorexigenic effects, and a single s.c. injection fully inhibited [Dpr^3] Ghrelin-induced food intake and GH release. In conclusion, the novel LEAP2 analog palm-LEAP2(1-14) has great potential for the treatment of obesity. Our future studies will focus on further examining the interplay between LEAP2 and ghrelin in an organism and the potential actions of LEAP2 analogs in the brain.

Acknowledgments

The authors thank Hedvika Vysusilova and Ales Marek (Institute of Organic Chemistry and Biochemistry, Czech Academy of Sciences, Prague, Czech Republic) for the technical assistance and peptide iodination, respectively.

Authorship Contributions

Participated in research design: Zelezna, Kunes, Fehrentz, Maletınska.

Conducted experiments: Hola, Karnosova, Myskova, Maletınska.

Contributed new reagents or analytic tools: Fehrentz, Denoyelle, Cantel, Blechova.

Performed data analysis: Hola, Karnosova, Sykora.

Wrote or contributed to the writing of the manuscript: Hola, Zelezna, Kunes, Denoyelle, Cantel, Sykora, Maletınska.

References

Bednarek MA, Feighner SD, Pong SS, McKee KK, Hreniuk DL, Silva MV, Warren VA, Howard AD, Van Der Ploeg LH, and Heck JV (2000) Structure-function studies on the new growth hormone-releasing peptide, ghrelin: minimal sequence of ghrelin necessary for activation of growth hormone secretagogue receptor 1a. J Med Chem 43:4370–4376.

Cowley MA, Smith RG, Diano S, Tschöp M, Pronchuk N, Grove KL, Strasburger CJ, Bidlingmaier M, Esterman M, Heiman ML et al. (2003) The distribution and mechanism of action of ghrelin in the CNS demonstrates a novel hypothalamic circuit regulating energy homeostasis. Neuron 37:649–661.

Fernandez G, Cabral A, De Francesco PN, Uriarte M, Reynaldo M, Castrogiovanni D, Zubirıa G, Giovambattista A, Cantel S, Denoyelle S et al. (2022) GHSR controls food deprivation-induced activation of CRF neurons of the hypothalamic paraventricular nucleus in a LEAP2-dependent manner. Cell Mol Life Sci 79:277.

Ge X, Yang H, Bednarek MA, Galon-Tilleman H, Chen P, Chen M, Lichtman JS, Wang Y, Dalmas O, Yin Y et al. (2018) LEAP2 Is an Endogenous Antagonist of the Ghrelin Receptor. Cell Metab 27:461–469.e6.

Henriques ST, Tan CC, Craik DJ, and Clark RJ (2010) Structural and functional analysis of human liver-expressed antimicrobial peptide 2. ChemBioChem 11:2148–2157.

Holubova M, Blechova M, Kakonova A, Kunes J, Zelezna B, and Maletınska L (2018) In Vitro and In Vivo Characterization of Novel Stable Peptidic Ghrelin Analogs: Beneficial Effects in the Settings of Lipopolysaccharide-Induced Anorexia in Mice. J Pharmacol Exp Ther 366:422–432.

Cheng Y and Prusoff WH (1973) Relationship between the inhibition constant (K1) and the concentration of inhibitor which causes 50 per cent inhibition (I50) of an enzymatic reaction. Biochem Pharmacol 22:3099–3108.

Islam MN, Mita Y, Maruyama K, Tanida R, Zhang W, Sakoda H, and Nakazato M (2020) Liver-expressed antimicrobial peptide 2 antagonizes the effect of ghrelin in rodents. J Endocrinol 244:13–23.

Karnosova A, Strnadova V, Hola L, Zelezna B, Kunes J, and Maletinska L (2021) Palmitoylation of Prolactin-Releasing Peptide Increased Affinity for and Activation of the GPR10, NPFF-R2 and NPFF-R1 Receptors: In Vitro Study. Int J Mol Sci 22:8904.

Kojima M, Hosoda H, Date Y, Nakazato M, Matsuo H, and Kangawa K (1999) Ghrelin is a growth-hormone-releasing acylated peptide from stomach. Nature 402:656–660.

Krause A, Sillard R, Kleemeier B, Klüver E, Maronde E, Conejo-Garcıa JR, Forssmann WG, Schulz-Knappe P, Nehls MC, Wattler F et al. (2003) Isolation and biochemical characterization of LEAP-2, a novel blood peptide expressed in the liver. Protein Sci 12:143–152.

Kurtzhals P, Havelund S, Jonassen I, Kiehr B, Larsen UD, Ribel U, and Markussen J (1995) Albumin binding of insulins acylated with fatty acids: characterization of the ligand-protein interaction and correlation between binding affinity and timing of the insulin effect in vivo. Biochem J 312:725–731.

Li HZ, Shou LL, Shao XX, Li N, Liu YL, Xu ZG, and Guo ZY (2021) LEAP2 has antagonized the ghrelin receptor GHSR1a since its emergence in ancient fish. Amino Acids 53:939–949.

M'Kadmi C, Cabral A, Barrile F, Giribaldi J, Cantel S, Damian M, Mary S, Denoyelle S, Dutertre S, Peraldi-Roux S et al. (2019) N-Terminal Liver-Expressed Antimicro-bial Peptide 2 (LEAP2) Region Exhibits Inverse Agonist Activity toward the Ghre-lin Receptor. J Med Chem 62:965–973.

M'Kadmi C, Leyris JP, Onfroy L, Gales C, Sauliere A, Gagne D, Damian M, Mary S, Maingot M, Denoyelle S et al. (2015) Agonism, Antagonism, and Inverse Agonism Bias at the Ghrelin Receptor Signaling. J Biol Chem 290:27021–27039.

Made V, Els-Heindl S, and Beck-Sickinger AG (2014) Automated solid-phase peptide synthesis to obtain therapeutic peptides. Beilstein J Org Chem 10:1197–1212.

Maletınska L, Pychova M, Holubova M, Blechova M, Demianova Z, Elbert T, and Zelezna B (2012) Characterization of new stable ghrelin analogs with prolonged orexigenic potency. J Pharmacol Exp Ther 340:781–786.

Mani BK, Puzziferri N, He Z, Rodriguez JA, Osborne-Lawrence S, Metzger NP, Chhina N, Gaylinn B, Thorner MO, Thomas EL et al. (2019) LEAP2 changes with body mass and food intake in humans and mice. J Clin Invest 129:3909–3923.

Motulsky H and Neubig R (2002) Analyzing radioligand binding data. Curr Protoc Neurosci 19:7.5.1–7.5.55.

Nakazato M, Murakami N, Date Y, Kojima M, Matsuo H, Kangawa K, and Matsukura S (2001) A role for ghrelin in the central regulation of feeding. Nature 409:194–198.

Sato T, Ida T, Nakamura Y, Shiimura Y, Kangawa K, and Kojima M (2014) Physiological roles of ghrelin on obesity. Obes Res Clin Pract 8:e405–e413.

Shankar K, Metzger NP, Singh O, Mani BK, Osborne-Lawrence S, Varshney S, Gupta D, Ogden SB, Takemi S, Richard CP et al. (2021) LEAP2 deletion in mice enhances ghrelin's actions as an orexigen and growth hormone secretagogue. Mol Metab 53:101327.

Wang JH, Li HZ, Shao XX, Nie WH, Liu YL, Xu ZG, and Guo ZY (2019) Identifying the binding mechanism of LEAP2 to receptor GHSR1a. FEBS J 286:1332–1345.

Zhang L and Bulaj G (2012) Converting peptides into drug leads by lipidation. Curr Med Chem 19:1602–1618.

Zigman JM, Jones JE, Lee CE, Saper CB, and Elmquist JK (2006) Expression of ghrelin receptor mRNA in the rat and the mouse brain. J Comp Neurol 494:528–548.

Address correspondence to: Dr. Lenka Maletınska, Institute of Organic Chemistry and Biochemistry, Flemingovo nam. 2, Prague 6, Czech Republic, 16610. E-mail: maletin@uochb.cas.cz

High-fat diet induces resistance to ghrelin and LEAP2 peptide analogs in mice

HF diet induces ghrelin and LEAP2 resistance

Lucie Holá[1,3], Theodora Tureckiová[1], Jaroslav Kuneš[1,2], Blanka Železná[1], Lenka Maletínská[1*]

[1]*Institute of Organic Chemistry and Biochemistry, Czech Academy of Sciences, Prague, Czech Republic*

[2]*Institute of Physiology, Czech Academy of Sciences, Prague, Czech Republic*

[3]*First Faculty of Medicine, Charles University, Prague, Czech Republic*

*Correspondence:
Lenka Maletínská
Institute of Organic Chemistry and Biochemistry
Czech Academy of Sciences
Flemingovo náměstí 542/2
166 10 Praha 6
Czech Republic
maletin@uochb.cas.cz
Tel.: +420 220 183567

Key words:

Palm-LEAP2(1-14), LEAP2, [Dpr[3]]Ghrelin, ghrelin, ghrelin resistance, LEAP2 resistance, diet-induced obesity, high-fat diet, mice

Word count: 5061

Abstract

Recent data suggest that the orexigenic peptide ghrelin and liver-expressed antimicrobial peptide 2 (LEAP2) have opposing effects on food intake regulation. Although circulating ghrelin is decreased in obesity, peripheral ghrelin administration does not induce food intake in obese mice. There is limited information available on ghrelin resistance in relation to LEAP2. In this study, we investigate the interplay between ghrelin and LEAP2 in obesity induced by a high-fat (HF) diet in mice.

First, we examined the progression of obesity and intolerance to glucose together with plasma levels of active and total ghrelin, leptin, as well as liver *LEAP2* mRNA expression at different time points of HF diet feeding. In addition, we investigated whether the switch from a HF diet to a standard diet would affect plasma ghrelin and LEAP2 production. Second, we assessed sensitivity to the stable ghrelin analogue [Dpr^3]Ghrelin or our novel LEAP2 analogue palm-LEAP2(1-14) during the progression of HF diet-induced obesity and after the switch for standard diet. Food intake was monitored after acute subcutaneous administration of each substance.

We found that HF diet feeding decreased both active and total plasma ghrelin and increased liver *LEAP2* mRNA expression along with intolerance to glucose and the switch from a HF diet to a standard diet normalised liver *LEAP2* mRNA expression as well as plasma level of active ghrelin, but not of total ghrelin. Additionally, our study demonstrates that a HF diet causes resistance to [Dpr^3]Ghrelin, reversible by switch to St diet, followed by resistance to palm-LEAP2(1-14). Further studies are needed in order to determine the long-term effects of LEAP2 analogues on obesity-related ghrelin resistance.

Introduction

Obesity is strongly associated with an increased risk of health problems such as type 2 diabetes, cardiovascular diseases, gastrointestinal disorders, and other comorbidities (Fruh 2017). Given that obesity is frequently caused by hyperphagia, a comprehensive understanding of food intake regulation is required in order to treat this chronic disease.

Ghrelin is the only known peripheral peptide that increases food intake and acts directly in the hypothalamus (Andrews 2011; Kojima, et al. 1999), stimulating secretion of the orexigenic neuropeptides agouti-related protein (AgRP) and neuropeptide Y (NPY) in AgRP/NPY neurons (Cowley, et al. 2003). Ghrelin entry to the brain is nowadays envisioned through the choroid plexus and the hypothalamus tanycytes, which form the blood-cerebrospinal fluid (CSF) barrier (Uriarte, et al. 2021).

Ghrelin is octanoylated on the Ser^3 of the 28 amino acid peptide chain, which makes ghrelin biologically active (Kojima *et al*. 1999). Ghrelin receptor, growth hormone secretagogue receptor (GHSR), has the constitutive activity which is almost 50% of activity reached by ghrelin, which is important for constitutive stimulation of basal food intake (Holst and Schwartz 2004; Holst, et al. 2003). Liver-expressed antimicrobial peptide 2 (LEAP2) inhibits the high constitutive activity of GHSR as well as ghrelin-induced actions (Ge, et al. 2018).

LEAP2 is a 40-amino acid-long peptide expressed mainly in the liver and jejunum (Ge et al. 2018). LEAP2 acts as an endogenous antagonist as well as an inverse agonist of GHSR (Hola, et al. 2022; M'Kadmi, et al. 2019). Subcutaneously (SC) administered LEAP2 alone does not affect food intake in *ad libitum*-fed mice (M'Kadmi *et al*. 2019), but inhibits the ghrelin-induced release of growth hormone (GH) (Ge et al. 2018). Mice deficient in LEAP2 display increased sensitivity to the acute effects of ghrelin on food intake and GH secretion (Shankar, et al. 2021). In healthy men, LEAP2 attenuates food intake and postprandial glucose excursions (Hagemann, et al. 2022).

Blood plasma levels of ghrelin and LEAP2 exhibit opposite trends during fasting and feeding/refeeding in both humans and mice. Plasma LEAP2 rises with body mass, body fat, blood glucose, serum triglycerides (TAG), and intrahepatocellular lipid content in humans and mice (Holm, et al. 2022; Mani, et al. 2019). In mice, liver *LEAP2* mRNA expression is selectively downregulated at fasting by ketone bodies and is upregulated by HF diet feeding (Holm et al. 2022). *LEAP2* mRNA expression in mice even selectively correlated with stores of hepatic glycogen and jejunal lipids (Gradel, et al. 2023). LEAP2 to ghrelin ratio is an

indicator of obesity (Mani *et al*. 2019). It also increases during pregnancy in humans and rats, which may be associated with pregnancy weight gain (Garces, et al. 2022).

Obesity lowers ghrelin secretion and its availability in the brain (Banks, et al. 2008). Fasting in mice with diet-induced obesity (DIO) does not increase ghrelin levels (Perreault, et al. 2004) and plasma ghrelin does not drop after the meal in obese humans (English, et al. 2002). Moreover, ghrelin administered peripherally does not acutely induce food intake in diet-induced obese (DIO) mice (Perreault *et al*. 2004) or agouti mice (Martin, et al. 2004), and has no effect at chronic administration in DIO mice (Gardiner, et al. 2010). The orexigenic effect of ghrelin in obesity is lowered via inefficient activation of AgRP/NPY neurons (Briggs, et al. 2010). In mice, 12 weeks of a HF diet has been shown to decrease not only plasma ghrelin and *GHRL* mRNA expression in the stomach, but also *GHSR* mRNA expression in the hypothalamus, indicating suppression of the neuroendocrine ghrelin axis. Neither peripherally nor centrally administered ghrelin induces food intake, *NPY* and *AgRP* mRNA expression, and NPY and AgRP peptide secretion in DIO mice. However, intracerebroventricular administration of NPY stimulates food intake in both lean and DIO mice, indicating that downstream ghrelin signalling is not affected by obesity (Briggs and Andrews 2011).

Ghrelin resistance is reversible by a low-calorie diet causing weight loss in obese individuals. However, an increase in ghrelin blood level indicating restoration of ghrelin sensitivity promotes rebound weight gain (Briggs, et al. 2013). There is still no knowledge if resistance to ghrelin is associated with resistance to LEAP2.

In this study, we hypothesized that switching from a HF diet to a St diet could not only improve metabolic and morphometric parameters, but also restore sensitivity to ghrelin and LEAP2 in mice. In the first experiment, the time course of HF diet-induced obesity related parameters were linked to active and total plasma ghrelin and liver *LEAP2* mRNA expression. As obesity is associated with the development of metabolic diseases connected with chronic low-grade inflammation and increased risk of liver steatosis and oxidative stress in the liver, CRP in blood, and peroxides and lipid droplets in the liver were observed in this sense. In the second experiment, sensitivity to ghrelin and LEAP2 was evaluated by monitoring food intake after acute SC administration of either ghrelin analogue [Dpr^3]Ghrelin (Bednarek, et al. 2000; Maletinska, et al. 2012) or our recently published palmitoylated LEAP2 analogue palm-LEAP2(1-14) (Hola *et al*. 2022) at particular times of feeding HF diet and after the switch to St diet. [Dpr^3]Ghrelin and palm-LEAP2(1-14) are stable analogs of the natural peptides with

affinity to and activation of GHSR similar to natural peptides. Besides, palm-LEAP2(1-14) attenuated food intake after acute SC administration in St diet fed mice (Hola *et al*. 2022).

Materials and methods

Peptides

[Dpr^3]Ghrelin (GS Dpr (N-octanoyl)FLSPEHQKAQQRKESKKPPAKLQPR) was synthesised and purified as previously described (Holubova, et al. 2018). Lipidization with the corresponding fatty acid was performed on a fully protected peptide on resin as the last step (Maletinska *et al*. 2012). Synthesis of palm-LEAP2(1-14) (Nle-TPFWRGVSLRPIG-βAla-Lys(Palm)-NH_2) was assembled using solid-phase peptide synthesis (Hola *et al*. 2022). Peptide purification and identification were carried out using analytical HPLC and the Q-Tof micro® MS technique (Waters, Milford, MA, USA). The purity of the synthesised peptides was greater than 95% (Dpr – diaminopropionic acid, palm – palmitoyl).

Experimental animals

All experiments followed ethical guidelines for animal experiments, met the regulations stipulated in Act No. 246/1992 of the Czech National Council, and were approved by the Committee for Experiments with Laboratory Animals of the Academy of Sciences of the Czech Republic (decision no. 96/2020 issued 10/12/2020).

Male C57Bl/6N mice (Charles River, Sulzfeld, Germany) were housed at a temperature of 23°C with a daily cycle of 12-h light- and dark (light on at 6:00 AM). The mice were given *ad libitum* water and fed either a HF diet containing 13%, 60%, and 27% of calories from protein, fat, and carbohydrate, respectively (Maletinska, et al. 2015), or a standard chow diet (St) (ssniff® R/M-H; cat. no. V1534; Spezialdiäten GmbH, Soest, Germany) containing 33%, 9%, and 58% of calories from protein, fat, and carbohydrate, respectively.

Experiment 1: Effect of HF diet on mice metabolic parameters – experimental design

An overview of the study design is described in Figure 1. At the age of 8 weeks, mice were divided into 12 groups (*n*=8), housed in groups of four animals per cage and fed either HF or St diet. After 8 weeks on HF diet, group 12 was switched from HF to St diet. Body weights were monitored weekly. Mice were sacrificed at different time points according to Figure 1. One week before sacrificing, an oral glucose tolerance test (OGTT) was performed after 6 h of fasting in each group. Free-fed mice were sacrificed by decapitation and trunk blood was then collected; plasma was separated and stored at -20°C. Plasma pre-treated with Pefabloc® (Carl Roth, Karlsruhe, Germany) and acidified using HCl was used for ELISA detection of ghrelin according to the manufacturer's protocol.

Epididymal white adipose tissue (eWAT), the liver, and the hypothalamus were dissected and weighed. Tissue samples were frozen in liquid nitrogen and then stored at -80°C. Morphometric and biochemical analyses, liver histology, and mRNA analysis of tissues were subsequently performed.

Oral glucose tolerance test

An OGTT was performed after 6 h of fasting one week before sacrificing in each experimental group. At time point 0 (09:00 h), blood was collected from the tail vein to measure insulin, cholesterol, and TAG. The animals were then gavaged with glucose at a dose of 2 g/kg body weight. Concentrations of blood glucose were determined in whole blood at 15, 30, 60, 120, and 180 min after glucose gavage using a glucometer (LifeScan, Inc., Milpitas, CA, USA).

Experiment 2: Effect of HF diet on development of ghrelin resistance – experimental design

The study design is shown in Figure 2. At the age of 8 weeks (week 0 of the experiment), mice were divided into 5 groups (n=8), and housed in separate cages. Two groups were fed a St diet and 3 groups a HF diet. Since week 8, all mice were fed St diet. Body weight was monitored weekly. The effect of SC administered [Dpr^3]Ghrelin and palm-LEAP2(1-14) on feeding behaviour was tested at weeks 0, 2, 4, 8, 10, and 12 in free-fed mice.

On the day of the food intake experiment, at 8:00 AM, the mice were SC injected with 150 µl of saline, palm-LEAP2(1-14) (dissolved in saline) at a dose of 5 mg/kg of body weight, or [Dpr^3]Ghrelin (dissolved in saline) at a dose of 1 mg/kg of body weight in order to achieve a significant change in food intake. Dose of [Dpr^3]Ghrelin was chosen based on the ED_{50} determined in our previous study (Maletinska et al. 2012). Dose of palm-LEAP2(1-14) was chosen based on acute food intake experiment after SC administration of palm-LEAP2(1-14) to lean animals (Hola et al. 2022). Fifteen minutes after the injection, the mice were given pre-weighed food pellets. Food intake was monitored every 30 min for at least 6 hours. The animals had free access to water during the experiment.

Determination of biochemical parameters in plasma

Fasted plasma was used to detect insulin on the Sensitive Rat Insulin RIA kit (MilliporeSigma, Burlington, MA, USA), and TAG and cholesterol using colorimetric assays (Erba Lachema, Brno, Czech Republic). Free-fed plasma was used to measure leptin, total ghrelin, active ghrelin (Millipore, St. Charles, MI, USA), and C-reactive protein (CRP) with mouse ELISA kits

(Thermo Fisher Scientific, Waltham, MA USA). All measurements were carried out according to the manufacturers' instructions.

Determination of mRNA expression

Samples of the hypothalamus and liver for mRNA determination were processed as previously described (Maletinska *et al*. 2015). The mRNA expressions of *AgRP*, *CART*, *GHSR*, *NPY*, and *POMC* in the hypothalamus, and *LEAP2* in the liver were determined using the ABI PRISM® 7500 instrument (Applied Biosystems, Foster City, CA, USA). Data were normalised to the expression of the reference genes beta-2-microglobulin (*B2m*) or glyceraldehyde3-phosphate dehydrogenase (*GAPDH*).

Oxidative stress

Liver samples were homogenised in ice-cold lysis buffer (62.5 mM Tris-HCl buffer with pH 6.8, 1% deoxycholate, 1% Triton X-100, 50mM NaF, 1mM Na_3VO_4 and complete protease inhibitor (Roche Applied Science, Mannheim, Germany)) using the Bullet Blender® tissue homogeniser (Next Advance, Inc., Averill Park, NY, USA). Lysates were sonicated for 1 min and centrifuged for 15 min at 13,500 × g at 4°C. Protein concentration was measured using the Pierce™ BCA Protein Assay Kit (Thermo Fisher Scientific, Inc., Waltham, MA, USA). Lysates were diluted to a final concentration of 10 µg/µl in lysis buffer. The Amplex™ Red Hydrogen Peroxide/Peroxidase Assay Kit (Thermo Fisher Scientific, Waltham, MA USA) was used to measure H_2O_2 concentration. All measurements were carried out according to the manufacturers' instructions.

Haematoxylin and eosin staining of the liver

The right lobe of each liver was carefully removed, fixed with 4% paraformaldehyde (PFA), and embedded in paraffin. Sections were cut with the Leica ASP200S Tissue Processor (Leica Biosystems, Buffalo Grove, IL, USA) at a thickness of 5 µm (n=3) as described previously (Prazienkova, et al. 2021). Samples were covered with DPX mounting medium (MilliporeSigma, Burlington, MA, United States). Photomicrographs of liver sections stained with haematoxylin and eosin were taken using the Olympus IX83 inverted microscope (Olympus Europa SE & Co. KG, Hamburg, Germany).

Statistical analysis

Data are presented as the mean ± SEM as analysed with GraphPad 8 Software (San Diego, CA, USA). Data were evaluated by two-way ANOVA with Bonferroni's post hoc test or one-way ANOVA with Tukey's test or multiple *t*-test with Bonferroni-Dunn's method for multiple

comparisons as described in the figure legends. Outliers were identified by Grubbs test. $P<0.05$ was considered statistically significant.

Results

Experiment 1

Switching from a HF diet to a St diet decreases body weight, eWAT weight and leptin in plasma

Mice were fed a HF diet from the 8th week of age (week 0 of the experiment). Body weight was monitored weekly over the following 15 weeks. Consumption of a HF diet caused higher body weight as well as eWAT weight and leptin level (Figure 3) compared to a St diet. These differences became significant as early as after 3 weeks of HF diet feeding. In mice that were switched to a St diet after 9 weeks on a HF diet (group 12), we observed a significant reduction in body weight as early as after 2 weeks St diet feeding and their final body weight was similar to that of control mice fed exclusively a St diet (Figure 3a). Their eWAT weight (Figure 3b) and plasma leptin (Figure 3c) followed a similar trend.

Switching from a HF diet to a St diet normalises *LEAP2* mRNA expression in liver as well as active plasma ghrelin

The level of *LEAP2* mRNA in the liver (Figure 4 C) increased with higher body weight. In the group fed a 9-week HF diet followed by a 6-week St diet, *LEAP2* mRNA in the liver proved similar to the group fed exclusively a St diet.

Levels of active (Figure 4 A) and total ghrelin (Figure 4 B) in plasma exhibited opposite trends to liver *LEAP2* mRNA expression. Mice fed a HF diet had lower active and total ghrelin compared to those fed a St diet. Switching from a HF to a St diet caused an increase in active ghrelin levels to the levels in mice fed exclusively a St diet. Interestingly, the total ghrelin level in mice fed a 9-week HF diet followed by a 6-week St diet was similar to the level in those fed exclusively a HF diet.

Switching from a HF diet to a St diet improves glucose tolerance

Glucose tolerance was assessed by the OGTT after glucose gavage. Three weeks of HF diet consumption increased glucose levels significantly over the course of oral glucose tolerance testing (Figure 5 A-F). In mice switched from a 9-week HF diet to a 6-week St diet, glucose levels were similar to mice fed exclusively a St diet over the course of oral glucose tolerance testing.

Fasted glucose plasma levels (Figure 5 G) and OGTT area under the curve (AUC) values (Figure 5 H) confirmed results from the courses of OGTT curves.

Fasted plasma insulin levels (Figure 5 I) were significantly higher in mice fed a HF diet for 9 weeks compared to mice fed a St diet. Plasma insulin was similar in mice fed a 9-week HF diet followed by a 6-week St diet and mice fed exclusively St diet.

Switching from a HF diet to a St diet lowers cholesterol and CRP plasma levels, liver steatosis, and oxidative stress in the liver

Fifteen weeks on a HF diet significantly increased the level of cholesterol in plasma (Figure 6 A) and switching from a HF diet to a St diet decreased cholesterol as well as CRP levels (Figure 6 C) to levels observed in mice fed exclusively St diet. Liver weight (Figure 6 D) tended toward a non-significant increase in the group of mice fed a 15-week HF diet compared to other groups. Oxidative stress expressed as H_2O_2 concentration (Figure 6 E) was significantly increased in groups fed a HF diet for 9 and 15 weeks and switching from a HF diet to a St diet tended to decrease it. 15 weeks of HF diet feeding induced reversible steatosis in the liver (Figure 6 F). Switching from a HF diet to a St diet decreased the amount of visible lipid droplets in the liver to those observed in mice fed a 15-week St diet.

Switching from a HF diet to a St diet does not affect hypothalamic mRNA expression of neuropeptides and *GHSR*

Hypothalamic mRNA expression of selected genes was compared between groups 6, 11, and 12 (Figure 7). *POMC* and *CART* mRNA expression in the hypothalamus tended toward a non-significant increase in the group of mice fed a 15-week HF diet compared to other groups. *AgRP*, *GHSR*, and *NPY* mRNA levels were not affected by the diet in free fed mice.

Experiment 2

HF diet attenuates food intake response to [Dpr^3]Ghrelin and palm-LEAP2(1-14)

The effect of acute SC administration of [Dpr^3]Ghrelin or palm-LEAP2(1-14) on feeding in mice fed a HF diet is shown in Figure 8 and 9. Mice fed a St diet were used as controls. The results in Figure 8 are expressed as grams of food consumed per 270 minutes, because we observed that after 270 minutes, a steady state of food intake occurs. The results in Figure 9 are expressed as grams of food consumed during the entire experiment (360 minutes). As early as two weeks after HF diet feeding, mice had lost sensitivity to acutely administered [Dpr^3]Ghrelin regarding to increase in food intake, while food intake had fallen below the basal level of food intake due to acute palm-LEAP2(1-14) administration. Resistance to palm-LEAP2(1-14) (i.e. the ability of palm-LEAP2(1-14) to decrease the basal level of food intake developed after 4

weeks of HF diet feeding. Four weeks after the switch of HF diet to a St diet, sensitivity to [Dpr^3]Ghrelin had been restored.

Discussion

Due to the key role ghrelin plays in regulating food intake and energy expenditure, the pharmaceutical industry has been developing anti-obesity drugs that target the ghrelin receptor GHSR, (Schalla and Stengel 2019). As ghrelin receptor is a constitutively active G-protein-coupled receptor (Holst, et al. 2004), attention has turned to inverse agonists that are able to reduce the high constitutive activity of GHSR. However, no drug that reduces body weight through GHSR has yet been developed. This may be due to ghrelin resistance, which reduces sensitivity to ghrelin in obese individuals even though their circulating ghrelin is lower than in lean individuals. Switching from a HF diet to a St diet enhances both ghrelin level and sensitivity to ghrelin and normalizes metabolic parameters (Briggs *et al*. 2013), but whether LEAP2 is also affected remains inconclusive. The plasma level of LEAP2, which is both an endogenous inverse agonist and an antagonist of GHSR, increases during obesity. However, it is not clear whether obesity affects sensitivity to LEAP2 or whether obesity-induced resistance to ghrelin is accompanied by resistance to LEAP2.

Previous studies have shown that plasma ghrelin levels are reduced in obesity (Cummings, et al. 2001; Tschop, et al. 2001). Three weeks of HF diet feeding decreased the levels of both active ghrelin and total ghrelin in Experiment 1, which is consistent with the work of Briggs and colleagues (Briggs, et al. 2014). They demonstrated that switching to a control diet after 12 weeks of HF diet feeding increased levels of active ghrelin, but did not lead to a re-increase in total ghrelin levels (Briggs *et al*. 2013). Nonetheless, we consider an increase in active ghrelin much more important for ghrelin sensitivity than an increase in total ghrelin.

While the plasma level of LEAP2 is increased in obese mice and humans (Andrews 2019), it is decreased during diet-induced weight loss (Mani *et al*. 2019). Even though higher liver mRNA expression was reported in mice with HF diet induced obesity (Holm et al. 2022), experiment 1 is the first to compare a time course of *LEAP2* mRNA expression in the livers of mice fed a HF diet, a St diet, or a diet that alternates between the two. After 3 weeks of HF diet feeding, we observed a non-significant increase in liver *LEAP2* mRNA, which became significant after 9 weeks of HF diet feeding. Switching from a HF diet to a St diet completely restored liver *LEAP2* mRNA expression to the level observed in mice exclusively fed a St diet. Here it is proper to mention two limitations of this study. The first is that we did not determine *LEAP2* mRNA expression in jejunum, another significant LEAP2 producer. We rather simplistically assumed that the liver LEAP2 production in mouse is the biggest one similarly as in rat (Islam,

et al. 2020). The second is that due to technical problems with LEAP2 ELISA kits and limited volume of plasma we were not able to determine plasma LEAP2.

In Experiment 1, we observed significantly increased glucose excursion at OGTT in mice fed a HF diet after only 3 weeks that were restored after switching to a St diet. Similarly, Reynolds and colleagues showed that 6 weeks of HF diet feeding led to glucose intolerance in mice, but after switching to a St diet, glucose tolerance was restored (Reynolds, et al. 2015).The time course of increase in body weight owing to the exclusive HF diet feeding was mirrored by increase in plasma leptin and cholesterol level, intolerance to glucose and also LEAP2 liver production and decrease in active ghrelin level. Analogously, increase in active ghrelin and decrease in *LEAP2* mRNA expression was accompanied by a normalized body weight, plasma cholesterol level and tolerance to glucose after the switch to St diet.

Low levels of active ghrelin in plasma have been demonstrated in individuals with non-alcoholic steatohepatitis (Sajjad, et al. 2005; Yalniz, et al. 2006). On the other hand, CRP levels were found correlated with LEAP2 plasma level (Francisco, et al. 2020). Similarly, obesity related chronic low-level inflammation is characterised by increased circulating CRP and permanently increased oxidative stress (Brooks and Maklakov 2010; Monteiro and Azevedo 2010). A negative correlation between ghrelin and CRP levels in plasma was proved (Peracchi, et al. 2006; Riedl, et al. 2007). Decreased plasma ghrelin correlates not only with increased immunoglobulin production, often observed in patients with chronic liver disease (Okamatsu, et al. 2009), but also with liver inflammation (Machado, et al. 2012).

Weight loss then could attenuate the low-level inflammation as it was seen in Experiment 1. An increase in active ghrelin and a decrease in LEAP2 liver production after the switch from HF to St diet was accompanied with a decrease in plasma CRP, and liver oxidative stress and steatosis. Clearly visible lipid droplets in the livers of mice fed a HF diet disappeared after switching to a St diet. Then LEAP2/ghrelin ration could become a measure of low-grade obesity related systemic and liver inflammation.

In our study, mRNA expression of neuropeptides did not differ between the St diet-fed group and the HF diet-fed group. Briggs and colleagues proved that hypothalamic *AgRP* and *NPY* expression in free-fed mice is the same in both HF- and control-fed groups. However, in fasted mice, mRNA expression of *AgRP* and *NPY* was higher in their control diet-fed group than in their HF diet-fed group (Briggs, et al. 2011). In agreement with Kohsaka and colleagues, mRNA

encoding *POMC* and *CART* tended to increase under diet-induced obesity conditions in our study (Kohsaka, et al. 2007).

Previous studies have indicated that both peripheral and central administration of ghrelin are not adept at inducing food intake in HF diet-fed mice (Briggs et al. 2010; Gardiner et al. 2010; Perreault et al. 2004). It has also been suggested that ghrelin resistance develops as early as after 3-4 weeks of HF diet feeding (Briggs et al. 2014; Naznin, et al. 2015) and that diet-induced weight loss restores ghrelin sensitivity (Briggs *et al*. 2013). In our previous study (Hola *et al*. 2022), we proved that acute SC administration of the LEAP2 analogue palm-LEAP2(1-14) lowered food intake in lean mice. In Experiment 2, we show for the first time that a HF diet induces [Dpr^3]Ghrelin resistance in mice as early as after 2 weeks on a HF diet, while palm-LEAP2(1-14) resistance develops after 4 weeks on a HF diet. Switching from a HF diet to a St diet restored [Dpr^3]Ghrelin sensitivity after 4 weeks. However, palm-LEAP2(1-14) sensitivity was not fully restored. Difference between [Dpr^3]Ghrelin-induced food intake and the control group was much higher than the reduction of food intake after palm-LEAP2(1-14) administration. Therefore, statistical evaluation might not reveal a significant difference in the latter case.

In conclusion, this study offers new insights into the interplay between ghrelin and LEAP2 in HF diet-induced obesity. Our data demonstrate that switching from a HF diet to a St diet restores *LEAP2* liver mRNA expression as well as plasma levels of active ghrelin to values in mice exclusively fed a St diet. Simultaneously, increased body weight due to HF diet feeding mirrored by enhanced leptin level, intolerance to glucose and liver steatosis were lowered by the switch to St diet. We also show that a HF diet induces not only reversible ghrelin resistance but also palm-LEAP2(1-14) resistance. Further studies are needed in order to determine the long-term effects of LEAP2 analogues on obesity-related ghrelin resistance

Declaration of interest

There is no conflict of interest that could be perceived as prejudicing the impartiality of the research reported.

Funding

This work was supported by the Czech Science Foundation (22-11155S) and the Czech Academy of Sciences (RVO:61388963, RVO:67985823).

Acknowledgements

We would like to thank Hedvika Vysušilová and Martina Kojecká (Institute of Organic Chemistry and Biochemistry, Czech Academy of Sciences, Prague, Czech Republic) for their technical assistance, Miloslava Čechová (Institute for Clinical and Experimental Medicine, Prague, Czech Republic) for mRNA analysis, and Miroslava Blechová (Institute of Organic Chemistry and Biochemistry, Czech Academy of Sciences, Prague, Czech Republic) for peptide synthesis.

References

Andrews ZB 2011 Central mechanisms involved in the orexigenic actions of ghrelin. *Peptides* **32** 2248-2255.

Andrews ZB 2019 The next big LEAP2 understanding ghrelin function. *J Clin Invest* **129** 3542-3544.

Banks WA, Burney BO & Robinson SM 2008 Effects of triglycerides, obesity, and starvation on ghrelin transport across the blood-brain barrier. *Peptides* **29** 2061-2065.

Bednarek MA, Feighner SD, Pong SS, McKee KK, Hreniuk DL, Silva MV, Warren VA, Howard AD, Van Der Ploeg LH & Heck JV 2000 Structure-function studies on the new growth hormone-releasing peptide, ghrelin: minimal sequence of ghrelin necessary for activation of growth hormone secretagogue receptor 1a. *J Med Chem* **43** 4370-4376.

Briggs DI & Andrews ZB 2011 Metabolic status regulates ghrelin function on energy homeostasis. *Neuroendocrinology* **93** 48-57.

Briggs DI, Lemus MB, Kua E & Andrews ZB 2011 Diet-induced obesity attenuates fasting-induced hyperphagia. *J Neuroendocrinol* **23** 620-626.

Briggs DI, Enriori PJ, Lemus MB, Cowley MA & Andrews ZB 2010 Diet-induced obesity causes ghrelin resistance in arcuate NPY/AgRP neurons. *Endocrinology* **151** 4745-4755.

Briggs DI, Lockie SH, Wu Q, Lemus MB, Stark R & Andrews ZB 2013 Calorie-restricted weight loss reverses high-fat diet-induced ghrelin resistance, which contributes to rebound weight gain in a ghrelin-dependent manner. *Endocrinology* **154** 709-717.

Briggs DI, Lockie SH, Benzler J, Wu Q, Stark R, Reichenbach A, Hoy AJ, Lemus MB, Coleman HA, Parkington HC, et al. 2014 Evidence that diet-induced hyperleptinemia, but not hypothalamic gliosis, causes ghrelin resistance in NPY/AgRP neurons of male mice. *Endocrinology* **155** 2411-2422.

Brooks R & Maklakov A 2010 Sex differences in obesity associated with total fertility rate. *PLoS One* **5** e10587.

Cowley MA, Smith RG, Diano S, Tschop M, Pronchuk N, Grove KL, Strasburger CJ, Bidlingmaier M, Esterman M, Heiman ML, et al. 2003 The distribution and mechanism of action of ghrelin in the CNS demonstrates a novel hypothalamic circuit regulating energy homeostasis. *Neuron* **37** 649-661.

Cummings DE, Purnell JQ, Frayo RS, Ma MK, Dellinger EP & Weigle DS 2001 Plasma ghrelin levels are markedly decreased after gastric bypass surgery in humans. *Obesity Research* **9** 73s-73s.

English PJ, Ghatei MA, Malik IA, Bloom SR & Wilding JP 2002 Food fails to suppress ghrelin levels in obese humans. *J Clin Endocrinol Metab* **87** 2984.

Francisco V, Tovar S, Conde J, Pino J, Mera A, Lago F, Gonzalez-Gay MA, Dieguez C & Gualillo O 2020 Levels of the Novel Endogenous Antagonist of Ghrelin Receptor, Liver-Enriched Antimicrobial Peptide-2, in Patients with Rheumatoid Arthritis. *Nutrients* **12**.

Fruh SM 2017 Obesity: Risk factors, complications, and strategies for sustainable long-term weight management. *J Am Assoc Nurse Pract* **29** S3-S14.

Garces MF, Buell-Acosta JD, Angel-Muller E, Parada-Banos AJ, Acosta-Alvarez J, Saavedra-Lopez HF, Franco-Vega R, Maldonado-Acosta LM, Escobar-Cordoba F, Vasquez-Romero K, et al. 2022 Study of the Ghrelin/LEAP-2 Ratio in Humans and Rats during Different Phases of Pregnancy. *International Journal of Molecular Sciences* **23**.

Gardiner JV, Campbell D, Patterson M, Kent A, Ghatei MA, Bloom SR & Bewick GA 2010 The hyperphagic effect of ghrelin is inhibited in mice by a diet high in fat. *Gastroenterology* **138** 2468-2476, 2476 e2461.

Ge X, Yang H, Bednarek MA, Galon-Tilleman H, Chen P, Chen M, Lichtman JS, Wang Y, Dalmas O, Yin Y, et al. 2018 LEAP2 Is an Endogenous Antagonist of the Ghrelin Receptor. *Cell Metab* **27** 461-469 e466.

Gradel AKJ, Holm SK, Byberg S, Merkestein M, Hogendorf WFJ, Lund ML, Buijink JA, Damgaard J, Lykkesfeldt J & Holst B 2023 The dietary regulation of LEAP2 depends on meal composition in mice. *FASEB J* **37** e22923.

Hagemann CA, Jensen MS, Holm S, Gasbjerg LS, Byberg S, Skov-Jeppesen K, Hartmann B, Holst JJ, Dela F, Vilsboll T, et al. 2022 LEAP2 reduces postprandial glucose excursions and ad libitum food intake in healthy men. *Cell Rep Med* **3** 100582.

Hola L, Zelezna B, Karnosova A, Kunes J, Fehrentz JA, Denoyelle S, Cantel S, Blechova M, Sykora D, Myskova A, et al. 2022 A Novel Truncated Liver Enriched Antimicrobial Peptide-2 Palmitoylated at its N-Terminal Antagonizes Effects of Ghrelin. *J Pharmacol Exp Ther* **383** 129-136.

Holm S, Husted AS, Skov LJ, Morville TH, Hagemann CA, Jorsal T, Dall M, Jakobsen A, Klein AB, Treebak JT, et al. 2022 Beta-Hydroxybutyrate Suppresses Hepatic Production of the Ghrelin Receptor Antagonist LEAP2. *Endocrinology* **163**.

Holst B & Schwartz TW 2004 Constitutive ghrelin receptor activity as a signaling set-point in appetite regulation. *Trends Pharmacol Sci* **25** 113-117.

Holst B, Cygankiewicz A, Jensen TH, Ankersen M & Schwartz TW 2003 High constitutive signaling of the ghrelin receptor--identification of a potent inverse agonist. *Mol Endocrinol* **17** 2201-2210.

Holst B, Holliday ND, Bach A, Elling CE, Cox HM & Schwartz TW 2004 Common structural basis for constitutive activity of the ghrelin receptor family. *J Biol Chem* **279** 53806-53817.

Holubova M, Blechova M, Kakonova A, Kunes J, Zelezna B & Maletinska L 2018 In Vitro and In Vivo Characterization of Novel Stable Peptidic Ghrelin Analogs: Beneficial Effects in the Settings of Lipopolysaccharide-Induced Anorexia in Mice. *J Pharmacol Exp Ther* **366** 422-432.

Islam MN, Mita Y, Maruyama K, Tanida R, Zhang W, Sakoda H & Nakazato M 2020 Liver-expressed antimicrobial peptide 2 antagonizes the effect of ghrelin in rodents. *J Endocrinol* **244** 13-23.

Kohsaka A, Laposky AD, Ramsey KM, Estrada C, Joshu C, Kobayashi Y, Turek FW & Bass J 2007 High-fat diet disrupts behavioral and molecular circadian rhythms in mice. *Cell Metab* **6** 414-421.

Kojima M, Hosoda H, Date Y, Nakazato M, Matsuo H & Kangawa K 1999 Ghrelin is a growth-hormone-releasing acylated peptide from stomach. *Nature* **402** 656-660.

M'Kadmi C, Cabral A, Barrile F, Giribaldi J, Cantel S, Damian M, Mary S, Denoyelle S, Dutertre S, Peraldi-Roux S, et al. 2019 N-Terminal Liver-Expressed Antimicrobial Peptide 2 (LEAP2) Region Exhibits Inverse Agonist Activity toward the Ghrelin Receptor. *J Med Chem* **62** 965-973.

Machado MV, Coutinho J, Carepa F, Costa A, Proenca H & Cortez-Pinto H 2012 How adiponectin, leptin, and ghrelin orchestrate together and correlate with the severity of nonalcoholic fatty liver disease. *Eur J Gastroenterol Hepatol* **24** 1166-1172.

Maletinska L, Pychova M, Holubova M, Blechova M, Demianova Z, Elbert T & Zelezna B 2012 Characterization of new stable ghrelin analogs with prolonged orexigenic potency. *J Pharmacol Exp Ther* **340** 781-786.

Maletinska L, Nagelova V, Ticha A, Zemenova J, Pirnik Z, Holubova M, Spolcova A, Mikulaskova B, Blechova M, Sykora D, et al. 2015 Novel lipidized analogs of prolactin-releasing peptide have prolonged half-lives and exert anti-obesity effects after peripheral administration. *Int J Obes (Lond)* **39** 986-993.

Mani BK, Puzziferri N, He Z, Rodriguez JA, Osborne-Lawrence S, Metzger NP, Chhina N, Gaylinn B, Thorner MO, Thomas EL, et al. 2019 LEAP2 changes with body mass and food intake in humans and mice. *J Clin Invest* **129** 3909-3923.

Martin NM, Small CJ, Sajedi A, Patterson M, Ghatei MA & Bloom SR 2004 Pre-obese and obese agouti mice are sensitive to the anorectic effects of peptide YY(3-36) but resistant to ghrelin. *Int J Obes Relat Metab Disord* **28** 886-893.

Monteiro R & Azevedo I 2010 Chronic inflammation in obesity and the metabolic syndrome. *Mediators Inflamm* **2010**.

Naznin F, Toshinai K, Waise TM, NamKoong C, Md Moin AS, Sakoda H & Nakazato M 2015 Diet-induced obesity causes peripheral and central ghrelin resistance by promoting inflammation. *J Endocrinol* **226** 81-92.

Okamatsu Y, Matsuda K, Hiramoto I, Tani H, Kimura K, Yada Y, Kakuma T, Higuchi S, Kojima M & Matsuishi T 2009 Ghrelin and leptin modulate immunity and liver function in overweight children. *Pediatr Int* **51** 9-13.

Peracchi M, Bardella MT, Caprioli F, Massironi S, Conte D, Valenti L, Ronchi C, Beck-Peccoz P, Arosio M & Piodi L 2006 Circulating ghrelin levels in patients with inflammatory bowel disease. *Gut* **55** 432-433.

Perreault M, Istrate N, Wang L, Nichols AJ, Tozzo E & Stricker-Krongrad A 2004 Resistance to the orexigenic effect of ghrelin in dietary-induced obesity in mice: reversal upon weight loss. *Int J Obes Relat Metab Disord* **28** 879-885.

Prazienkova V, Funda J, Pirnik Z, Karnosova A, Hruba L, Korinkova L, Neprasova B, Janovska P, Benzce M, Kadlecova M, et al. 2021 GPR10 gene deletion in mice increases basal neuronal activity, disturbs insulin sensitivity and alters lipid homeostasis. *Gene* **774** 145427.

Reynolds KA, Boudoures AL, Chi MM, Wang Q & Moley KH 2015 Adverse effects of obesity and/or high-fat diet on oocyte quality and metabolism are not reversible with resumption of regular diet in mice. *Reprod Fertil Dev* **27** 716-724.

Riedl M, Maier C, Handisurya A, Luger A & Kautzky-Willer A 2007 Insulin resistance has no impact on ghrelin suppression in pregnancy. *J Intern Med* **262** 458-465.

Sajjad A, Mottershead M, Syn WK, Jones R, Smith S & Nwokolo CU 2005 Ciprofloxacin suppresses bacterial overgrowth, increases fasting insulin but does not correct low acylated ghrelin concentration in non-alcoholic steatohepatitis. *Aliment Pharmacol Ther* **22** 291-299.

Shankar K, Metzger NP, Singh O, Mani BK, Osborne-Lawrence S, Varshney S, Gupta D, Ogden SB, Takemi S, Richard CP, et al. 2021 LEAP2 deletion in mice enhances ghrelin's actions as an orexigen and growth hormone secretagogue. *Mol Metab* **53** 101327.

Schalla MA & Stengel A 2019 Pharmacological Modulation of Ghrelin to Induce Weight Loss: Successes and Challenges. *Curr Diab Rep* **19** 102.

Tschop M, Weyer C, Tataranni PA, Devanarayan V, Ravussin E & Heiman ML 2001 Circulating ghrelin levels are decreased in human obesity. *Diabetes* **50** 707-709.

Uriarte M, De Francesco PN, Fernandez G, Castrogiovanni D, D'Arcangelo M, Imbernon M, Cantel S, Denoyelle S, Fehrentz JA, Praetorius J, et al. 2021 Circulating ghrelin crosses the blood-cerebrospinal fluid barrier via growth hormone secretagogue receptor dependent and independent mechanisms. *Molecular and Cellular Endocrinology* **538**.

Yalniz M, Bahcecioglu IH, Ataseven H, Ustundag B, Ilhan F, Poyrazoglu OK & Erensoy A 2006 Serum adipokine and ghrelin levels in nonalcoholic steatohepatitis. *Mediators Inflamm* **2006** 34295.

Figure legends

Figure 1

Experiment 1 – scheme of experimental design. Ninety-six C57Bl/6N male mice were divided into 12 groups. Group 1 was sacrificed at the beginning of the experiment as a control group. Every three weeks, one group fed a St diet (from groups 2-6) and one group fed a HF diet (from groups 7-11) were sacrificed until week 15. Group 12 was fed a HF diet for the first 9 weeks and then switched to a St diet for a further 6 weeks before being sacrificed at week 15. The white triangles indicate the week of the experiment when the OGTT was performed. The black triangles indicate the week of the experiment when the dissection was performed.

Figure 2

Experiment 2 – scheme of experimental design. Forty C57Bl/6N male mice were divided into 5 groups. 2 groups were fed a St diet and 3 groups were fed a HF diet. In the 8^{th} week of the experiment, the diet of all mice was changed to St diet. Food intake was monitored after SC injection of saline, palm-LEAP2(1-14), or [Dpr^3]Ghrelin at 0^{th}, 2^{nd}, 4^{th}, 8^{th}, 10^{th}, and 12^{th} week of experiment (marked by black triangle).

Figure 3

Effect of HF diet on body weight (A), eWAT weight (B) an leptin in plasma (C) in C57Bl/6N mice. Data are presented as means ± SEM. Statistical analysis was performed by two-way ANOVA with Bonferroni's post hoc test (A) and multiple *t*-test with Bonferroni-Dunn's method for multiple comparisons (B, C). eWAT – epididymal white adipose tissue. Significance is **P*<0.05, ***P*<0.01, ****P*<0.001 HF vs St; #*P*<0.05, ##*P*<0.01, ###*P*<0.001 HF-St vs St; †*P*<0.05, ††*P*<0.01, †††*P*<0.001 HF-St vs HF (*n*=8).

Figure 4

Levels of active and total ghrelin in plasma (A and B), and *LEAP2* mRNA in the liver (C). Data are presented as means ± SEM. Statistical analysis was performed using the multiple *t*-test with Bonferroni-Dunn's method for multiple comparisons. Significance is **P*<0.05, ***P*<0.01, ****P*<0.001 HF vs St; #*P*<0.05, ##*P*<0.01, ###*P*<0.001 HF-St vs St; †*P*<0.05, ††*P*<0.01, †††*P*<0.001 HF-St vs HF (*n*=8).

Figure 5

Blood glucose levels (A-F) after oral glucose gavage (dose 2 g/kg) and corresponding plasma levels of fasting glucose (G), AUC (H), and insulin plasma levels (I). OGTT at 0 weeks (A), 3 weeks (B), 6 weeks (C), 9 weeks (D), 12 weeks (E), and 15 weeks of the experiment are expressed as means ± SEM and

determined by two-way ANOVA with Bonferroni's post hoc test (A-F) and multiple *t*-test with Bonferroni-Dunn's method for multiple comparisons (G and H). Fasting glucose, area under the OGTT curves, and insulin plasma levels are expressed as means ± SEM and determined by the multiple *t*-test. Significance is **P*<0.05, ***P*<0.01, ****P*<0.001 HF vs St; †*P*<0.05, ††*P*<0.01, †††*P*<0.001 HF-St vs HF (*n*=8).

Figure 6

Liver weight and metabolic parameters at the end of the experiment. Cholesterol (A), TAG (B), and CRP (C) in plasma, liver weight (D), oxidative stress in the liver (E), and morphological changes in liver tissue (F). Data (A-E) are presented as means ± SEM. Statistical analysis was performed by one-way ANOVA with Tukey's method for multiple comparisons. Significance is **P*<0.05, ***P*<0.01, ****P*<0.001 HF vs St; #*P*<0.05; †*P*<0.05, ††*P*<0.01, †††*P*<0.001 HF-St vs HF (*n*=8). (F) Representative microphotographs of a liver stained by haematoxylin and eosin are magnified 200x.

Figure 7

Effect of HF diet on hypothalamic mRNA expression of *AgRP*, *CART*, *GHSR*, *NPY*, and *POMC* in mice fed a HF diet or a St diet. Data were normalised to B2M and presented as means ± SEM. Statistical analysis was performed by one-way ANOVA with Tukey's method for multiple comparisons (*n*=5). *AgRP* – agouti-related peptide, *CART* – cocaine- and amphetamine-regulated transcript, *GHSR* – growth hormone-secretagogue receptor, *NPY* – neuropeptide Y, *POMC* – pro-opiomelanocortin.

Figure 8

Cumulative food intake 270 minutes after SC [Dpr^3]Ghrelin (1mg/kg) or palm-LEAP2(1-14) (5 mg/kg) administration in mice fed a HF diet or a St diet for 0 (A), 2 (B), 4 (C), and 8 (D) weeks followed by a St diet only for a further 2 (E) and 4 (F) weeks. Data are presented as means of AUC ± SEM. Statistical analysis was performed by *t*-test. Significance is **P*<0.05, ***P*<0.01, ****P*<0.001 [Dpr^3]Ghrelin vs saline; #*P*<0.05, ##*P*<0.01, ###*P*<0.001 palm-LEAP2(1-14) vs saline (*n*=6-8).

Figure 9

Cumulative food intake after SC [Dpr^3]Ghrelin (1mg/kg) or palm-LEAP2(1-14) (5 mg/kg) administration in mice at the beginning of experiment (A) and after feeding a HF diet for 2 (B), 4 (C), and 8 (D) weeks followed by a St diet only for a further 2 (E) and 4 (F) weeks or exclusively St diet for 2 (G), 4 (H), 8 (I), 10 (J), and 12 (K). Data are presented as means ± S.E.M. Statistical analysis was performed by two-way ANOVA with Bonferroni's post hoc test. Significance is **P*<0.05, ***P*<0.01, ****P*<0.001 [Dpr^3]Ghrelin vs saline; #*P*<0.05, ##*P*<0.01, ###*P*<0.001 palm-LEAP2(1-14) vs saline (*n*=6-8).

Figure 1

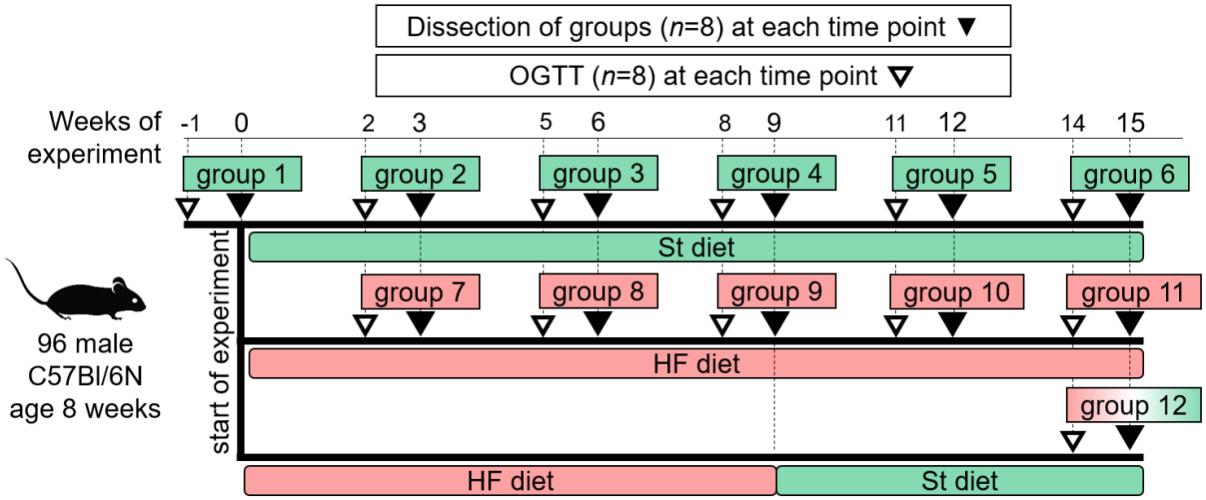

Figure 2

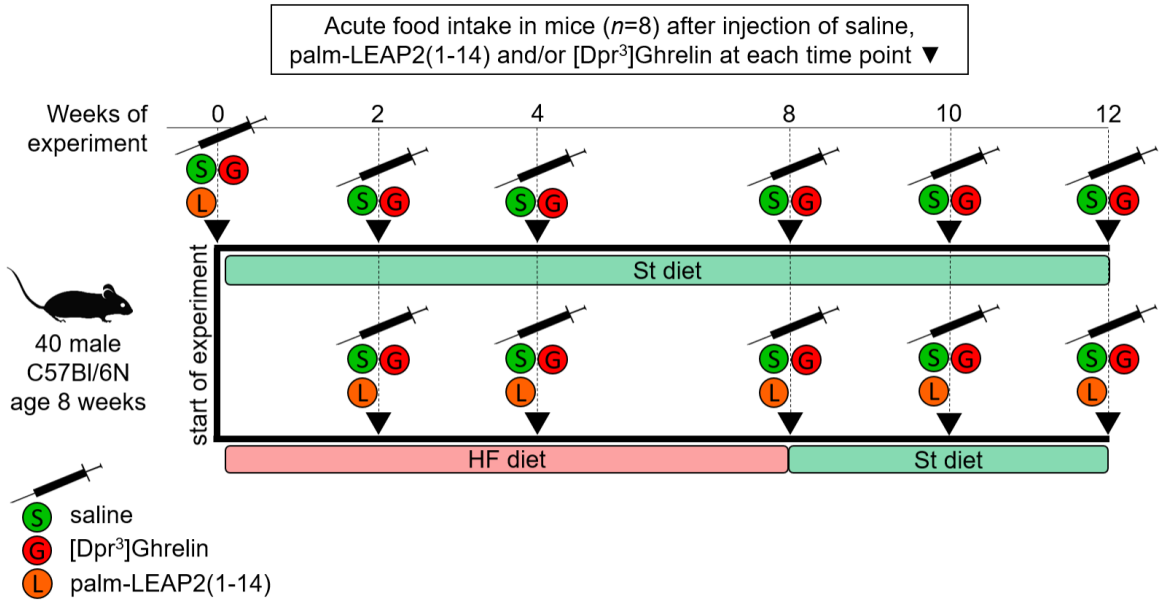

Figure 3

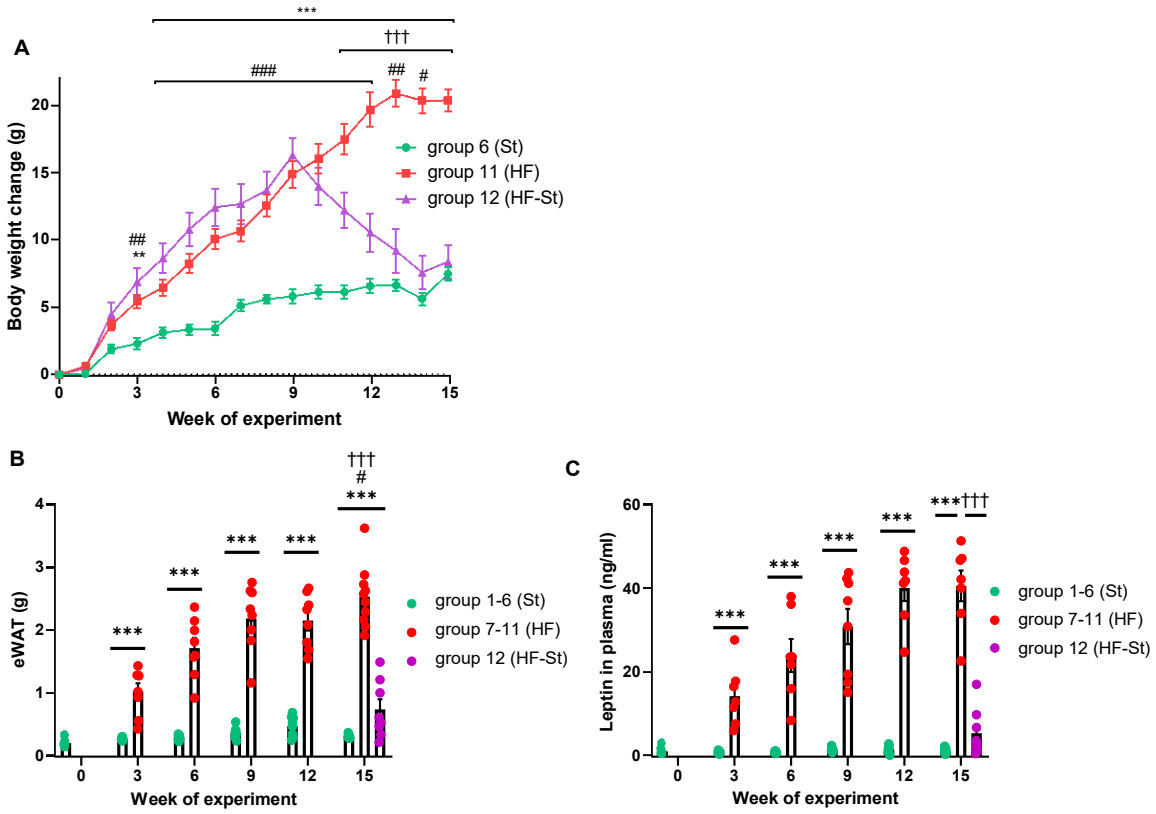

Figure 4

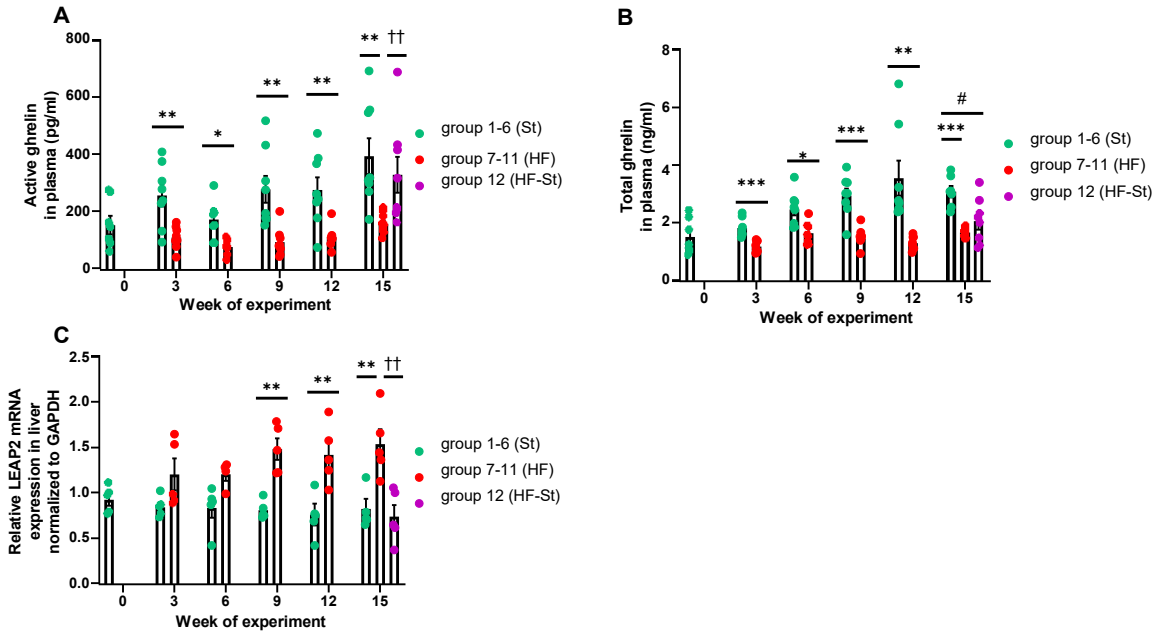

Figure 5

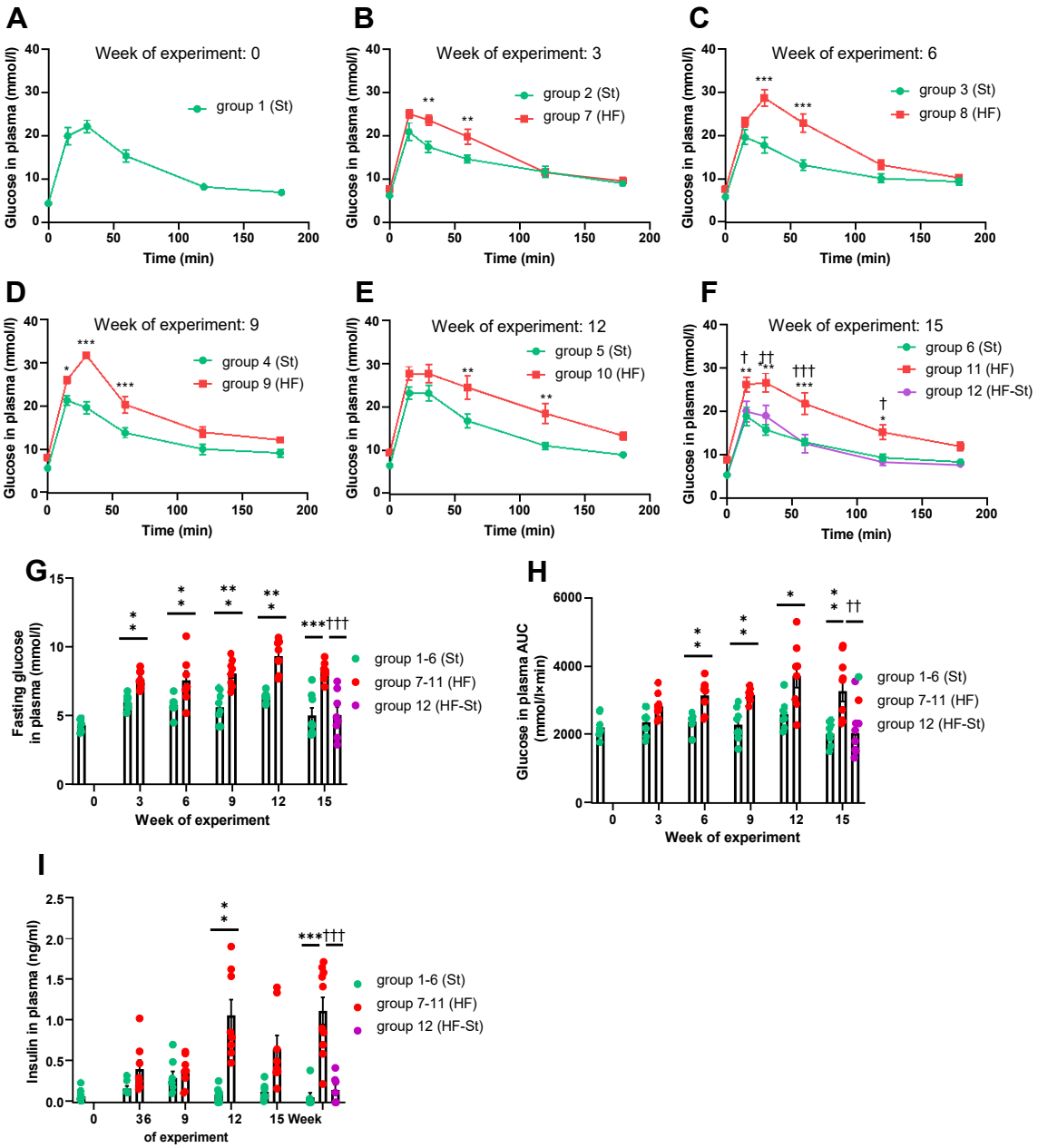
A
Week of experiment: 0
group 1 (St)
B
Week of experiment: 3
group 2 (St)
group 7 (HF)
C
Week of experiment: 6
group 3 (St)
group 8 (HF)
D
Week of experiment: 9
group 4 (St)
group 9 (HF)
E
Week of experiment: 12
group 5 (St)
group 10 (HF)
F
Week of experiment: 15
group 6 (St)
group 11 (HF)
group 12 (HF-St)
Glucose in plasma (mmol/l)
Time (min)
G
Fasting glucose in plasma (mmol/l)
Week of experiment
group 1-6 (St)
group 7-11 (HF)
group 12 (HF-St)
H
Glucose in plasma AUC (mmol/l×min)
Week of experiment
I
Insulin in plasma (ng/ml)
of experiment

Figure 6

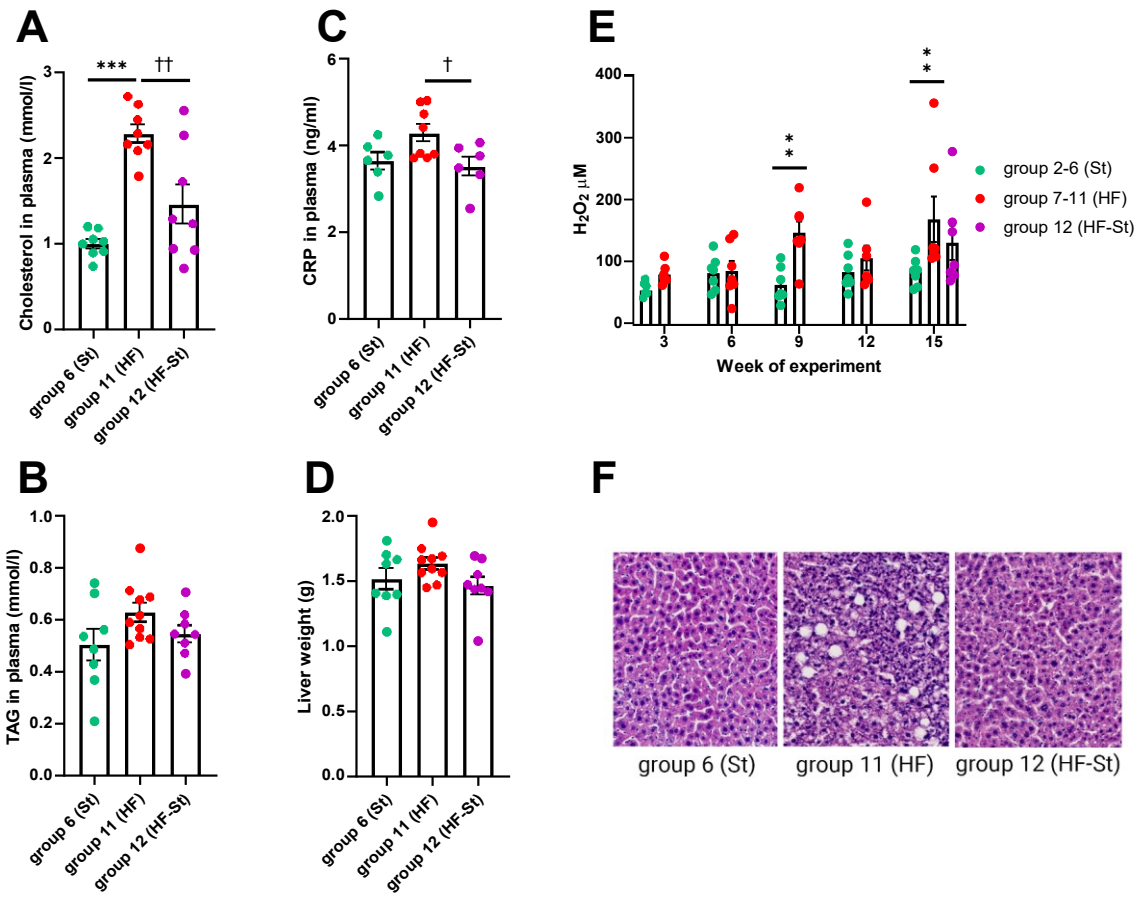

Figure 7

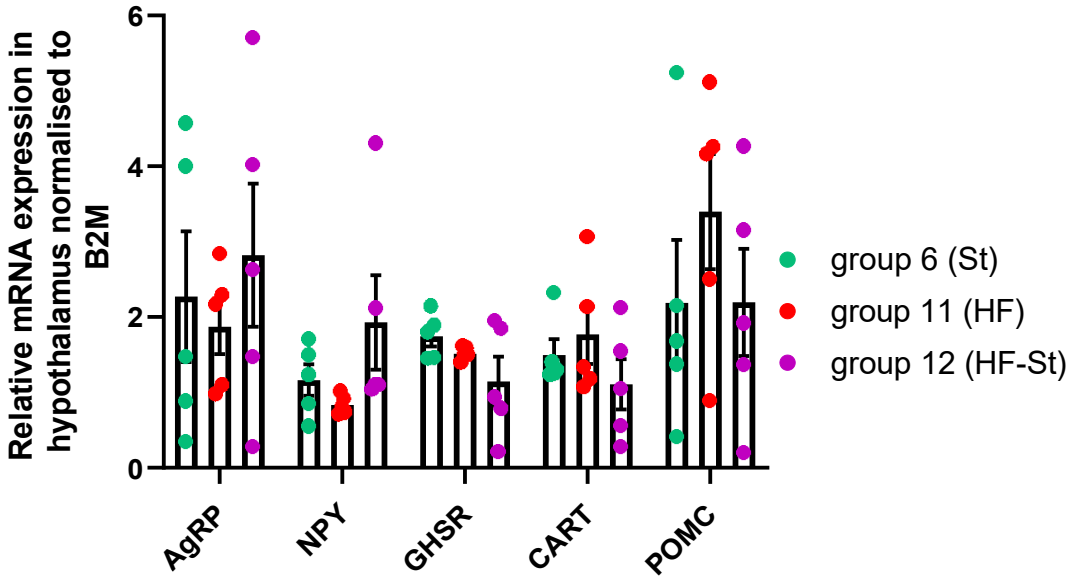

Figure 8

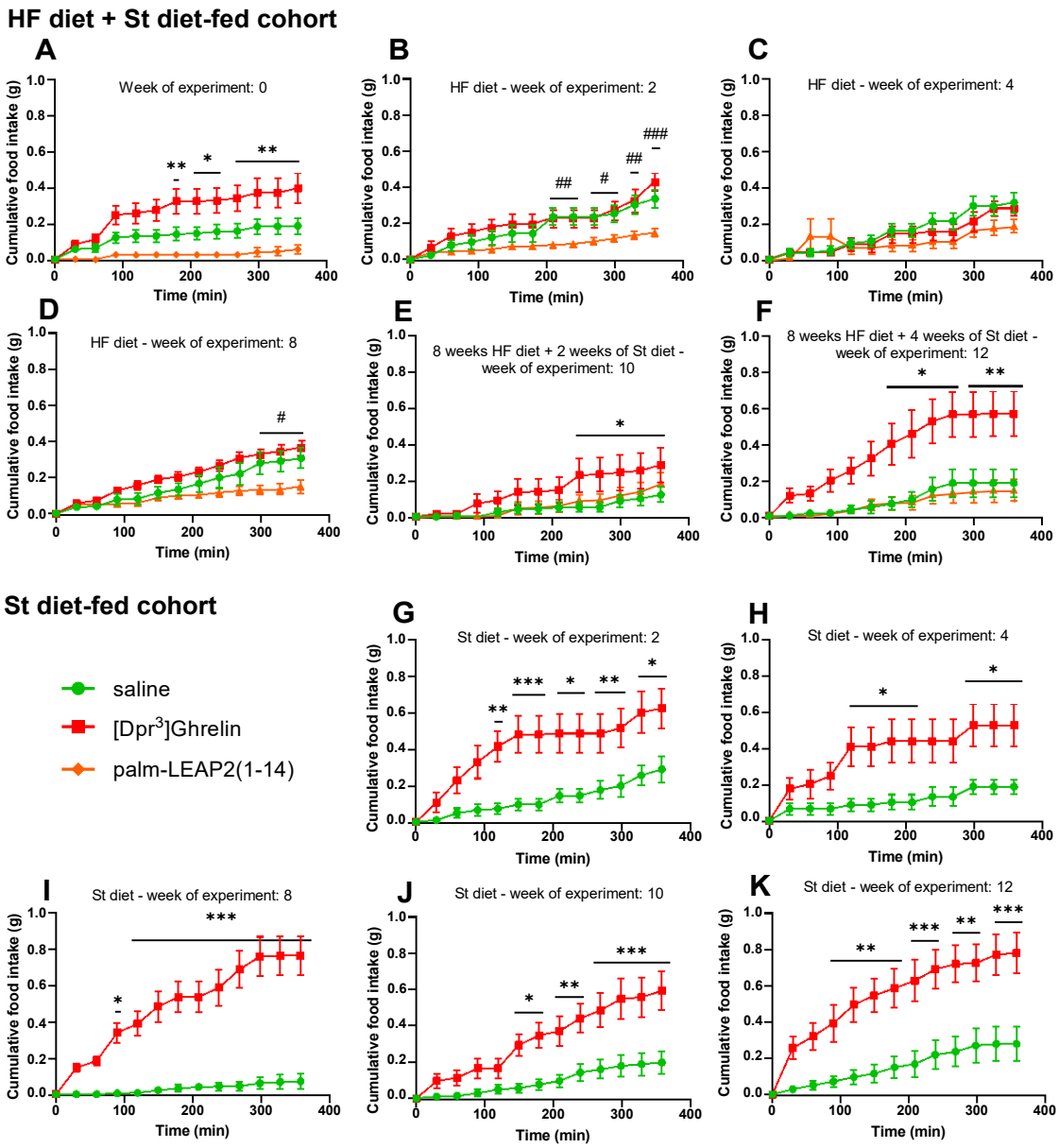
HF diet + St diet-fed cohort
A
Week of experiment: 0
B
HF diet - week of experiment: 2
C
HF diet - week of experiment: 4
D
HF diet - week of experiment: 8
E
8 weeks HF diet + 2 weeks of St diet - week of experiment: 10
F
8 weeks HF diet + 4 weeks of St diet - week of experiment: 12
St diet-fed cohort
saline
[Dpr3]Ghrelin
palm-LEAP2(1-14)
G
St diet - week of experiment: 2
H
St diet - week of experiment: 4
I
St diet - week of experiment: 8
J
St diet - week of experiment: 10
K
St diet - week of experiment: 12
Cumulative food intake (g)
Time (min)

Figure 9

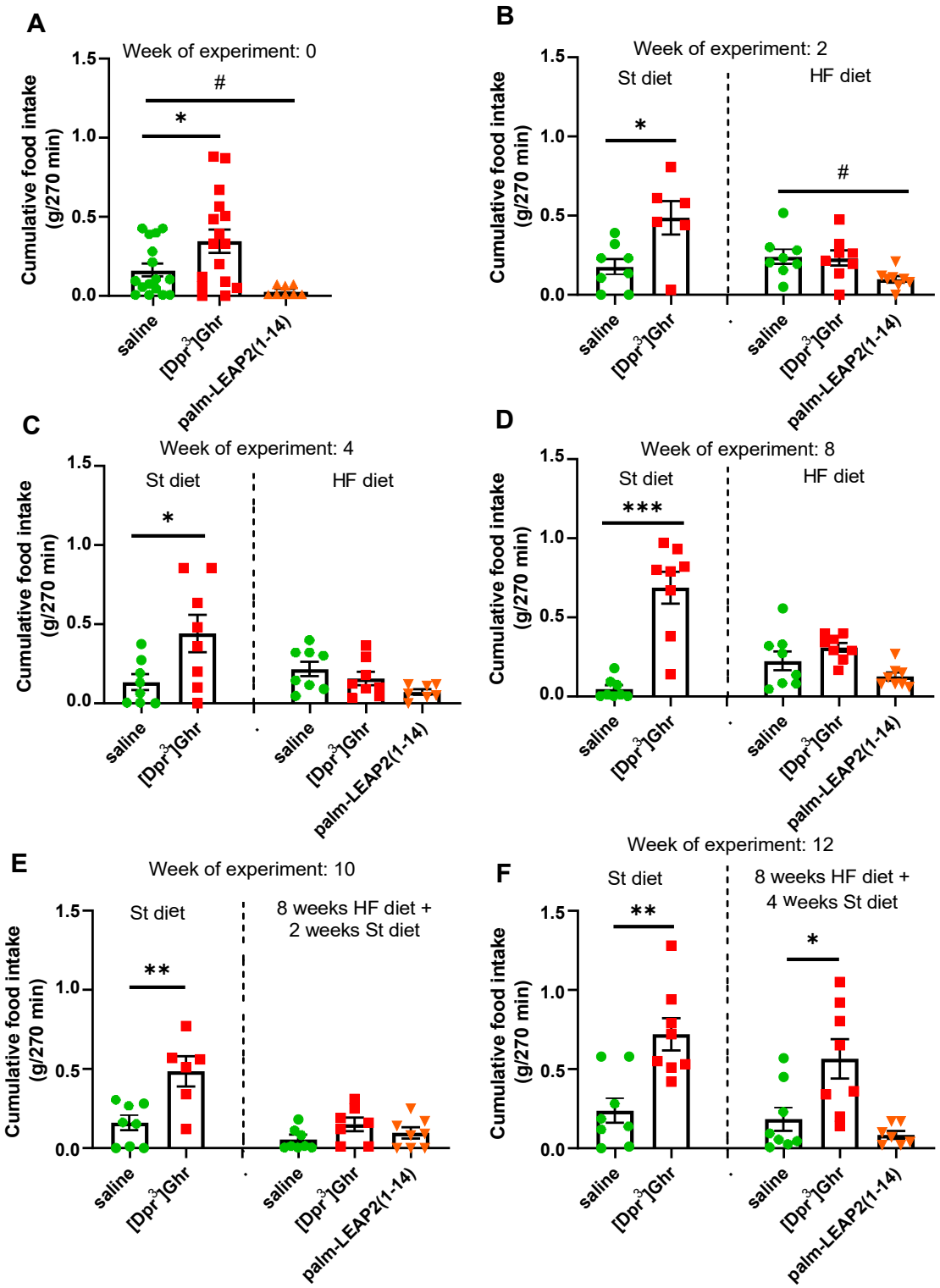
A
Week of experiment: 0
Cumulative food intake (g/270 min)
1.5
1.0
0.5
0.0
#
*
saline
[Dpr3]Ghr
palm-LEAP2(1-14)
B
Week of experiment: 2
St diet
HF diet
*
#
C
Week of experiment: 4
St diet
HF diet
*
D
Week of experiment: 8
St diet
HF diet
***
E
Week of experiment: 10
St diet
8 weeks HF diet + 2 weeks St diet
**
F
Week of experiment: 12
St diet
8 weeks HF diet + 4 weeks St diet
**
*

International Journal of
Molecular Sciences

MDPI

Article

Palmitoylation of Prolactin-Releasing Peptide Increased Affinity for and Activation of the GPR10, NPFF-R2 and NPFF-R1 Receptors: In Vitro Study

Alena Karnošová [1,2], Veronika Strnadová [1], Lucie Holá [1,2], Blanka Železná [1], Jaroslav Kuneš [1,3] and Lenka Maletínská [1,*]

[1] Biochemistry and Molecular Biology, Institute of Organic Chemistry and Biochemistry of the Czech Academy of Sciences, 16610 Prague, Czech Republic; alena.karnosova@uochb.cas.cz (A.K.); veronika.strnadova@uochb.cas.cz (V.S.); lucie.cerna@uochb.cas.cz (L.H.); zelezna@uochb.cas.cz (B.Ž.); kunes@biomed.cas.cz (J.K.)
[2] First Faculty of Medicine, Charles University, 12108 Prague, Czech Republic
[3] Experimental Hypertension, Institute of Physiology of the Czech Academy of Sciences, 14200 Prague, Czech Republic
* Correspondence: maletin@uochb.cas.cz; Tel.: +420-220-183567

Abstract: The anorexigenic neuropeptide prolactin-releasing peptide (PrRP) is involved in the regulation of food intake and energy expenditure. Lipidization of PrRP stabilizes the peptide, facilitates central effect after peripheral administration and increases its affinity for its receptor, GPR10, and for the neuropeptide FF (NPFF) receptor NPFF-R2. The two most potent palmitoylated analogs with anorectic effects in mice, palm^{11}-PrRP31 and palm-PrRP31, were studied in vitro to determine their agonist/antagonist properties and mechanism of action on GPR10, NPFF-R2 and other potential off-target receptors related to energy homeostasis. Palmitoylation of both PrRP31 analogs increased the binding properties of PrRP31 to anorexigenic receptors GPR10 and NPFF-R2 and resulted in a high affinity for another NPFF receptor, NPFF-R1. Moreover, in CHO-K1 cells expressing GPR10, NPFF-R2 or NPFF-R1, palm^{11}-PrRP and palm-PrRP significantly increased the phosphorylation of extracellular signal-regulated kinase (ERK), protein kinase B (Akt) and cAMP-responsive element-binding protein (CREB). Palm^{11}-PrRP31, unlike palm-PrRP31, did not activate either c-Jun N-terminal kinase (JNK), p38, c-Jun, c-Fos or CREB pathways in cells expressing NPFF-1R. Palm-PrRP31 also has higher binding affinities for off-target receptors, namely, the ghrelin, opioid (KOR, MOR, DOR and OPR-L1) and neuropeptide Y (Y_1, Y_2 and Y_5) receptors. Palm^{11}-PrRP31 exhibited fewer off-target activities; therefore, it has a higher potential to be used as an anti-obesity drug with anorectic effects.

Keywords: prolactin-releasing peptide; GPR10; neuropeptide FF; NPFF-R2; NPFF-R1; binding properties; signaling pathways

•€••,ƒ„…†
•€•,ƒ„…

Citation: Karnošová, A.; Strnadová, V.; Holá, L.; Železná, B.; Kuneš, J.; Maletínská, L. Palmitoylation of Prolactin-Releasing Peptide Increased Affinity for and Activation of the GPR10, NPFF-R2 and NPFF-R1 Receptors: In Vitro Study. Int. J. Mol. Sci. **2021**, 22, 8904. https://doi.org/10.3390/ijms22168904

Academic Editor: Clara Balsano

Received: 1 July 2021
Accepted: 12 August 2021
Published: 18 August 2021

Publisher's Note: MDPI stays neutral with regard to jurisdictional claims in published maps and institutional affiliations.

1. Introduction

Prolactin-releasing peptide (PrRP) was discovered as an endogenous ligand of the orphan G-protein coupled receptor GPR10 (also known as hGR3) in the hypothalamus and has been suggested to stimulate prolactin secretion [1,2]. However, soon after this finding, Lawrence et al. showed a reduction in food intake and body weight and an increase in energy expenditure after intracerebroventricular (ICV) PrRP injection in rats and questioned the role of PrRP in prolactin secretion [3,4]. The effects of PrRP, mostly mediated through the GPR10 receptor, which is widely expressed throughout the brain mainly in areas related to the regulation of food intake and energy homeostasis, confirm GPR10 knockout (KO) mouse studies showing an increase in body weight in KO mice [5–7].

PrRP occurs in two biologically active isoforms, PrRP31 and PrRP20. Our previous studies showed the induction of central c-Fos activation of regions related to food intake

after peripheral administration of PrRP31 or PrRP20 modified with either myristoyl or palmitoyl, but this central effect was not observed after peripheral administration of natural PrRP31 or PrRP20. Lipidized PrRP31 and PrRP20 analogs decrease food intake and body weight in mice, increase stability and prolong half-life compared to natural peptides [8–12]. PrRP20 and PrRP31 also strongly interact with the receptor of neuropeptide FF (NPFF), NPFF-R2 [13]. Lipidization of PrRP20 and PrRP31 increases in vitro binding affinities not only to GPR10 but also to NPFF-R2 [8,9]. However, lipidized PrRP20 showed lower solubility and bioavailability [8]; therefore, our further studies were focused on lipidized PrRP31 analogs.

PrRP, together with NPFF, belongs to the RF-amide peptide family, which contains a typical C-terminal amino acid sequence motif (RF-NH_2) essential for receptor activation. All RF-amide peptides have a high affinity for and activity on both NPFF receptors NPFF-R2 and NPFF-R1 and may also exert in vivo effects through these receptors [14]. Expression of both NPFF receptors has been found in hypothalamic areas that regulate feeding and energy homeostasis. Moreover, the ability of NPFF to regulate food intake was previously demonstrated, when ICV administration of NPFF was shown to result in decreased food intake in fasted rats [15,16].

Both NPFF receptors show the ability to regulate the cardiovascular system and modulate pain perceptions [17–19]. Despite the fact that antagonist of NPFF-R1 and NPFF-R2 RF9 prevents opioid-induced hyperalgesia and that NPFF induces an increase in arterial blood pressure in rats [20], our previous study did not prove the antagonistic activity of RF9 on NPFF-induced anorexigenic effects [21]. Conversely, RF9 exhibits an anorectic effect after ICV or subcutaneous administration in fasted mice [21].

Similar to NPFF, PrRP also appears to have antinociceptive properties [22,23]. Although PrRP has a high affinity for NPFF receptors, its ability to modulate pain perception through NPFF-1R and NPFF-2R has not been proven. Kalliomäki et al. studied the nociceptive properties of 1DMe, a stable NPFF analog, and PrRP in the central nervous system of rats and refuted the ability of PrRPs to regulate pain perception through NPFF receptors [22].

Many G-protein coupled receptors (GPCRs) share similar characteristic features. Receptors GPR10, NPFF-R1 and NPFF-R2 are members of the -type rhodopsin GPCR family, which has important roles in the regulation of food intake and energy homeostasis [24]. GPR10 has a high percentage of amino sequence identity, especially in the transmembrane regions, with neuropeptide Y receptors, members of the -type rhodopsin GPCR family, which are involved in food intake regulation [25]. Furthermore, Y receptors share a high percentage of amino sequence homology with NPFF-R1 and NPFF-R2 [26].

The mechanism of action of PrRP is not yet fully understood. PrRP31 and PrRP20 have been shown to mobilize Ca^{2+} from intracellular stores via GPR10 by activating the second messenger IP3 (inositol-1,4,5-trisphosphate), leading to an increase in cytoplasmic Ca^{2+} [27,28], which can subsequently activate the extracellular signal-regulated kinase (ERK) signaling cascade [29]. PrRPs displayed the ability to activate the phosphorylation of ERK, the c-Jun N-terminal kinase (JNK) pathway, the cAMP-responsive element binding protein (CREB) pathway and the protein kinase B (Akt/PKB) pathway, which plays a key role in the regulation of protein synthesis and maintenance of glucose homeostasis [30–32].

Maixnerová et al. previously showed that the first 20 amino acids of PrRP31 are important for the preservation of full in vivo activity [31]. This study compares the activity of two most potent PrRP31 analogs, palm^{11}-PrRP31 and palm-PrRP31, which contain palmitic acid attached to the N-terminus of the amino acid chain (palm-PrRP31) or to the position 11, where original Arg^{11} was replaced with Lys^{11} (palm^{11}-PrRP31) (Table 1). These analogs previously showed the ability to significantly decrease food intake and body weight after repeated peripheral administration [8,9], but the mechanism of action is still unclear. We aimed to identify the off-target activity of palm^{11}-PrRP31 and palm-PrRP31 to map the mechanism of action and to compare intracellular transduction pathways of anorexigenic receptors GPR10, NPFF-R2, and new strong target of PrRP31 analogs, NPFF-

R1. GPR10 is a highly selective receptor for PrRP31 and analogs related to PrRP31. To control the selectivity of PrRP31 for GPR10s, we used NPFF and its stable analog 1DMe in this study. To determine whether the possible analgesic effect of PrRPs is caused by off-target activity, opioid receptors were investigated.

Table 1. Structures of human prolactin-releasing peptide 31 (PrRP31), neuropeptide FF (NPFF) and its analogs.

Analog	Sequence
PrRP31	SRAHQHSMETRTPDINPAWYTGRGIRPVGRF-NH_2
$Palm^{11}$-PrRP31	SRTHRHSMEIK(-E (N-palm))TPDINPAWYASRGIRPVGRF-NH_2
Palm-PrRP31	(N-palm)SRTHRHSMEIRTPDINPAWYASRRGIRPVGRF-NH_2
NPFF	FLFQPQRF-NH_2
1DMe	yL(N-Me)FQPQRF-NH_2

2. Results

2.1. Binding Affinity for GPR10, NPFF-R2 and Potential Off-Target Receptors

2.1.1. Palmitoylated PrRP31 Analogs Have a High Binding Affinity for GPR10, NPFF-R2 and NPFF-R1

Based on previously published data, affinity for the GPR10 and NPFF-R2 of PrRP31 and its analogs was studied [8,9]. PrRP31 and its two palmitoylated analogs of PrRP31 (see Table 1 for structures) have a high binding affinity for the GPR10 and NPFF-R2 receptors, and their K_i values were in the nanomolar range (Table 2). Compared to natural PrRP31, palmitoylated analogs had a higher binding affinity for both of these receptors. $Palm^{11}$-PrRP31 showed a higher affinity for the receptor GPR10 than for the receptor NPFF-R2. NPFF and its stable analog 1DMe displayed negligible affinity for the GPR10 receptor. The affinities of NPFF and 1DMe to NPFF-R2 were detected to be in the nanomolar range (Table 2).

Table 2. Binding affinities of natural PrRP31, its analogs and other peptides to tested receptors.

Receptor	**GPR10**	**NPFF-R2**	**NPFF-R1**	**KOR**
	[^{125}I]-PrRP31	**[^{125}I]-1DMe**	**[^{125}I]-1DMe**	**[^{125}I]-Dynorphin**
		K_i [nM]		
PrRP31	4.58 0.66	26.73 9.01	40.39 4.20	>10,000
$Palm^{11}$-PrRP31	3.44 0.36	7.66 1.33	13.52 1.57	4278 866
Palm-PrRP31	4.04 0.01	0.77 0.19	0.78 0.11	106 15 --
NPFF	>10,000	0.28 0.06	1.08 0.09	0.36 0.03
1DMe	>10,000	1.03 0.23 -	0.79 0.06 -	
Dynorphin	-			**GHSR**
Receptor	**Y_1**	**Y_2**	**Y_5**	**[^{125}I]-Ghrelin**
	[^{125}I]-PYY	**[^{125}I]-PYY**	**[^{125}I]-PYY**	
		K_i [nM]		
PYY	2.92 0.28	6.51 0.71	3.06 0.49	-
PrRP31	>10,000	>10,000	2863 43 362	>10,000
$Palm^{11}$-PrRP31	>10,000	>10,000	96 32.62	2800 466
Palm-PrRP31	3147 31 -	>10,000	6.16 -	160 16 4.59
Ghrelin		-		0.41

- not determined; data presented as the means K_i values SEM and analyzed in Graph-Pad Software were performed in 2–5 independent experiments in duplicates. K_i was calculated using the Cheng-Prusoff equation [33].

To find another possible target of the two most potent palmitoylated analogs of PrRP31, binding to NPFF-R1 was tested. Membranes from CHO-K1 cells expressing the NPFF-R1 were isolated, and the K_d was determined to be 0.94 0.06 nM by saturation experiments using the radioligand [^{125}I]-1DMe. Although natural PrRP31 bound to NPFF-R1 with a

lower affinity than to NPFF-R2, the binding affinity was still in the 10 ^{8} M range (Table 2). Palmitoylation increased the binding affinities of both analogs to NPFF-R1. Palm-PrRP31 showed binding affinities in the nanomolar range to both NPFF receptors compared to palm^{11}-PrRP31 (Table 2).

2.1.2. Palm-PrRP31 Shows a Higher Affinity for Other Potential Off-Target Receptors than Palm^{11}-PrRP31

Several other potential off-target receptors of PrRP31 and its palmitoylated analogs were tested. The binding properties of PrRP31, palm^{11}-PrRP and palm-PrRP31 to receptors Y_1, Y_2, and Y_5, ghrelin receptor (also growth hormone secretagogue receptor—GHSR) and kappa-opioid receptor (KOR) were determined. The natural ligand PYY of Y receptors bound in the nanomolar range to the Y_1, Y_2, and Y_5 receptors (Table 2). From saturation binding experiments with [^{125}I]-PYY as a radioligand, the K_d for each receptor was determined. The K_d for Y_1 was 1.53 0.08 nM, for Y_2 was 2.18 0.85 nM and for Y_5 was 1.01 0.27 nM. Natural PrRP31 had no affinity to the Y_1 and Y_2 receptors in the range of measured concentrations, but it showed a very low affinity to the Y_5 receptor. Compared to palm^{11}-PrRP31, palm-PrRP31 exhibited a relatively high affinity for the Y_5 receptor. Both palmitoylated analogs bound to Y_1 and Y_2 with a negligible low affinity (Table 2).

The K_d determined by a saturation binding experiment with [^{125}I]-dynorphin as a radioligand was 2.38 nM. The agonist dynorphin showed a very high affinity for the KOR receptor, but no binding was observed with natural PrRP31 (Table 2). Palmitoylation enhanced binding to the KOR receptor. Palm-PrRP31 bound to KOR with a higher affinity than palm^{11}-PrRP31, but both were in the 10 ^{7}–10 ^{6} M range.

Another tested potential off-target receptor was the ghrelin receptor GHSR. From saturation experiments using [^{125}I]-ghrelin as a radioligand, a K_d of 0.44 0.12 nM was determined. Natural PrRP31 showed no binding to GHSR in competitive binding experiments in the measured range, but palmitoylated analogs showed a low binding affinity for this receptor (Table 2). Palm-PrRP31 had a higher affinity for GHSR than palm^{11}-PrRP31.

2.2. PrRP31 and Its Palmitoylated Analogs Stimulate Ca^{2+} Mobilization in CHO-K1 Cells Expressing GPR10 or NPFF-R2

Stimulation of Ca^{2+} in CHO-K1 cells expressing the GPR10 receptor was monitored using the calcium-sensitive dye Fura 2. No calcium mobilization was observed after stimulation with the NPFF-R2 agonists NPFF and 1DMe (Figure 1). On the other hand, natural PrRP31, palm^{11}-PrRP31 and palm-PrRP31 stimulated Ca^{2+} mobilization. Both of the lipidized analogs showed a similar Ca^{2+} release response, which was observed at lower concentrations compared to PrRP31.

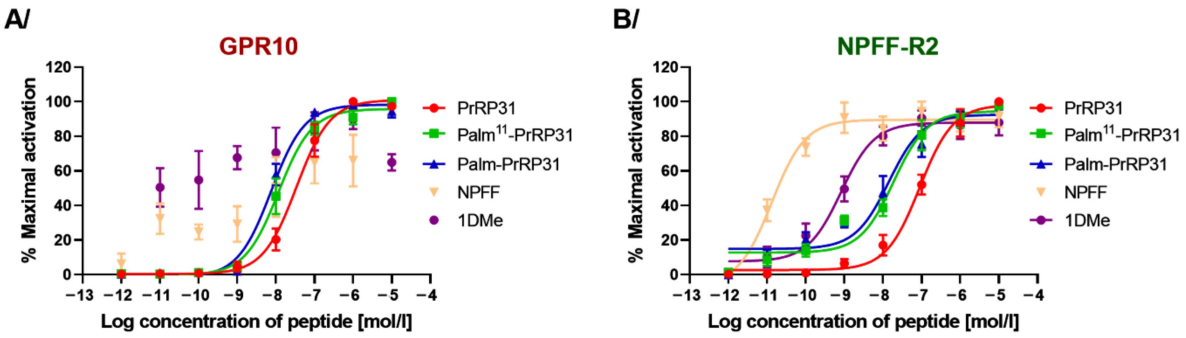

Figure 1. Intracellular Ca^{2+} mobilization in CHO-K1 cells expressing (**A**) GPR10 or (**B**) NPFF-R2. Data are presented as mean SEM, and the experiments were performed in duplicates and repeated two (GPR10) or three (NPFF-R2) times in duplicates.

The CHO-K1 cell line expressing NPFF-R2 with aequorin protein, which detects intracellular Ca^{2+} release, was used to study the agonist properties of PrRP31, its palmitoylated

analogs, NPFF and 1DMe. NPFF (EC_{50}, 0.24 0.02 pM) and 1DMe (EC_{50}, 0.82 0.15 nM) stimulated intracellular Ca^{2+} release at much lower concentrations than the GPR10 agonist PrRP31 (EC_{50}, 89.33 0.84 nM) and its lipidized analogs. Palmitoylation of PrRP31 increased agonist activity at NPFF-R2, where the EC_{50} of palm^{11}-PrRP31 was 18.71 1.31 nM and that of palm-PrRP31 was 14.16 1.52 nM (Figure 1).

2.3. Palmitoylated PrRP31 Analogs Activate Different Intracellular Signaling Pathways in GPR10-, NPFF-R2- or NPFF-R1-Expressing Cells

To determine the intracellular mechanism of action of PrRP31 and its palmitoylated analogs, several signaling pathways were tested in cells expressing GPR10, NPFF-R2 or NPFF-R1 receptors using immunoblotting (Figures 2–5; Supplementary Figure S1). No changes in total protein levels were observed (Supplementary Figure S1B); therefore, only activated/phosphorylated proteins were quantified and compared. NPFF and 1DMe were used as negative controls to validate GPR10 selective properties.

To study PKB/Akt pathway activation, phosphorylation of Akt at Ser473 (Figure 2A) and Thr308 (Figure 2B) was tested. Both PrRP31 analogs, palm^{11}-PrRP31 and palm-PrRP31, showed significantly increased phosphorylation of Akt at Ser473 (Figure 2A) and Thr308 (Figure 2B) in cells with GPR10 and NPFF-R2 but also in cells expressing NPFF-R1. Natural PrRP31 did not significantly activate Akt (Figure 2) in cells with NPFF-R1. NPFF and 1DMe increased the phosphorylation of Akt at either Ser473 (Figure 2A) or Thr308 (Figure 2B) in cells containing NPFF-R2 and NPFF-R1, but they were less effective at GPR10.

The activation of the cAMP-dependent protein kinase (PKA) was also studied (Supplementary Figure S1A). No significant changes were observed after treatment with PrRP31, palmitoylated PrRP31 analogs, NPFF or 1DMe in cells expressing GPR10, NPFF-R2 and NPFF-R1.

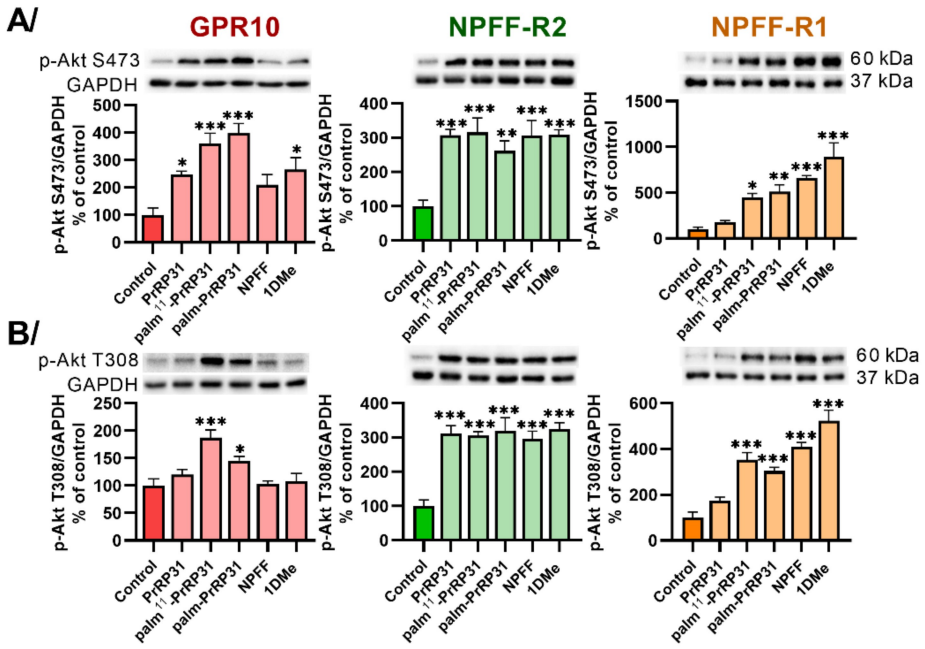

Figure 2. Induction of (**A**) Akt (S473) and (**B**) Akt (T308) phosphorylation after 5 min of incubation at 37 C with peptides at final concentrations of 10 ^{6} M in CHO-K1 cells expressing receptors GPR10, NPFF-R2 and NPFF-R1. Densitometric quantification was normalized to GAPDH, and the phosphorylation level in the untreated control was standardized as 100%. Data are presented as the mean SEM and analyzed by two-way ANOVA followed by Dunnett's post hoc test. Experiments were performed independently at least three times. Statistically significant differences from the control are indicated (* $p < 0.05$, ** $p < 0.01$, *** $p < 0.001$).

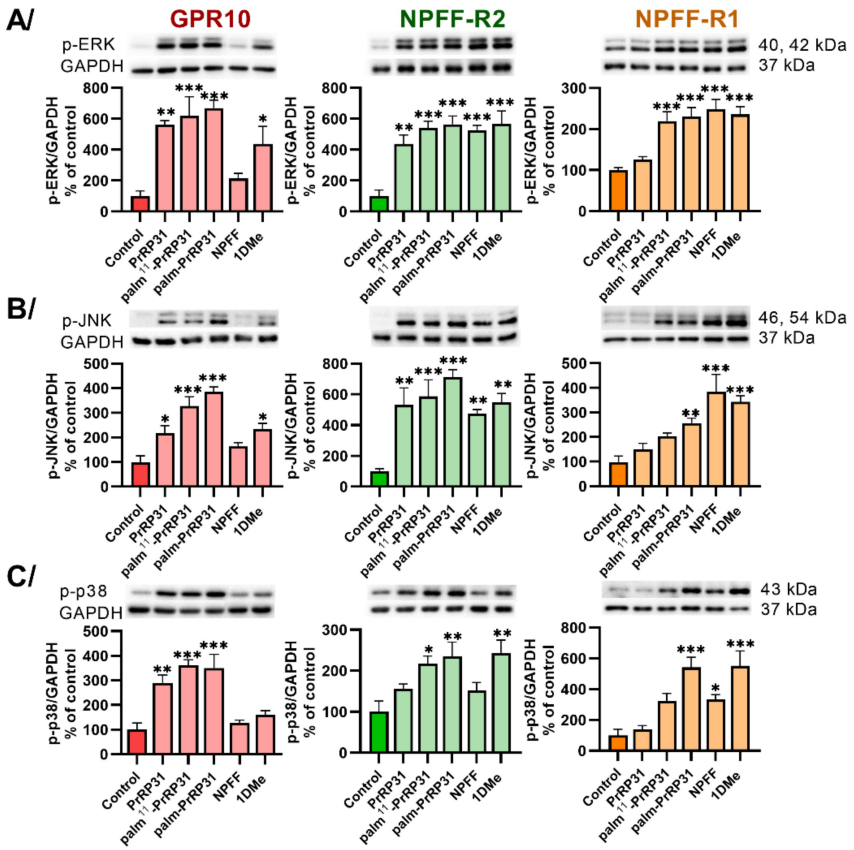

Figure 3. Induction of MAPK pathways: phosphorylation of (**A**) ERK and (**B**) JNK after 5 min and (**C**) p38 after 60 min of incubation at 37 C with peptides at final concentrations of 10 ^{6} M in CHO-K1 cells expressing receptors GPR10, NPFF-R2 and NPFF-R1. Densitometric quantification was normalized to GAPDH, and the phosphorylation level in the untreated control was standardized as 100%. Data are presented as the mean SEM and analyzed by two-way ANOVA followed by Dunnett's post hoc test. Experiments were performed independently at least three times. Statistically significant differences from the control are indicated (* $p < 0.05$, ** $p < 0.01$, *** $p < 0.001$).

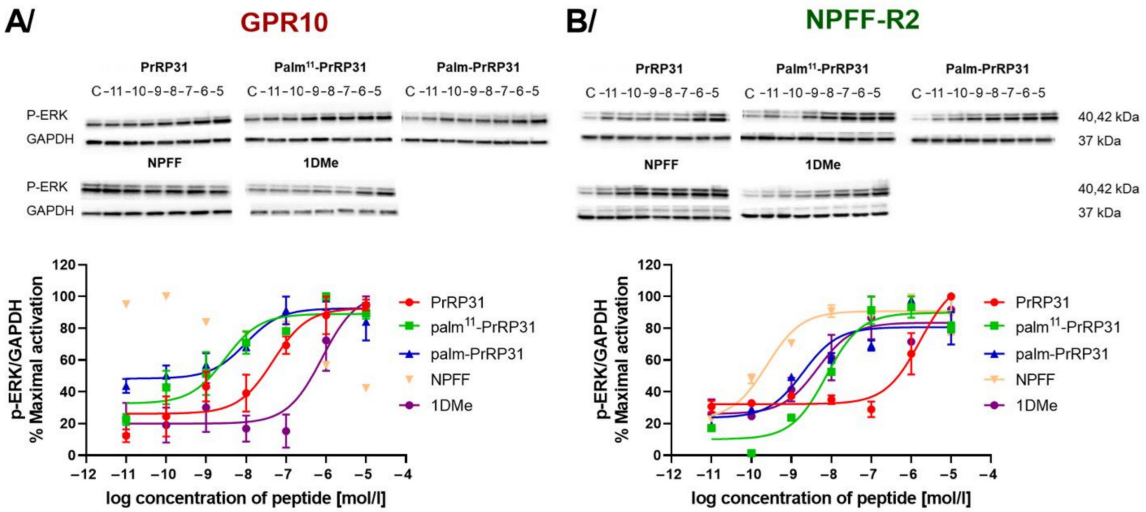

Figure 4. Dose-response phosphorylation of ERK in CHO-K1 cells expressing (**A**) GPR10 and (**B**) NPFF-R2 after 5 min of incubation at 37 C with peptides at final concentrations from 10 ^{11} to 10 ^{5} M. Densitometric quantification was normalized to GAPDH. Data are presented as the mean SEM, and the experiments were performed independently at least two times and were analyzed using nonlinear regression.

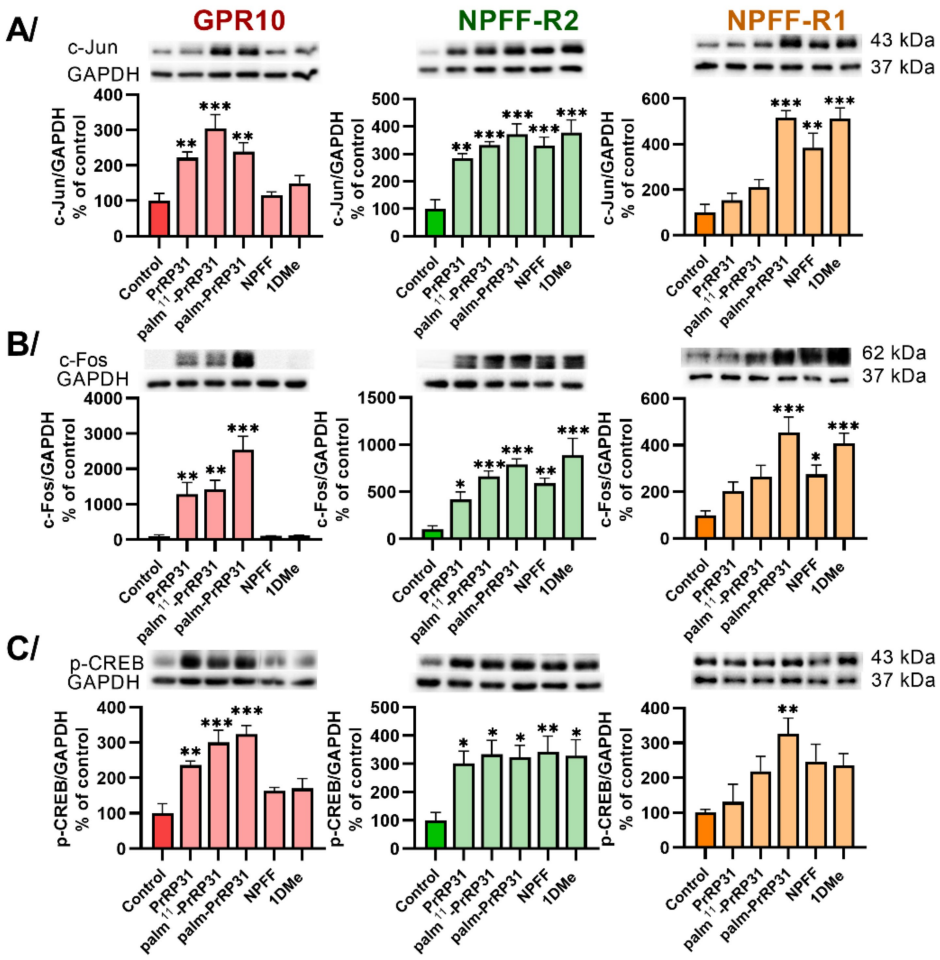

Figure 5. Activation of (**A**) c-Jun and (**B**) c-Fos after 60 min incubation and induction of (**C**) CREB phosphorylation after 5 min incubation at 37 C with peptides in final concentrations 10 ^{6} M in CHO-K1 cells expressing receptors GPR10, NPFF-R2 and NPFF-R1. Densitometric quantification was normalized to GAPDH and the phosphorylation level in the untreated control was standardized as 100%. Data are presented as mean SEM and analyzed by two-way ANOVA followed by Dunnett's post hoc test. Experiments were performed independently at least three times. Statistically significant differences from the control are indicated (* $p < 0.05$, ** $p < 0.01$, *** $p < 0.001$).

One of the key signaling pathways of GPCR signaling, the mitogen-activated protein kinase (MAPK) pathway, was also studied. The phosphorylation of MAPKs, ERK, JNK and p38 was significantly increased in CHO-K1 cells expressing receptors GPR10, NPFF-R2 and NPFF-R1 after stimulation with palm-PrRP31 (Figure 3A–C). Palm^{11}-PrRP31 significantly increased the phosphorylation of ERK, JNK and p38 in CHO-K1 cells expressing GPR10 and NPFF-R2 (Figure 3A–C), but no significant increase in JNK and p38 was observed in cells with NPFF-R1 (Figure 3B,C). Natural PrRP31 was effective in cells expressing GPR10 and NPFF-R2 but did not activate ERK (Figure 3A), JNK (Figure 3B) or p38 (Figure 3C) in cells transfected with NPFF-R1.

To further characterize the signaling of receptors GPR10 and NPFF-R2, dose-response experiments were performed. The EC_{50} of ERK activation in cells expressing GPR10 was in the nanomolar range after stimulation with PrRP31, palm^{11}-PrRP and palm-PrRP31 (Figure 4A). Cells expressing NPFF-R2 showed a strong response with EC_{50} in nanomolar concentrations after stimulation with natural PrRP31, palmitoylated PrRP31 analogs, NPFF or 1DMe (Figure 4B).

Finally, three DNA-binding proteins, cyclic AMP-responsive element-binding (CREB), c-Jun and c-Fos protein, which activate transcription factors, were tested (Figure 5). Palm-

PrRP31 significantly increased the activation of c-Jun (Figure 5A) and c-Fos (Figure 5B) and the phosphorylation of CREB (Figure 5C) compared to the nontreated control in the CHO-K1 cells expressing GPR10, NPFF-R2 or NPFF-R1. Stimulation with palm^{11}-PrRP31 significantly increased the activation of all three DNA-binding proteins (Figure 5) in cells with GPR10 and NPFF-R2, but was ineffective in cells expressing the NPFF-R1 receptor. No activation in GPR10 after stimulation with NPFF and its stable analog 1DMe was observed, unlike in NPFF-R2 or NPFF-R1, where significantly increased activation was monitored.

The results showing signaling pathway activation determined using immunoblotting in CHO-K1 cells expressing GPR10, NPFF-R2 and NPFF-R1 incubated with peptides at final concentrations of 10 ^{6} M are summarized in Table 3.

Table 3. Summary table of signaling pathways tested using immunoblot in cells expressing GPR10, NPFF-R2 and NPFF-R1.

	PrRP31			Palm^{11}-PrRP31			Palm-PrRP31			NPFF			1DMe		
Receptor	**GPR10**	**NPFF-R2**	**NPFF-R1**	**GPR10**	**NPFF-R2**	**NPFF-R1**	**GPR10**	**NPFF-R2**	**NPFF-R1**	**GPR10**	**NPFF-R2**	**NPFF-R1**	**GPR10**	**NPFF-R2**	**NPFF-R1**
p-ERK	" **	" **	-	" ***	" ***	" ***	" ***	" ***	" ***	-	" ***	" ***	" *	" ***	" ***
p-JNK	" *	" **	-	" ***	" ***	-	" ***	" ***	" **	-	" **	" ***	" *	" **	" ***
p-p38	" **	-	-	" ***	" *	-	" ***	" **	" ***	-	-	" *	-	" **	" ***
p-Akt S473	" *	" ***	-	" ***	" ***	" *	" ***	" **	" **	-	" ***	" ***	" *	" ***	" ***
p-Akt T308	-		" ***	" ***	" ***	" ***	" *	" ***	" ***	-	" ***	" ***	-	" ***	" ***
-p-PKA	-	-	-	-	-	-	-	-	-	-	-	-	-	-	-
c-Jun		" **	" **	" ***	" ***	-	" **	" ***	" ***	-	" ***	" **	-	" ***	" ***
-c-Fos		" **	" *	" **	" ***	-	" ***	" ***	" ***	-	" **	" *	-	" ***	" ***
			-	" ***	" *	-	" ***	" *	" **	-	" **	-	-	" *	-
p-CREB	" **	" *	-												

" significant activation (* $p < 0.05$, ** $p < 0.01$, *** $p < 0.001$), - no significant changes.

2.4. Agonist and Antagonist Properties of PrRP31 and Its Palmitoylated Analogs at Other Potential Off-Target Receptors

Using the beta-lactamase reporter gene assay with a FRET substrate, receptor activation was studied to establish agonist and antagonist properties of natural PrRP31 and palmitoylated PrRP31 analogs.

Both tested palmitoylated PrRP analogs were strong agonists of the GPR10 receptor, and their EC_{50} values were in the picomolar range (Table 4). Palm^{11}-PrRP31 had stronger agonist activity on GPR10 than the analog palm-PrRP31.

Table 4. Agonist properties on GPR10 and other potential off-target receptors determined using -lactamase assay.

Receptor	**GPR10**	**Y_5**	**GHSR**	**KOR**	**DOR**	**MOR**	**ORL-1**
	EC_{50} [pM]			**EC_{50} [nM]**			
PrRP31	530.3 70.5	N	N	N	N	N	N
PYY		19.4 2.5					
Ghrelin			2.8 2.5				
U-50488				1.4 1.0			
Deltorphin II					5.6 9.9		
DAMGO						14.7 1.9	
Nociceptin							3.8 0.6
Palm^{11}-PrRP31	39.1 5.1	583.3 121.1	1068.1 272.2	>10,000	N	N	N
Palm-PrRP31	71.8 6.4	56.5 18.4	1273.5 167.9	>10,000	N	N	N

Data presented as the means EC_{50} values SEM and analyzed in Graph-Pad Software and performed in 2–3 independent experiments in duplicates; N-no agonist properties.

Natural PrRP31 was not effective at any tested possible off-target receptor. Both palm^{11}-PrRP31 and palm-PrRP31 did not show any agonist activity on the DOR, MOR and

ORL-1 opioid receptors, but they did have very weak agonist activity on the KOR (Table 4). In addition, lipidized analogs exerted weak agonist effects on GHSR.

Compared to palm^{11}-PrRP31, palm-PrRP31 showed much stronger agonist activity on GHSR and the Y_5 receptor (Table 4); therefore, antagonist activity on receptors Y_5, GHSR and opioid receptors was tested only with PrRP31 and palm^{11}-PrRP31. No antagonist properties of PrRP31 and palm^{11}-PrRP31 were observed with receptors Y_5 (Figure 6), GHSR or opioid receptors (KOR, DOR, MOR, ORL-1) (Supplementary Figure S2A,B). Palm^{11}-PrRP31 was shown to be a positive allosteric modulator for the Y_5 receptor, enhancing PYY activity (Figure 6B).

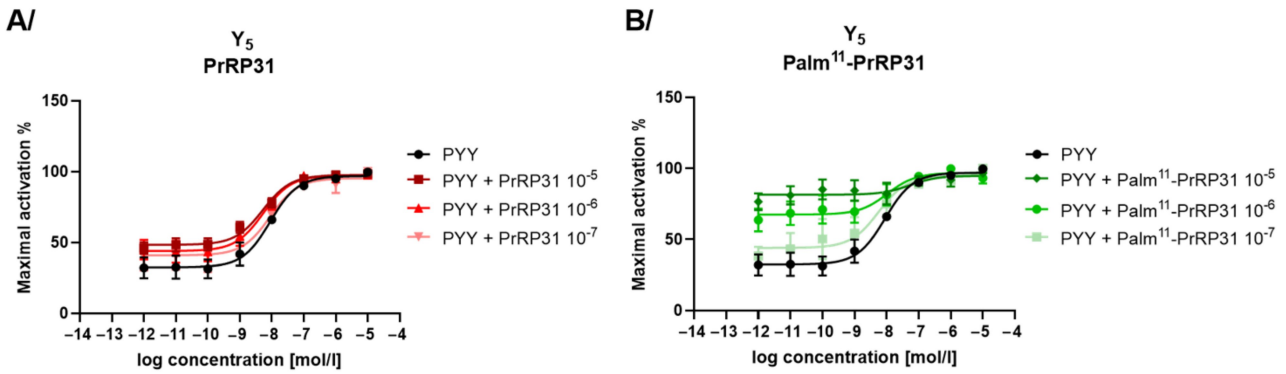

Figure 6. Antagonist mode assay showing effect of (**A**) PrRP31 and (**B**) palm^{11}-PrRP31 at Y_5 receptor together with PYY agonist. Data are presented as mean SEM, and the experiments were performed in duplicates and repeated at least two times and analyzed using nonlinear regression.

3. Discussion

Palmitoylated analogs of neuropeptide PrRP31 previously showed anorexigenic effects and central c-Fos activation after peripheral administration, as well as increased central insulin and leptin signaling, suggesting great potential for the treatment of not only obesity but also neurodegenerative disorders [9,34,35]. PrRP31 has a high affinity for its receptor GPR10, but it also binds to NPFF-R2 [13]. Based on the results of our previous studies the mechanism of action of the two most potent palmitoylated PrRP31 analogs, palm^{11}-PrRP31 and palm-PrRP31 on the anorexigenic receptors GPR10 and NPFF-R2 was mapped.

Palmitoylation increased the binding properties of PrRP31 to both of these receptors. Palm^{11}-PrRP31 had a higher affinity for the GPR10 receptor than palm-PrRP31, and both analogs displayed an affinity for the NPFF-R2 in the nanomolar range. In this study, several possible off-target receptors of PrR31 were tested. Both of the PrRP31 analogs showed a stronger affinity for the NPFF-R1 than natural PrRP31. Therefore, NPFF-R1 is now considered another relevant target of lipidized PrRP31 analogs.

The activation of intracellular Ca^{2+} mobilization in the CHO-K1 AequoScreen cell line expressing NPFF-R2 showed the agonist properties of PrRP31 and its palmitoylated analogs. Palmitoylation increased the agonist properties of PrRP31 on the receptor NPFF-R2. However, NPFF and its stable analog 1DMe have much stronger agonist activity on its NPFF-R2 receptor than palm^{11}-PrRP31 and palm-PrRP31. The activation of GPR10 was studied using the -lactamase assay with a FRET substrate and a FLIPR calcium assay measuring intracellular Ca^{2+} mobilization. The EC_{50} values of palm^{11}-PrRP31 and palm-PrRP31 were in the picomolar range, and the activation was increased three times after palmitoylation. Previous studies suggested that GPR10 is coupled with Gi/o proteins [30,32]. Other studies have shown the ability of PrRP to stimulate cAMP in rat PC12 cells [36] and CHO-K1 cells expressing GPR10 [37], which pointed to Gs protein coupling. However, Langmead et al. revealed the PrRP-induced mobilization of intracellular Ca^{2+} after GPR10 activation, and the PrRP's inability to suppress cAMP levels after forskolin stimulation in HEK293 cells transfected with GPR10. These results suggested that GPR10 is coupled with the Gq

protein [27]. We observed intracellular Ca^{2+} mobilization after stimulation with PrRP31 and its palmitoylated analogs, which may suggest that GPR10 is coupled with either Gi or Gq. This also supported our finding that PKA was not activated after stimulation with PrRP31 and its palmitoylated analogs; thus, GPR10 was not coupled with Gs proteins.

In this study, the intracellular signaling pathways of PrRP31 and its palmitoylated analogs in CHO-K1 cells transfected with GPR10, NPFF-R2, or NPFF-R1 were explored using immunoblotting, and the possible signal transduction of GPR10 was suggested (Figure 7). Haykawa et al. previously showed the activation of Akt in rat pituitary GH3 cells after 5 min of stimulation with PrRP [32]. Our study found significant induction of Akt phosphorylation at T308 and S473 in CHO-K1 cells expressing GPR10, NPFF-R2 and NPFF-R1 after 5 min of stimulation with palm^{11}-PrRP31 and palm-PrRP31, but no significantly increased phosphorylation was observed after stimulation with natural PrPR31 in cells with NPFF-R1. Palmitoylation helped stabilize PrRP31 and increased the induction activity of Akt through the receptors GPR10, NPFF-R2 and NPFF-R1. Previous studies demonstrated that PrRP activated the MAP kinases ERK and JNK in rat GH3 cells [30] and PC12 cells [38]. Our results showed significant activation of JNK, ERK and p38 MAPKs after PrRP31 incubation in CHO-K1 cells expressing GPR10, and of JNK and ERK in cells with NPFF-R2. Both palmitoylated PrRP31 analogs also significantly increased the phosphorylation of all three tested MAPKs in GPR10 and NPFF-R2-expressing cells. Dose-response experiments showed the ability of PrRP31, palm^{11}-PrRP31 and palm-PrRP31 to activate ERK phosphorylation in cells with GPR10 and NPFF-R2 in the nanomolar range. JNK and ERK activation play important roles in cell proliferation, differentiation and apoptosis by promoting the formation of AP1 complexes, important transcription factors controlling the cell cycle, through the activation of c-Fos and c-Jun [39]. Similar to ERK and JNK, p38 is also connected with cell cycle regulation, regulation of stress responses, immune responses and cell differentiation [40]. Palm^{11}-PrRP31 and palm-PrRP31 were found to significantly increase p38 phosphorylation in cells expressing GPR10 and NPFF-R2, and stimulation with palm-PrRP31 induced p38 phosphorylation in cells expressing NPFF-R1. Both inducible transcription factors, c-Fos and c-Jun, were significantly activated after stimulation with PrRP31 and its palmitoylated analogs in cells with GPR10 and NPFF-R2. Conversely, NPFF-R1 significantly activated c-Fos and c-Jun only after stimulation with palm-PrRP31. The transcription factor CREB is also important for the regulation of cell pro-liferation, cell survival and differentiation, for maintaining glucose homeostasis, and has an important role in activating immune responses [40,41]. Likewise, c-Fos and c-Jun activation and phosphorylation of the transcription factor CREB were significantly increased in cells expressing GPR10 and NPFF-R2 after stimulation with PrRP31 and its analogs. Compared to palm^{11}-PrRP31, palm-PrRP31 showed a higher activity in cells transfected with NPFF-R1 in all tested signaling pathways. The results show that PrRP31, palm^{11}-PrRP31 and palm-PrRP31 may play important roles in the regulation of cell proliferation and affect immune responses. These findings suggest that dysregulation of glucose homeostasis and inflammatory responses linked with obesity could be treated with PrRP31 analogs.

In this study, we tested potential off-target receptors of PrRP31, which are related to food intake and energy metabolism. Because PrRP and NPFF were found to have antinociceptive properties [16,17,22,23], their agonist and antagonist activities on opioid receptors were studied using a -lactamase assay. In our study, palmitoylation increased the binding properties of natural PrRP31. Palm^{11}-PrRP31 was found to have a lower affinity for KOR than palm-PrRP31, but they both had negligible ability to activate the KOR receptor in either agonist mode or antagonist mode. We did not observe any agonist or antagonist activity of either PrRP31 palmitoylated analog on the other opioid receptors MOR, DOR and ORL-1. The possible pain modulation properties of PrRP do not seem to be linked to opioid receptors, which supports the idea that GPR10 is involved in pain processing regulation. A study by Laurent et al. using GPR10 KO suggested that the central anti-opioid activity of NPFF in mice is regulated by GPR10. Moreover, they suggested that the dual coupling of GPR10 with Gq and Gi may be the reason for PrRP's involvement in

different neuronal networks [23]. GPR10 could be involved either in pain modulation or food intake regulation, depending on the type of G protein coupled with GPR10.

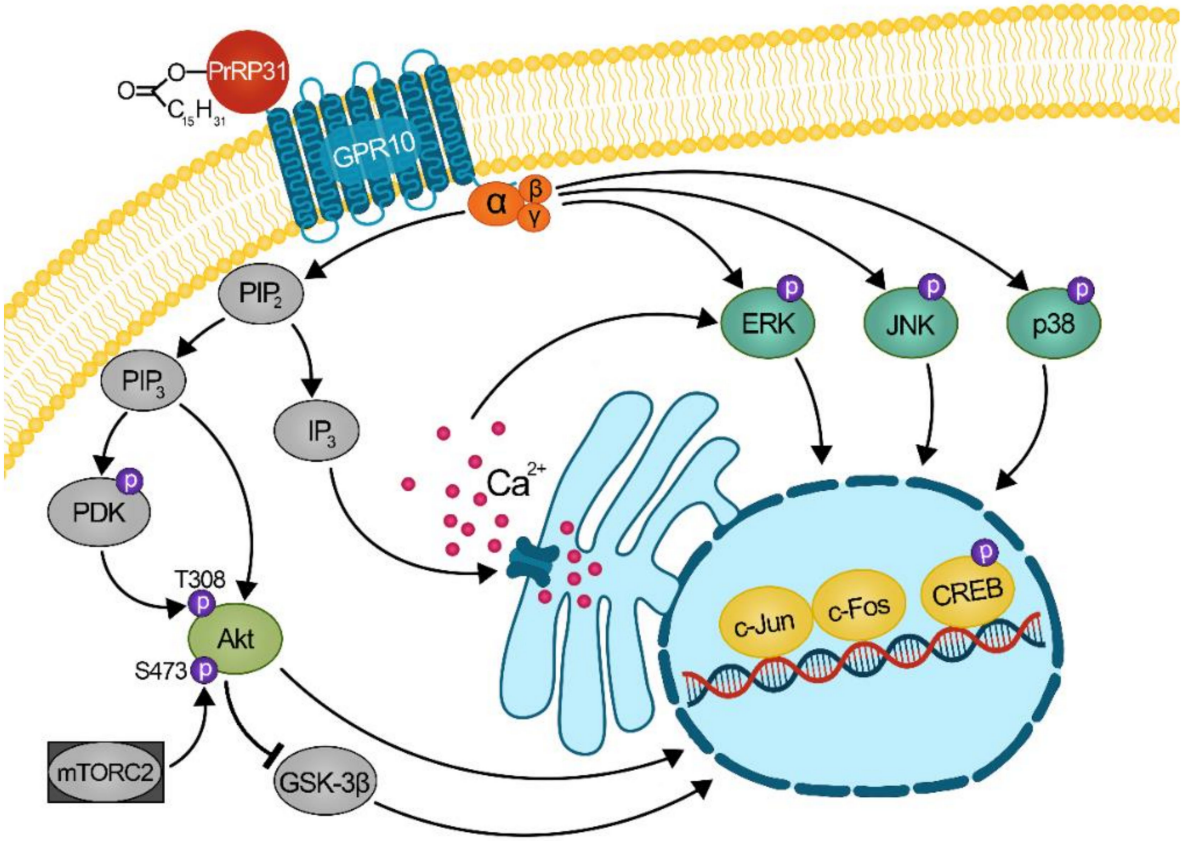

Figure 7. Scheme of mechanism of action of palmitoylated PrRP31 analogs at GPR10: ERK, extracellular signal-regulated kinase; JNK, c-Jun N-terminal kinase; CREB, cAMP-responsive element binding protein; PIP_2, phosphatidylinositol 4,5-bisphosphate; IP_3, inositol 1,4,5-triphosphate; PIP_3, phosphatidylinositol (3,4,5)-trisphosphate; PDK, phosphoinositide-dependent kinase 1; Akt, protein kinase B; mTORC2, mammalian target of rapamycin complex 2; GSK-3, glycogen synthase kinase-3.

NPY, together with PYY and pancreatic polypeptide (PP), controls energy homeostasis though NPY receptors. NPY receptors are expressed throughout the central nervous system but can also be found in the peripheral nervous system [42]. The affinity of PrRP31 and its palmitoylated analogs for the receptors Y_1, Y_2 and Y_5 was tested. No binding affinity of PrRP31 and palmitoylated analogs for the Y_2 receptor was observed and a negligible affinity of palm-PrRP31 for Y_1 was detected. However, natural PrRP31, palm^{11}-PrRP31 and palm-PrRP31 bound and activated the Y_5 receptor with a K_i and an EC_{50} in the micromolar range. PrRP31 affinity and agonist activity were increased with the attached palmitoyl group. Y_1 and Y_5 receptors are expressed in the same neurons, and they both have important regulatory functions in food intake and energy balance [42]. Although NPY is an orexigenic peptide, Y_1 and Y_5 receptor deletion leads to obesity and decreases food intake [43]. This study showed that palm^{11}-PrRP31 and palm-PrRP31 had agonist activity ranging from 10^{-7} to 10^{-8} M on the Y_5 receptor, and palm^{11}-PrRP31 was also shown to be a positive allosteric modulator, which suggests that PrRP31 analogs could mediate the in vivo ability to reduce food intake through Y_5 receptors.

Finally, the off-target properties of the palmitoylated PrRP31 analogs on the receptor of the orexigenic peptide ghrelin were studied. Palm-PrRP31 had a higher affinity for the GHSR receptor than palm^{11}-PrRP31, but both analogs had negligible activity on GHSR.

Palm^{11}-PrRP31 and palm-PrRP31 displayed higher affinity for GPR10 and NPFF-R2 receptors than natural PrRP31, and stimulation with PrRP31 analogs activated transcription factors c-Fos, c-Jun and CREB and also activated PKB/Akt, MAPK pathways in cells expressing these receptors. A new strong target of palmitoylated analogs was found to be NPFF-R1. Palm-PrRP31 induced activation of tested signaling pathways in cells expressing NPFF-R1. Both analogs revealed negligible affinity and ability to activate receptors Y, opioid receptors and GHSR, but palm-PrRP31 showed higher off-target binding affinity for these possible off-target receptors. Palm^{11}-PrRP31 was a more selective agonist of anorexigenic receptors GPR10 and NPFF-R2, with less off-target activity; therefore, it has higher potential for the treatment of obesity and neurodegenerative diseases.

4. Materials and Methods

4.1. Material

Human PrRP31, palm^{11}-PrRP31, palm-PrRP31, neuropeptide FF (NPFF), its stable analog 1DMe (see Table 1 for structures), and ghrelin (ghr) were synthetized and purified as described previously [9,31]. PrRP31 palmitoylation was performed on fully protected peptide on resin as a last step [44]. Peptide purification and identification were determined by analytical high-performance liquid chromatography and by using a Q-TOF micro MS technique (Waters, Milford, MA, USA). Purity of the synthesized peptides was greater than 95%.

Human peptide YY (PYY) (#SC319) was obtained from the PolyPeptide Group (Strasbourg, France). The selective KOR agonists ()-trans-U-50488 methanesulfonate salt (#D8040) were purchased from Sigma-Aldrich (St. Louis, MS, USA). [D-Pro10]-dynorphin A (#021-17), used as an agonist of KOR in binding experiments, was purchased from Phoenix Pharmaceuticals (Burlingame, CA, USA). Selective agonists of mu-opioid receptor (MOR) DAMGO (#1171), opioid receptor-like 1 (ORL-1) agonist nociceptin (#0910) and agonist of delta-opioid receptor (DOR) [D-Ala2]-deltorphin II (#1180) were obtained from Tocris (Bristol, UK).

4.2. Peptide Iodination

Human PrRP31 and 1DMe were iodinated at Tyr20 and D-Tyr1, respectively, with Na[^{125}I] purchased from Izotop (Budapest, Hungary) using IODO-GEN (Pierce, Rockford, IL, USA), as described previously [44]. Radioligands [^{125}I]-PYY, [^{125}I]-dynorphin A and [^{125}I]-ghrelin were iodinated at Tyr20 (Tyr27), Tyr1 and His9, respectively. The identity of peptides was determined by a MALDI-TOF Reflex IV mass spectrometer (Bruker Daltonics, Billerica, MA, USA). The specific activity of all ^{125}I-labeled peptides was approximately 2100 Ci/mmol. The radiolabeled peptides were kept in aliquots at 20 C and used in experiments within 1 month.

4.3. Cell Cultures

All used cells were maintained at 37 C in a humified incubator with 5% CO_2. Growth and assay media were prepared according to manufacturer protocols, and cells were cultured as required. Chinese hamster ovary cells (CHO-K1) stably expressing receptors GPR10 (#K1732) or kappa-opioid receptor (KOR) (#K1533) and human bone osteosarcoma epithelial cells (U2OS) stably expressing receptors of NPY (Y_1 (#K1803), Y_2 (#K149), Y_5 (#K1782)), mu-opioid receptor (MOR) (#K1523), delta-opioid receptor (DOR) (#K1778), opioid receptor-like 1 (ORL-1) (#K1786) and ghrelin receptor (GHSR) (#K1819) were all obtained from Thermo Fisher Scientific Inc. Brand (Waltham, MA, USA). CHO-K1 cell lines containing NPFF-R2 (#ES-490-A) and NPFF-R1 (#ES-491-C) were obtained from Perkin Elmer (Waltham, MA, USA).

4.4. Cell Membrane Isolation

Pellets of CHO-K1 cells containing NPFF-R2, NPFF-R1 and KOR receptors were homogenized in ice-cold homogenizing buffer (20 mM HEPES pH 7.1, 5 mM $MgCl_2$,

0.7 mM bacitracin) with a DIAX 100 Homogenizer (Heidolph Instruments, Schwabach, Germany) and centrifuged in an ultracentrifuge (Beckman Coulter, Fullerton, CA, USA) at 26,000 g for 15 min at 4 C. The pellets were homogenized in ice-cold homogenization buffer, and the previous steps were repeated 2 more times. After the third centrifugation, pellets were resuspended in ice-cold storage buffer (50 mM Tris-Cl pH 7.4, 0.5 mM EDTA, 10 mM $MgCl_2$, 10% sucrose), and aliquots were stored at 80 C. The concentration of isolated membrane proteins was determined by a PierceTM BCA Protein Assay Kit (Pierce, Rockford, IL, USA).

4.5. Competitive Binding Experiments

Competition binding experiments were performed according to [45]. [^{125}I]-PrRP31 was used to compete with human PrRP31, palmitoylated PrRP31 analogs, NPFF, and 1DMe in CHO-K1 cells expressing human GPR10 as described previously [31]. Binding experiments using U2OS cells were optimized and performed in assay buffer (50 mM Tris-Cl pH 7.4, 118 mM NaCl, 5 mM $MgCl_2$, 4.7 mM KCl, 0.1% BSA) for cells stably expressing GHSR and (25 mM HEPES, 120 mM NaCl, 5 mM $MgCl_2$, 4.7 mM KCl, 1 mM $CaCl_2$, 0.5% BSA, 2 g/L glucose) for cells containing receptors Y_1, Y_2 and Y_5. PrRP31 or lipidized analogs of PrRP31,ghr, or PYY were used at final concentrations from 10 ^{12} to 10 ^{5} M to compete with 0.1 nM [^{125}I]-ghr, or [^{125}I]-PYY radioligands. Cells were incubated for 60 min at room temperature (RT).

Plasma membranes isolated from CHO-K1 cells containing receptors NPFF-R2, NPFF-R1 and KOR were used at a concentration of 5 g of protein/tube, and binding experiments were performed in assay buffer (50 mM Tris-HCl pH 7.4 + 60 mM NaCl + 1 mM MgCl2 + 0.5% BSA). [^{125}I]-1DMe was used to compete with human PrRP31, palmitoylated PrRP31 analogs, NPFF or 1DMe in isolated membranes with NPFF-R2 or NPFF-R1, and [^{125}I]-dynorphin A was used to compete with human PrRP31 and palmitoylated PrRP31 analogs in isolated membranes with KOR. The studied peptides and radioligands were incubated with plasma membranes for 60 min at RT and subsequently filtered in a Brandel cell harvester (Biochemical and Development Laboratories, Gaithersburg, MD, USA) using Whatman GF/B filters preincubated in 0.3% polyethylenimine. Filters were rinsed three times with 2 mL of wash buffer (50 mM Tris pH 7.4 + 60 mM NaCl).

Radioactivity was determined by a -counter Wizard 1470 Automatic Gamma Counter (Perkin Elmer). Experiments were carried out in duplicate at least three times, and K_i was calculated using the Cheng-Prusoff equation.

4.6. Cell Signaling Detection by Immunoblotting

Activation of signaling pathways was studied in the CHO-K1 cell lines containing GPR10, NPFF-R2 and NPFF-R1. Cells were seeded in 24-well plates at 30,000 cells/well in assay medium (growth medium without selective antibiotics) and were grown for 2 days. The day before the experiment, the medium was changed to serum-free medium. On the day of the experiment, cells were incubated with PrRP31, lipidized PrRP31 analogs, NPFF or 1DMe at final concentrations from 10 ^{11} to 10 ^{5} M for 5 min or 60 min at 37 C and then washed three times with ice-cold phosphate-buffered saline (PBS) pH 7.4. Cells were lysed with Laemmli sample buffer (62.5 mM Tris-HCl at pH 6.8, 2% SDS, 10% glycerol, 0.01% bromophenol blue, 5% -mercaptoethanol, 50 mM NaF, and 1 mM Na_3VO_4). Samples were stored at 20 C. Electrophoresis and immunoblotting were performed as described previously [45]. For detection of signaling pathways, primary monoclonal antibodies (see Table 5 for the antibodies used) purchased from Cell Signaling Technology (Danvers, MA, USA) were used.

Table 5. Primary antibodies used for immunoblotting and their dilutions.

Antibody Against	Source	Dilution
Phospho-Akt (Thr308) (#2965)	Rabbit	1:1000, 5% BSA, TBS/T-20
Phospho-Akt (Ser473) (#4060)	Rabbit	1:1000, 5% BSA, TBS/T-20
Akt (#4691S)	Rabbit	1:1000, 5% BSA, TBS/T-20
Phospho-CREB (Ser133) (#9196)	Mouse	1:1000, 5% milk, TBS/T-20
CREB (#9104S)	Mouse	1:1000, 5% milk, TBS/T-20
Phospho-p44/42 MAPK (Erk1/2) (Thr202/Tyr204) (#4370S)	Rabbit	1:2000, 5% BSA, TBS/T-20
p44/42 MAPK (Erk1/2) (#9107S)	Mouse	1:2000, 5% milk, TBS/T-20
Phospho-SAPK/JNK (Thr183/Tyr185) (#4668)	Rabbit	1:1000, 5% BSA, TBS/T-20
SAPK/JNK (#9252)	Rabbit	1:1000, 5% BSA, TBS/T-20
Phospho-p38 MAPK (Thr180/Tyr182) (#4511)	Rabbit	1:1000, 5% BSA, TBS/T-20
p38 MAPK (#9212)	Rabbit	1:1000, 5% BSA, TBS/T-20
Phospho-PKA C (Thr197) (#5661)	Rabbit	1:1000, 5% BSA, TBS/T-20
c-Fos (#2250)	Rabbit	1:1000, 5% BSA, TBS/T-20
c-Jun (#9165)	Rabbit	1:1000, 5% BSA, TBS/T-20
GAPDH (#97166)	Mouse	1:1000, 5% milk, TBS/T-20

4.7. Calcium Mobilization Assays

Measuring the intracellular Ca^{2+} level in CHO-K1 cells containing GRP10 was performed using the calcium-sensitive dye Fura-2 according to the manufacturer's protocol (Molecular Devices, Sunnyvale, CA, USA). The day before the experiment, cells were seeded at 40,000 cells/well in 96-well plates in growth media and kept at 37 C in an incubator with 5% CO_2 overnight. Peptides were tested at concentrations from 10^{-12} to 10^{-5} M. Fura-2 fluorescent dye was detected using a FlexStation 3 fluorometric plate reader (Molecular Devices), and excitation was measured at 340 nm and 380 nm and emission at 510 nm.

The intracellular Ca^{2+} level was measured using the AequoScreen stable CHO-K1 cell line containing NPFF-R2 purchased from Perkin Elmer according to the manufacturer's protocol. Cells at 80–90% confluence cultured in media without selective antibiotics were detached (PBS pH 7.4 + 0.5 mM EDTA) and centrifuged. Cells resuspended in phenol red-free DMEM with 0.1% protease-free BSA and 5 M coelenterazine h (Thermo Fisher Scientific Inc. Brand) were seeded at 50,000 cells/well in 96-well plates and incubated in the dark at RT with gentle agitation for 4 h. Peptides were tested at concentrations from 10^{-12} to 10^{-5} M. Luminescent light emission was recorded using a FlexStation 3 plate reader.

4.8. Cell Signaling Determined Using Beta-Lactamase Reporter System

Cell lines containing beta-lactamase reporter genes with different receptors, GPR10, Y_5, GHSR and opioid receptors, were used to study the agonist/antagonist properties of PrRP31 and lipidized PrRP31 analogs. Cells were seeded at 10,000 cells/well in a 384-well plate in assay medium, and the assay was performed according to Thermo Fisher's protocol and according to our previous study [10]. Receptor agonists were tested at concentrations from 10^{-12} to 10^{-5} M. The concentration of the agonist in antagonist assay mode ranged from 10^{-12} to 10^{-5} M, and the potential antagonists PrRP31 and palm^{11}-PrRP31 were tested at concentrations from 10^{-7} or 10^{-6} to 10^{-5} M. Fluorescence was detected at 409 nm excitation and 460 and 530 nm emissions using the FlexStation 3 fluorometric plate reader.

4.9. Statistical Analysis

Data were analyzed by GraphPad Software (San Diego, CA, USA) and are presented as the means SEM. The saturation and competitive binding experiments were analyzed according to [46] using the Cheng-Prusoff equation [33]. The competitive binding curves were plotted compared to the best fit for single-binding site models, and half maximal inhibitory concentration (IC_{50}) values were obtained from nonlinear regression analysis. From saturation binding experiments, the dissociation constant (K_d) and number of binding

sites/cell (Bmax) were calculated. Inhibition constants (K_i) were calculated from IC_{50} values, K_d and the concentration of radioligands.

Experiments using immunoblotting were analyzed using one-way ANOVA followed by Dunnett's post hoc test; $p < 0.05$ was considered statistically significant. Dose-response curves were obtained from nonlinear regression.

The beta-lactamase assay results were analyzed by nonlinear regression as log agonist versus response, and EC_{50} values were determined in agonist mode using GraphPad software. Data are representative of at least two experiments, each performed in duplicate.

Ca^{2+} release assay data are shown as the percentage of maximal response, and the results were analyzed by nonlinear regression as log agonist versus response using GraphPad software. Data are representative of at least three experiments, each performed in duplicate.

5. Conclusions

Lipidized PrRP31 analogs have great potential for the treatment of obesity and neurodegenerative diseases. The in vitro properties of the two most potent palmitoylated analogs, palm-PrRP31 and palm^{11}-PrRP31, were tested and compared. Palmitoylation of PrRP31 increased not only the activity and binding affinity to GPR10 and NPFF-R2, which are both connected with food intake regulation, but also the binding properties and activity to NPFF-R1. Therefore, NPFF-R1 is a new target of lipidized PrRP31 analogs. Both analogs activated the cellular signaling of the PKB/Akt and MAPK pathways and activated the transcription factors c-Fos, c-Jun and CREB in cells expressing GPR10 and NPFFR-2. Activation of all previously mentioned cellular pathways in cells expressing NPFF-R1 was observed only after incubation with palm-PrRP31. Palm-PrRP31 also showed higher off-target activity on GHSR receptors and Y receptors than palm^{11}-PrRP31; therefore, the more selective palm^{11}-PrRP31 has a better potential for obesity treatment. Our future studies will focus on further development of palmitoylated PrRP analogs with minimized off-target activity.

Supplementary Materials: The following are available online at https://www.mdpi.com/article/10.3390/ijms22168904/s1, Supplementary Figure S1: Induction of (A) PKA phosphorylation after 5 min incubation at 37 C with peptides in final concen-18 trations 10-6 M in CHO-K1 cells expressing receptors GPR10, NPFF-R2 and NPFF-R1, Supplementary Figure S2: Antagonist mode of FRET assay showing effect of PrRP31 and palm11-PrRP31 at (A) opioid receptors and 23 (B) GHSR.

Author Contributions: A.K. measured the data, wrote the manuscript and prepared the figures; V.S. measured the data and contributed to the writing of the manuscript, L.H. assisted in data measurements and preparation of the pictures; L.M., B.Ž. and J.K. designed the experiments, contributed to the writing and revised the manuscript. All authors have read and agreed to the published version of the manuscript.

Funding: This work was supported by the Grant Agency of the Czech Republic (GACR 21-03691S, RVO:67985823 and RVO:61388963) of the Academy of Sciences of the Czech Republic.

Institutional Review Board Statement: Not applicable.

Informed Consent Statement: Not applicable.

Data Availability Statement: Not applicable.

Acknowledgments: We gratefully acknowledge the generous help of Miroslava Blechová., for peptide synthesis and Aleš Marek, for radioiodination.

Conflicts of Interest: The authors declare no conflict of interest. The funders had no role in the design of the study, the collection, analyses, or interpretation of data, the writing of the manuscript or in the decision to publish the results.

References

1. Hinuma, S.; Habata, Y.; Fujii, R.; Kawamata, Y.; Hosoya, M.; Fukusumi, S.; Kitada, C.; Masuo, Y.; Asano, T.; Matsumoto, H.; et al. A prolactin-releasing peptide in the brain. Nature **1998**, 393, 272–276. [CrossRef]

2. Matsumoto, H.; Noguchi, J.; Horikoshi, Y.; Kawamata, Y.; Kitada, C.; Hinuma, S.; Onda, H.; Nishimura, O.; Fujino, M. Stimulation of Prolactin Release by Prolactin-Releasing. Biochem. Biophys. Res. Commun. **1999**, 259, 321–324. [CrossRef]
3. Lawrence, C.B.; Celsi, F.; Brennand, J.; Luckman, S.M. Alternative role for prolactin-releasing peptide in the regulation of food intake. Nat. Neurosc. **2000**, 3, 645–646. [CrossRef] [PubMed]
4. Lawrence, C.B.; Ellacott, K.L.J.; Luckman, S.M. PRL-releasing peptide reduces food intake and may mediate satiety signaling. Endocrinology **2002**, 143, 360–367. [CrossRef] [PubMed]
5. Bjursell, M.; Lenneras, M.; Goransson, M.; Elmgren, A.; Bohlooly, Y.M. GPR10 deficiency in mice results in altered energy expenditure and obesity. Biochem. Biophys. Res. Commun. **2007**, 363, 633–638. [CrossRef] [PubMed]
6. Gu, W.; Geddes, B.J.; Zhang, C.; Foley, K.P.; Stricker-Krongrad, A. The prolactin-releasing peptide receptor (GPR10) regulates body weight homeostasis in mice. J. Mol. Neurosc. **2004**, 22, 93–103. [CrossRef]
7. Prazienkova, V.; Funda, J.; Pirnik, Z.; Karnosova, A.; Hruba, L.; Korinkova, L.; Neprasova, B.; Janovska, P.; Benzce, M.; Kadlecova, M.; et al. GPR10 gene deletion in mice increases basal neuronal activity, disturbs insulin sensitivity and alters lipid homeostasis. Gene **2021**, 774, 145427. [CrossRef]
8. Maletinska, L.; Nagelova, V.; Ticha, A.; Zemenova, J.; Pirnik, Z.; Holubova, M.; Spolcova, A.; Mikulaskova, B.; Blechova, M.; Sykora, D.; et al. Novel lipidized analogs of prolactin-releasing peptide have prolonged half-lives and exert anti-obesity effects after peripheral administration. Int. J. Obesity **2015**, 39, 986–993. [CrossRef]
9. Prazienkova, V.; Holubova, M.; Pelantova, H.; Buganova, M.; Pirnik, Z.; Mikulaskova, B.; Popelova, A.; Blechova, M.; Haluzik, M.; Zelezna, B.; et al. Impact of novel palmitoylated prolactin-releasing peptide analogs on metabolic changes in mice with diet-induced obesity. PLoS ONE **2017**, 12, e0183449. [CrossRef]
10. Prazienkova, V.; Ticha, A.; Blechova, M.; Spolcova, A.; Zelezna, B.; Maletinska, L. Pharmacological characterization of lipidized analogs of prolactin-releasing peptide with a modified C-terminalaromatic ring. J. Physiol. Pharmacol. **2016**, 67, 121–128. [PubMed]
11. Pirnik, Z.; Kolesarova, M.; Zelezna, B.; Maletinska, L. Repeated peripheral administration of lipidized prolactin-releasing peptide analog induces c-fos and FosB expression in neurons of dorsomedial hypothalamic nucleus in male C57 mice. Neurochem. Int. **2018**, 116, 77–84. [CrossRef]
12. Pirnik, Z.; Zelezna, B.; Kiss, A.; Maletinska, L. Peripheral administration of palmitoylated prolactin-releasing peptide induces Fos expression in hypothalamic neurons involved in energy homeostasis in NMRI male mice. Brain Res. **2015**, 1625, 151–158. [CrossRef]
13. Engstrom, M.; Brandt, A.; Wurster, S.; Savola, J.M.; Panula, P. Prolactin releasing peptide has high affinity and efficacy at neuropeptide FF2 receptors. J. Pharmacol. Exp. Therapeut. **2003**, 305, 825–832. [CrossRef]
14. Elhabazi, K.; Humbert, J.P.; Bertin, I.; Schmitt, M.; Bihel, F.; Bourguignon, J.J.; Bucher, B.; Becker, J.A.; Sorg, T.; Meziane, H.; et al. Endogenous mammalian RF-amide peptides, including PrRP, kisspeptin and 26RFa, modulate nociception and morphine analgesia via NPFF receptors. Neuropharmacology **2013**, 75, 164–171. [CrossRef]
15. Murase, T.; Arima, H.; Kondo, K.; Oiso, Y. Neuropeptide FF reduces food intake in rats. Peptides **1996**, 17, 353–354. [CrossRef]
16. Sunter, D.; Hewson, A.K.; Lynam, S.; Dickson, S.L. Intracerebroventricular injection of neuropeptide FF, an opioid modulating neuropeptide, acutely reduces food intake and stimulates water intake in the rat. Neurosci. Lett. **2001**, 313, 145–148. [CrossRef]
17. Mouledous, L.; Mollereau, C.; Zajac, J.M. Opioid-modulating properties of the neuropeptide FF system. BioFactors **2010**, 36, 423–429. [CrossRef] [PubMed]
18. Nicklous, D.M.; Simansky, K.J. Neuropeptide FF exerts pro- and anti-opioid actions in the parabrachial nucleus to modulate food intake. Am. J. Physiol. Regulat. Integr. Compar. Physiol. **2003**, 285, 1046–1054. [CrossRef] [PubMed]
19. Panula, P.; Aarnisalo, A.A.; Wasowicz, K. Neuropeptide FF, a mammalian neuropeptide with multiple functions. Progress Neurobiol. **1996**, 48, 461–479. [CrossRef]
20. Simonin, F.; Schmitt, M.; Laulin, J.-P.; Laboureyras, E.; Jhamandas, J.H.; MacTavish, D.; Matifas, A.; Mollereau, C.; Laurent, P. RF9, a potent and selective neuropeptide FF receptor antagonist, prevents opioid-induced tolerance associated with hyperalgesia. Proc. Natl. Acad. Sci. USA **2006**, 103, 466–471. [CrossRef]
21. Maletinska, L.; Ticha, A.; Nagelova, V.; Spolcova, A.; Blechova, M.; Elbert, T.; Zelezna, B. Neuropeptide FF analog RF9 is not an antagonist of NPFF receptor and decreases food intake in mice after its central and peripheral administration. Brain Res. **2013**, 1498, 33–40. [CrossRef] [PubMed]
22. Kalliomäki, M.L.; Pertovaara, A.; Brandt, A.; Wei, H.; Pietilä, P.; Kalmari, J.; Xu, M.; Kalso, E.; Panula, P. Prolactin-releasing peptide affects pain, allodynia and autonomicreflexes through medullary mechanisms. Neuropharmacology **2004**, 46, 412–424. [CrossRef] [PubMed]
23. Laurent, P.; Becker, J.A.; Valverde, O.; Ledent, C.; de Kerchove d'Exaerde, A.; Schiffmann, S.N.; Maldonado, R.; Vassart, G.; Parmentier, M. The prolactin-releasing peptide antagonizes the opioid system through its receptor GPR10. Nat. Neurosci. **2005**, 8, 1735–1741. [CrossRef]
24. Cardoso, J.C.; Felix, R.C.; Fonseca, V.G.; Power, D.M. Feeding and the rhodopsin family g-protein coupled receptors in nematodes and arthropods. Front. Endocrinol. **2012**, 3, 157. [CrossRef] [PubMed]
25. Marchese, A.; Heiber, M.; Nguyen, T.; Heng, H.H.Q.; Saldivia, V.R.; Cheng, R.; Murphy, P.M.; Tsui, L.C.; Shi, X.; Gregor, P.; et al. Cloning and Chromosomal Mapping of Three Novel Genes, GPR9, GPR10, and GPR14, Encoding Receptors Related to Interleukin 8, Neuropeptide Y, and Somatostatin Receptors. Genomics **1995**, 29, 335–344. [CrossRef]

26. Bonini, J.A.; Jones, K.A.; Adham, N.; Forray, C.; Artymyshyn, R.; Durkin, M.M.; Smith, K.E.; Tamm, J.A.; Boteju, L.W.; Lakhlani, P.P.; et al. Identification and characterization of two G protein-coupled receptors for neuropeptide FF. J. Biol. Chem. **2000**, 275, 39324–39331. [CrossRef] [PubMed]
27. Langmead, C.J.; Szekeres, P.G.; Chambers, J.K.; Ratcliffe, S.J.; Jones, D.N.; Hirst, W.D.; Price, G.W.; Herdon, H.J. Characterization of the binding of [(125)I]-human prolactin releasing peptide (PrRP) to GPR10, a novel G protein coupled receptor. British J. Pharmacol. **2000**, 131, 683–688. [CrossRef]
28. Roland, B.L.; Sutton, S.W.; Wilson, S.J.; Luo, L.; Pyati, J.; Huvar, R.; Erlander, M.G.; Lovenberg, T.W. Anatomical distribution of prolactin-releasing peptide and its receptor suggests additional functions in the central nervous system and periphery. Endocrinology **1999**, 140, 5736–5745. [CrossRef]
29. Chuderland, D.; Seger, R. Calcium regulates ERK signaling by modulating its protein-protein interactions. Commun. Integr. Biol. **2008**, 1, 4–5. [CrossRef] [PubMed]
30. Kimura, A.; Ohmichi, M.; Tasaka, K.; Kanda, Y.; Ikegami, H.; Hayakawa, J.; Hisamoto, K.; Morishige, K.; Hinuma, S.; Kurachi, H.; et al. Prolactin-releasing peptide activation of the prolactin promoter is differentially mediated by extracellular signal-regulated protein kinase and c-Jun N-terminal protein kinase. J. Biol. Chem. **2000**, 275, 3667–3674. [CrossRef] [PubMed]
31. Maixnerova, J.; Spolcova, A.; Pychova, M.; Blechova, M.; Elbert, T.; Rezacova, M.; Zelezna, B.; Maletinska, L. Characterization of prolactin-releasing peptide: Binding, signaling and hormone secretion in rodent pituitary cell lines endogenously expressing its receptor. Peptides **2011**, 32, 811–817. [CrossRef]
32. Hayakawa, J.; Ohmichi, M.; Tasaka, K.; Kanda, Y.; Adachi, K.; Nishio, Y.; Hisamoto, K.; Mabuchi, S.; Hinuma, S.; Murata, Y. Regulation of the PRL promoter by Akt through cAMP response element binding protein. Endocrinology **2002**, 143, 13–22. [CrossRef] [PubMed]
33. Cheng, Y.; Prusoff, W.H. Relationship between the inhibition constant (K1) and the concentration of inhibitor which causes 50 per cent inhibition (I50) of an enzymatic reaction. Biochem. Pharmacol. **1973**, 22, 3099–3108. [CrossRef] [PubMed]
34. Holubova, M.; Zemenova, J.; Mikulaskova, B.; Panajotova, V.; Stohr, J.; Haluzik, M.; Kunes, J.; Zelezna, B.; Maletinska, L. Palmitoylated PrRP analog decreases body weight in DIO rats but not in ZDF rats. J. Endocrinol. **2016**, 229, 85–96. [CrossRef]
35. Maletinska, L.; Popelova, A.; Zelezna, B.; Bencze, M.; Kunes, J. The impact of anorexigenic peptides in experimental models of Alzheimer's disease pathology. J. Endocr. **2019**, 240, R47–R72. [CrossRef]
36. Nanmoku, T.; Takekoshi, K.; Isobe, K.; Kawakami, Y.; Nakai, T.; Okuda, Y. Prolactin-releasing peptide stimulates catecholamine release but not proliferation in rat pheochromocytoma PC12 cells. Neurosci. Lett. **2003**, 350, 33–36. [CrossRef]
37. Wang, Y.; Wang, C.Y.; Wu, Y.; Huang, G.; Li, J.; Leung, F.C. Identification of the receptors for prolactin-releasing peptide (PrRP) and Carassius RFamide peptide (C-RFa) in chickens. Endocrinology **2012**, 153, 1861–1874. [CrossRef]
38. Nanmoku, T.; Takekoshi, K.; Fukuda, T.; Ishii, K.; Isobe, K.; Kawakami, Y. Stimulation of catecholamine biosynthesis via the PKC pathway by prolactin-releasing peptide in PC12 rat pheochromocytoma cells. J. Endocrinol. **2005**, 186, 233–239. [CrossRef]
39. Cargnello, M.; Roux, P.P. Activation and function of the MAPKs and their substrates, the MAPK-activated protein kinases. Microbiol. Mol. Biol. Rev. **2011**, 75, 50–83. [CrossRef]
40. Canovas, B.; Nebreda, A.R. Diversity and versatility of p38 kinase signalling in health and disease. Nat. Rev. Mol. Cell Biol. **2021**. [CrossRef]
41. Wen, A.Y.; Sakamoto, K.M.; Miller, L.S. The role of the transcription factor CREB in immune function. J. Immunol. **2010**, 185, 6413–6419. [CrossRef] [PubMed]
42. Loh, K.; Herzog, H.; Shi, Y.C. Regulation of energy homeostasis by the NPY system. Trends Endocrinol. Metab. **2015**, 26, 125–135. [CrossRef] [PubMed]
43. Nguyen, A.D.; Mitchell, N.F.; Lin, S.; Macia, L.; Yulyaningsih, E.; Baldock, P.A.; Enriquez, R.F.; Zhang, L.; Shi, Y.C.; Zolotukhin, S.; et al. Y1 and Y5 receptors are both required for the regulation of food intake and energy homeostasis in mice. PLoS ONE **2012**, 7, e40191. [CrossRef] [PubMed]
44. Maletinska, L.; Pychova, M.; Holubova, M.; Blechova, M.; Demianova, Z.; Elbert, T.; Zelezna, B. Characterization of new stable ghrelin analogs with prolonged orexigenic potency. J. Pharmacol. Exp. Ther. **2012**, 340, 781–786. [CrossRef] [PubMed]
45. Spolcova, A.; Mikulaskova, B.; Holubova, M.; Nagelova, V.; Pirnik, Z.; Zemenova, J.; Haluzik, M.; Zelezna, B.; Galas, M.C.; Maletinska, L. Anorexigenic lipopeptides ameliorate central insulin signaling and attenuate tau phosphorylation in hippocampi of mice with monosodium glutamate-induced obesity. J. Alzheimers Dis. **2015**, 45, 823–835. [CrossRef] [PubMed]
46. Motulsky, H.; Neubig, R. Analyzing radioligand binding data. Curr. Protoc. Neurosci. **2002**, 7. [CrossRef] [PubMed]